

Published in final edited form as:

*Chem Sci.* 2012 January 1; 2012(3): 633–658. doi:10.1039/C2SC00907B.

## Synergistic Catalysis: A Powerful Synthetic Strategy for New Reaction Development

Anna E. Allen and David W. C. MacMillan

Merck Center for Catalysis at Princeton University, Princeton, New Jersey, 08544, USA; Fax: +1 609 2585922; Tel: +1 609 2582254

David W. C. MacMillan: dmacmill@princeton.edu

### Abstract

Synergistic catalysis is a synthetic strategy wherein both the nucleophile and the electrophile are simultaneously activated by two separate and distinct catalysts to afford a single chemical transformation. This powerful catalysis strategy leads to several benefits, specifically synergistic catalysis can (i) introduce new, previously unattainable chemical transformations, (ii) improve the efficiency of existing transformations, and (iii) create or improve catalytic enantioselectivity where stereocontrol was previously absent or challenging. This perspective aims to highlight these benefits using many of the successful examples of synergistic catalysis found in the literature.

### 1. Introduction

Catalysis is, without question, one of the most efficient and powerful mechanistic strategies for identifying or engineering new chemical reactions. Within the realm of chemical synthesis, traditional catalytic pathways generally rely on the interaction of a unique catalyst with a single substrate, thereby lowering the energetic barrier to bond formation with a second, unactivated substrate. While this mono-catalysis strategy has successfully delivered vast numbers of new reactions over many decades, multi-catalysis concepts have recently begun to emerge that allow access to many difficult or unattainable transformations. In particular, *synergistic catalysis*, wherein two catalysts and two catalytic cycles work in concert to create a single new bond, has emerged as a powerful new mechanistic approach to reaction engineering. In its simplest form (Fig. 1), synergistic catalysis involves the concurrent activation of both a nucleophile and an electrophile using distinct catalysts. This simultaneously creates two reactive species, one with a higher HOMO (highest occupied molecular orbital) and the other with a lower LUMO (lowest unoccupied molecular orbital), in comparison to the respective ground state starting materials. If selected judiciously, these activated species can rapidly couple, in many cases enabling chemical reactions that are impossible or inefficient using traditional mono-catalysis methods.

Importantly, there are a number of multicyclic mechanisms that do not fall under the classification of synergistic catalysis, and we feel it is important to define them herein. First, if both the nucleophile and electrophile are activated separately by discrete functional groups *on the same catalyst*, this has been classified as *bifunctional catalysis* (Fig 2A).<sup>1</sup> When both catalysts work in concert to *activate only one* of the reacting partners, we term this *double activation catalysis* (Fig 2B).<sup>2</sup> Similarly, if both catalysts activate the same reacting partner, but *in a sequential fashion* (i.e. an activated substrate produces an intermediate, which is further activated by the second catalyst), we have previously classified this strategy as *cascade catalysis* (Fig 2C).<sup>3</sup> In contrast, and as defined above, when the nucleophile and electrophile are *simultaneously activated by two separate catalysts* to afford a single chemical transformation, we classify this strategy as *synergistic catalysis* (Fig 2D).

While synergistic catalysis is now beginning to emerge as a recognized and valuable approach to bond forming processes, the concept itself is not a new one. Indeed, synergistic catalysis is prevalent in nature, as many enzymes function through the cooperation of two or more catalysts (or catalytic moieties within an active site) to afford a specific transformation.<sup>4</sup> For example, tetrahydrofolate, an important coenzyme for the transfer of one-carbon units, is produced from the folic acid metabolite dihydrofolate via a hydride transfer to the imine moiety. The enzyme dihydrofolate reductase binds dihydrofolate and activates it towards hydride addition through protonation of the imine. A hydride is also catalytically activated by coenzyme NADP<sup>+</sup>, generating NADPH. This cofactor binds to the enzyme and delivers the hydride, producing tetrahydrofolate and regenerating NADP<sup>+</sup> (Fig 3).<sup>5</sup>

There are some perceived challenges surrounding this strategy. While nature has the advantage of physical separation between catalytic sites in an enzyme, when applying the concept in synthesis the catalysts are free to interact with one another. This can potentially result in self-quenching, which renders both catalysts inactive. This can happen through a variety of processes, such as strong complexation of a Lewis acid and a Lewis base or a redox event. The key to overcoming this challenge is the judicious selection of appropriate catalyst combinations. For example, many Lewis acids and Lewis bases form labile complexes that exhibit reversible binding; these weak interactions can still allow respective substrate activation. Often combining hard Lewis acids with soft Lewis bases will accomplish this and avoid the formation of strongly coordinated complexes.<sup>6</sup>

Another perceived challenge of synergistic catalysis surrounds kinetics. At first glance, it may appear that any reaction between two catalytic intermediates that are present in low sub-stoichiometric concentrations should be inherently difficult. This assumption neglects to consider an integral part of the rate equation, the *rate constant*  $k$ . When considering the reaction between two activated intermediates, the narrowing of the HOMO-LUMO gap that occurs in synergistic catalysis ( $\Delta E$ , Fig 1) causes a large decrease in the activation energy, which in turn increases the rate constant to drive the desired pathway in preference to possible side reactions.

While we recognize the challenges in implementing synergistic catalysis, there have been many successful applications reported in the recent literature. Indeed, a survey of asymmetric catalysis based on this synergistic paradigm reveals a 10-fold increase in publication numbers over the last decade (Fig 4). We believe this emergence of synergistic catalysis in the community is founded upon the realization of the inherent utility and benefits provided by this multi-catalysis concept. In this perspective, we aim to illustrate these benefits through various literature examples that demonstrate the (i) development of new, previously unattainable chemical transformations; (ii) improvements of existing transformations; (iii) introduction or improvement of catalytic enantioselectivity in systems where stereocontrol was previously absent or difficult.

## 2. Carbonyl $\alpha$ -Functionalization

### 2.1 Synthesis of $\alpha$ -Allyl carbonyls via $\pi$ -allyl intermediates

Palladium-catalyzed allylic alkylation (Tsuji-Trost allylation) is an attractive strategy to install an allyl substituent on a nucleophile via transient palladium(II)  $\pi$ -allyl intermediates.<sup>7</sup> For aldehyde and ketone nucleophiles, traditional  $\alpha$ -allylic alkylations often require stoichiometric preactivation to metal enolates, silyl enol ethers, or enamines prior to the allylation protocol. The concept of synergistic catalysis has enabled the development of several direct syntheses of  $\alpha$ -allylic aldehydes and ketones through the merger of palladium catalysis with other catalytic cycles. Described below are various methods of catalytically

activating carbonyls (or carbonyl precursors) to combine successfully with palladium(II)  $\pi$ -allyl complexes to forge  $\alpha$ -allyl bonds.

An early example from the Ito group merges rhodium and palladium catalysis for enantioselective allylic alkylations of  $\alpha$ -cyano carbonyls (Scheme 1).<sup>8</sup> Chiral rhodium(I)-activated enolates combine with  $\pi$ -allylpalladium(II) complexes derived from allyl carbonates (**2**) to form optically active  $\alpha$ -allyl- $\alpha$ -cyano esters (**3**), amides (**4**), and phosphonates (**5**) in high yield and selectivity. As shown in Scheme 2, chiral rhodium(I) complex **6** coordinates to the  $\alpha$ -cyano group of **1** forming rhodium(I)-coordinated enolate **7**. Simultaneously, the decarboxylative oxidative addition of allyl carbonate **2** to palladium(0) forms the  $\pi$ -allylpalladium(II) intermediate. The two catalytic cycles merge as rhodium-bound enolate **7** adds to the  $\pi$ -allyl electrophile, in a highly enantioselective fashion, to produce the stereogenic  $\alpha$ -cyano- $\alpha$ -allyl carbonyl **3** and regenerate both catalysts.

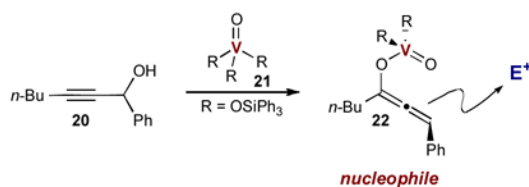
No reaction occurs in the absence of palladium, and while the reaction does proceed without the rhodium catalyst (with chiral ligand on palladium), the rate is considerably slower and racemic product is generated. These results indicate that a chiral environment around palladium imparts no stereocontrol on the transition state. This is not surprising as stabilized carbon nucleophiles attack the  $\pi$ -allyl electrophile from the face opposite the chiral palladium.<sup>7c</sup> The addition of the rhodium catalyst accelerates the rate of the reaction by activating the  $\alpha$ -cyano carbonyl and also creates an opportunity to impart stereocontrol during the bond-forming step.

While the allylic alkylation of  $\alpha$ -cyano carbonyls requires a synergistic strategy to create enantiocontrol in the transition state,  $\alpha$ -allylic alkylations of unactivated aldehydes and ketones do not proceed without activation of both reacting partners, due to the weak nucleophilicity of the carbonyl compounds (a result of the low concentration of the moderately nucleophilic enol tautomer).

In 2006, Córdova and coworkers reported the direct  $\alpha$ -allylic alkylation of unactivated aldehydes and cyclic ketones with allyl acetate **10** through the merger of enamine and palladium catalysis (Scheme 3).<sup>9</sup> Using pyrrolidine to activate the carbonyl and tetrakis(triphenylphosphine)palladium(0) to activate allyl acetate **10**, the reaction proceeds with high efficiency to yield the racemic  $\alpha$ -allyl carbonyls (**11**).

The organocatalytic cycle begins as pyrrolidine condenses with **9** to form a transient pyrrolidine enamine **12**. At the same time, allyl acetate **10** oxidatively adds to the palladium(0) complex, to form the  $\pi$ -allylpalladium(II) electrophile. The metal- and organocatalytic cycles intersect as the two intermediates combine to form  $\alpha$ -allyl iminium ion **13**. Hydrolysis releases  $\alpha$ -allyl carbonyl **11** and regenerates both the amine and palladium catalysts.

Replacing pyrrolidine with a chiral amine catalyst was only moderately successful in the Córdova system for generating stereogenic  $\alpha$ -allyl carbonyls. Enantiomeric excesses of up to 74% ee were obtained; however, reaction yields decreased dramatically. Zhang and coworkers, however, recently built upon Córdova's synergistic strategy and were able to achieve an asymmetric variant of the  $\alpha$ -allylic alkylation of unactivated aldehydes and ketones.<sup>10</sup> Taking a different approach to enantioinduction than previously described (i.e. chiral carbonyl activation), palladium catalysts bearing  $C_2$ -symmetric chiral metallocene-based ligands were used to activate secondary allyl acetates (**14**), generating chiral  $\pi$ -allyl electrophiles (Scheme 5). The chiral environment created around palladium is able to induce high levels of enantioselectivity in the  $\alpha$ -allyl products (**15**). Unfortunately, using catalytic quantities of pyrrolidine provides poor efficiency ( $\leq 50\%$  yield) and a stoichiometric amount of the amine is needed.



(1)

In 2001, Takemoto and coworkers investigated a different approach to carbonyl activation and used a phase-transfer strategy to activate *tert*-butyl glycinate-benzophenone (**16**) to react with styrenyl acetates **17** in the presence of palladium(0) (Scheme 6).<sup>11</sup> As outlined in Scheme 7, the aqueous base deprotonates glycine imino ester **16** and the resulting enolate **19** associates with the chiral cinchonidium phase transfer catalyst in the organic phase of the biphasic mixture. The chiral phase transfer catalyst acts as the counterion to Schiff base enolate **19** and enables differentiation of the two faces of the prochiral nucleophile, allowing enantioselective addition to the  $\pi$ -allylpalladium(II) complex. The result is the highly enantioenriched  $\alpha$ -allyl glycine imino ester **18** (up to 96% ee), which could not be generated using either catalyst individually.

Until recently, synergistic catalysis strategies toward  $\alpha$ -allyl carbonyls had focused exclusively on the direct  $\alpha$ -allylation of saturated carbonyls. In 2011, however, Trost and Luan developed a unique synergistic approach to the synthesis of  $\alpha$ -allyl- $\alpha,\beta$ -unsaturated ketones.<sup>12</sup> In previous studies, it was demonstrated that oxyvanadium catalysts **21** induces a 1,3-transposition of propargylic alcohols via nucleophilic vanadium-allenoate complex **22** (Eq 1).<sup>13</sup> The authors hypothesized that this catalytic nucleophile should also participate in a Tsuji-Trost allylation and couple with electrophilic  $\pi$ -allyl palladium complexes, forming  $\alpha$ -allyl- $\alpha,\beta$ -unsaturated ketones. A challenging aspect of this transformation is that both vanadium-allenoate intermediate **21** and the  $\pi$ -allyl palladium complex can be trapped with a second propargyl alcohol (present in stoichiometric quantities), forming the Meyer-Schuster rearrangement product **24** (Scheme 8A) and propargylic ether **25** (Scheme 8B) respectively. The success of the desired synergistic transformation depends on the relative rates of the three potential reaction pathways. Despite the potential side reactions, the authors found that treating propargyl alcohol **20** and allyl carbonate **23** with a combination of vanadium and palladium catalysts provides the desired  $\alpha$ -allyl enones **26** in excellent yield with no trace of the side products (Scheme 8C). Despite the low concentrations of both reactive intermediates, the desired  $\alpha$ -allylation reaction outcompeted both possible side reactions.

The mechanism of this remarkable transformation is outlined in Scheme 9. Vanadium catalyst **21** undergoes transesterification with propargyl alcohol **20** to form vanadium ester **27**. A 1,3-transposition of the ester generates key vanadium-allenoate intermediate **22**. At the same time, allyl carbonate **23** reacts with the palladium(0) catalyst to form the palladium  $\pi$ -allyl electrophile. Before either catalytic intermediate can react with unactivated propargyl alcohol **20**, the two activated metal complexes combine to form the desired  $\alpha$ -allyl enone **26**.

## 2.2 Enamine catalysis with metal-bound electrophiles

Traditional enamine catalysis relies on a relatively limited electrophile scope. An examination of these transformations reveals that electrophiles can generally be characterized as either unsaturated nucleophile acceptors (e.g. carbonyls, imines, enals) or electrophilic sources of heteroatoms.<sup>14</sup> Using electrophiles outside these classes, enamine catalysis often suffers from side reactions, such as self-aldolization. To avoid this, the rate of enamine addition to the desired electrophile must be greater than addition to unreacted

aldehyde. By combining enamine and transition metal catalysis, the desired chemoselectivity can increase through catalytic activation of the electrophile. This extends the traditional electrophile scope in order to develop new, previously unattainable chemical reactions.

The following transformations follow the same general mechanism (Scheme 10). The aldehyde (or ketone) condenses with an amine catalyst to form a transient enamine intermediate.

A metal catalyst also activates an electrophile, generating a metal-bound electrophilic intermediate. This metal-bound electrophile interacts with the enamine, transferring the desired functional group, and creates an  $\alpha$ -substituted iminium ion while regenerating the metal catalyst. Hydrolysis of the iminium ion releases the  $\alpha$ -substituted product and returns the amine catalyst.

Shortly after Córdova reported the first example of merging transition metal catalysis and organocatalysis (Scheme 3), Wu and coworkers introduced a synergistic 3-component coupling reaction. 2-Alkynylbenzaldehydes, primary amines, and ketones combine under proline and Ag(I) catalysis to form 1,2-dihydroisoquinoline derivatives (**31**) via the first reported merger of enamine and  $\pi$ -acid catalysis (Scheme 11).<sup>15</sup> They propose 2-alkynylbenzaldehyde **28** condenses with primary amine **29** to form 2-alkynylbenzimine **33** while ketone **30** condenses with proline to form enamine **32**. Intermediate **33** coordinates AgOTf, which triggers a hydroamination/Mannich cascade to furnish the 1,2-dihydroisoquinoline framework. Hydrolysis of iminium **34** releases dihydroisoquinoline **31**. Aryl substituted 2-alkynylbenzaldehydes and anilines react smoothly, however, when either of these components are alkyl substituted the yields obtained are much lower ( $\leq 35\%$ ). In addition, although proline forms chiral enamines, only racemic products are formed.

Recently, our group has also become interested in the use of transition metal-activated electrophiles in enamine catalysis as a strategy to develop new asymmetric reactions. This approach enabled an enantioselective  $\alpha$ -trifluoromethylation of aldehydes to be developed using Togni's reagent (**35**), an electrophilic trifluoromethyl source (Scheme 12).<sup>16</sup> Although Togni's reagent has been shown to react efficiently with a variety of nucleophiles,<sup>17</sup> when exposed to a transient chiral enamine, based on imidazolidinone catalyst **36**, only low yields are observed (14% yield, 92% ee). As the most likely mechanism of trifluoromethylation is attack of the Togni reagent at iodine, followed by reductive elimination of the aryl iodide, it was reasoned that a Lewis acid should facilitate cleavage of the I–O bond and create activated electrophilic iodonium intermediate **39** (Scheme 12). Copper-bound **39** should render iodine more susceptible to nucleophilic attack by enamine **38** when compared to the unactivated Togni reagent. By adding catalytic CuCl as a Lewis acid, in conjunction with chiral imidazolidinone catalyst **36**, excellent yield and enantioselectivity are obtained for the resultant  $\alpha$ -trifluoromethyl aldehydes **37**.

By combining enamine and transition metal catalysis, the Nishibayashi group developed two complementary methods for enantioselective  $\alpha$ -propargylation of aldehydes using propargyl alcohols **42** and benzoates **43** – classes of electrophiles previously outside the scope of enamine catalysis. Diruthenium and ligated copper catalysts activate **42** and **43**, respectively, to form metal-allenylidene complex **46** that is electrophilic at the  $\gamma$ -position (Scheme 13).<sup>18</sup> These metal-bound electrophiles are trapped by transient chiral enamine **47** to provide enantioenriched  $\alpha$ -propargyl aldehyde **45**, a product unattainable via enamine catalysis alone. Ruthenium appears to provide the product in higher yields,<sup>18a</sup> while copper delivers higher selectivities.<sup>18b</sup>

The allenylidene intermediate **46** initially limited the scope of this transformation to terminal alkynes, as they cannot be formed with internal alkynes. Recently, however, Nishibayashi expanded the scope to include internal alkynes by using an alternative method of activating propargylic alcohols (Scheme 14).<sup>19</sup> Using  $\text{InBr}_3$  as a Lewis acid, propargylic alcohol **49** is converted to the corresponding propargylic cation **51**. These cations are trapped by transient enamines to provide enantioenriched  $\alpha$ -propargyl aldehyde **50** bearing an internal alkyne.

In 2007, Sibi and Hasegawa reported an enantioselective  $\alpha$ -oxyamination of aldehydes using  $\text{FeCl}_3$  and a chiral amine catalyst.<sup>20</sup> Initially, this transformation was not described as an example of synergistic catalysis. It was initially proposed that  $\text{FeCl}_3$  oxidizes the transient enamine to produce a radical cation, which traps TEMPO at the  $\alpha$ -position. Recently, through mechanistic studies performed in the MacMillan group this mechanism was shown to be incorrect; the transformation most likely proceeds via synergistic catalysis wherein the  $\text{FeCl}_3$  coordinates to TEMPO, creating a complex that is electrophilic at oxygen and therefore activated towards enamine addition.<sup>21</sup> Based on this mechanistic insight, MacMillan and coworkers improved this transformation by switching to  $\text{CuCl}_2$  (known to form stable complexes with TEMPO) and using amine catalyst **53**. This broadened the functional group tolerance of the reaction and increased both yield and enantioselectivity (Scheme 15). Under these conditions, TEMPO coordinates copper(II) to form electrophilic complex **56**. Transient enamine **55** adds to the oxygen of the TEMPO-bound copper(II) complex **56**, generating iminium ion **57** and a copper(I) salt. The copper(I) is reoxidized by ambient oxygen to regenerate the copper(II) catalyst.

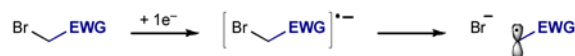
In all of the examples discussed, the transition metal catalyst is only directly involved with the electrophile, activating it towards enamine addition. An enamine, however, contains an electron-rich  $\pi$ -system and can also coordinate to a transition metal catalyst, helping to bring together the enamine and the electrophile to forge a bond at the  $\alpha$ -position. Although less common in the literature, recently, the MacMillan group published an example using this synergistic strategy. Using copper catalysis in combination with a chiral amine catalyst, an enantioselective  $\alpha$ -arylation of aldehydes was developed that uses diaryliodonium salts as the electrophilic arene source (Scheme 16).<sup>22</sup> Although diaryliodonium salts are not electrophilic enough to react with a transient enamine under organocatalytic conditions alone, they can be activated by copper(I) salts to generate highly electrophilic arylcopper(III) intermediate **60**.<sup>23</sup> These highly reactive arylcopper(III) species react smoothly with enamines (derived from amine catalyst **58**) to generate copper-bound iminium ion **61** that undergoes reductive elimination, followed by hydrolysis, to provide enantioenriched  $\alpha$ -aryl aldehyde **59** in excellent yield and selectivity. A wide variety of arenes can be transferred by this protocol, ranging from electron rich to electron poor and even some heteroaromatics. Prior to this report, organocatalytic  $\alpha$ -arylation reactions had only been developed for intramolecular substrates and intermolecular reactions with highly activated quinone substrates.<sup>24</sup> Using synergistic catalysis a more general intermolecular reaction was developed through in situ activation of both reacting partners.

### 2.3 Photoredox $\alpha$ -alkylation of aldehydes

In all of the synergistic catalysis examples outlined above, both catalysts have been directly involved in the key bond forming step. In an alternate mechanistic scenario, a catalyst may induce formation of a reactive intermediate, but not be involved in the actual coupling event; this strategy is key to the success of photoredox organocatalysis.<sup>25</sup>

The catalytic enantioselective  $\alpha$ -alkylation of aldehydes has been an ongoing challenge in organic synthesis that has yet to be solved in a general sense.<sup>26</sup> In enamine catalysis, which traditionally proceeds through a closed-shell, two-electron pathway, the use of alkyl halides has been generally unsuccessful, commonly leading to catalyst alkylation and/or self-

aldolization.<sup>27</sup> In an effort to circumvent these problems, MacMillan and Nicewicz reasoned that the electron-rich  $\pi$ -system of enamines should combine efficiently with electron-deficient radicals through a one-electron pathway.<sup>28</sup> To implement this strategy, enamine catalysis could be merged with the catalytic formation of electron-deficient radicals through the reductive cleavage of alkyl halide C–X bonds (Eq 2). Recognizing that photoredox catalysis is an attractive method for reductive cleavage of C–X bonds via photo-induced electron transfer (PET) from  $\text{Ru}(\text{bpy})_3\text{Cl}_2$ ,<sup>29</sup> the concepts



(2)

of enamine catalysis and photoredox catalysis were combined in an effort towards the enantioselective  $\alpha$ -alkylation of aldehydes (Scheme 17).<sup>28</sup>

The general mechanism of organocatalytic photoredox  $\alpha$ -alkylations is outlined in Scheme 18. When exposed to weak visible light,  $\text{Ru}(\text{bpy})_3^{2+}$  accepts a photon and populates the metal-to-ligand charge transfer (MLCT) excited state,  $^*\text{Ru}(\text{bpy})_3^{2+}$ . Initially, this excited state is quenched by a sacrificial amount of enamine **65** (0.5 mol%) to generate the highly reducing  $\text{Ru}(\text{bpy})_3^+$  (not shown). This reductant delivers an electron to alkyl halide **63**, generating the required electron-deficient radical **64** and returning the photocatalyst to its original oxidation state. In the organocatalytic cycle, chiral transient enamine **65** is formed via condensation of the aldehyde with amine catalyst **62**. The two catalytic cycles intersect and electron-deficient radical **63** adds to the accessible face of the electron-rich  $\pi$ -system of **65**, achieving the key alkylation step. The coupling event results in  $\alpha$ -amino radical **66**, whose low barrier to oxidation allows for a second convergence of the two catalytic cycles. After accepting a photon,  $^*\text{Ru}(\text{bpy})_3^{2+}$  oxidizes **66** to provide an  $\alpha$ -alkylated iminium ion and regenerate the strong reductant  $\text{Ru}(\text{bpy})_3^+$ . Upon hydrolysis of iminium ion **67**, the enantioenriched  $\alpha$ -alkylated aldehyde is released and chiral amine catalyst **62** is returned. The first successful execution of this synergistic design was realized in 2008 for the  $\alpha$ -alkylation of aldehydes using  $\alpha$ -bromocarbonyls **68** as radical precursors.<sup>29</sup> The combination of chiral amine organocatalyst **62** and  $\text{Ru}(\text{bpy})_3^{2+}$  delivers the desired  $\alpha$ -alkylated aldehydes **69** in excellent yields and enantioselectivities (Scheme 19A). This mild, yet powerful alkylation strategy supports high functional group tolerance and highly congested substrates as well as the formation of  $\beta$ -quaternary centers.

Recognizing the generality of this synergistic strategy, MacMillan and coworkers turned to other  $\alpha$ -alkyl substrate classes that have proven challenging under traditional catalysis. Shortly following the initial report, a photoredox strategy towards the  $\alpha$ -trifluoromethylation and  $\alpha$ -perfluoroalkylation of aldehydes was described using  $\text{CF}_3\text{I}$  (or the corresponding perfluoroalkyl iodide) as the radical source (Scheme 19B).<sup>30</sup> In this case,  $\text{Ir}(\text{ppy})_2(\text{dtbbpy})\text{PF}_6$  is used as the photocatalyst, rather than  $\text{Ru}(\text{bpy})_3\text{Cl}_2$ , since after single electron transfer, the reduced form,  $\text{Ir}(\text{ppy})_2(\text{dtbbpy})$ , is a stronger reductant than  $\text{Ru}(\text{bpy})_3^+$  ( $-1.51$  V vs SCE in  $\text{CH}_3\text{CN}$  for  $\text{Ir}(\text{ppy})_2(\text{dtbbpy})$  compared to  $-1.33$  V vs SCE in  $\text{CH}_3\text{CN}$  for  $\text{Ru}(\text{bpy})_3^+$ ).<sup>29,30</sup> The trifluoromethyl (or perfluoroalkyl) radical adds smoothly to the *in situ* generated enamine to furnish the  $\alpha$ - $\text{CF}_3$  or  $\alpha$ -perfluoroalkylated aldehydes in excellent yields and enantioselectivities. To maintain the stereochemical integrity of these products, the reaction must be run under cryogenic conditions.

Another challenging alkylation that was addressed using photoredox organocatalysis is the enantioselective  $\alpha$ -benzylation of aldehydes (Scheme 19C).<sup>31</sup> Previous direct

organocatalytic methods to form  $\alpha$ -benzylated aldehydes require multiple and/or electron-rich aryl rings on the electrophilic coupling partner to stabilize intermediate benzylic carbocations.<sup>32</sup> Since photoredox organocatalysis relies on the formation of electron-deficient radicals, this strategy complements existing benzylation protocols. The  $\alpha$ -benzylation of aldehydes proceeds through a slightly different photoredox catalytic cycle than described above. This protocol uses the commercially available photocatalyst *fac*-Ir(ppy)<sub>3</sub>. In the excited state, *fac*-\*Ir(ppy)<sub>3</sub> is a strong enough reductant (−1.73 V vs SCE in CH<sub>3</sub>CN) to induce reductive cleavage of aryl and heteroaryl methylene halides **73** directly (Scheme 20). After single electron transfer and addition of benzyl radical **74** to enamine **75** (derived from chiral amine catalyst **71**), *fac*-Ir(ppy)<sub>3</sub> merges with the organocatalytic cycle to oxidize  $\alpha$ -amino radical **76**, which closes the photoredox cycle. The  $\alpha$ -benzylation is successful for a range of electron-deficient aryl and heteroaryl methylene substrates and aldehyde functionality to form enantioenriched  $\alpha$ -benzyl aldehydes in high yield and selectivity.

Recently, Zeidler and coworkers also became interested in the concept of photoredox organocatalysis. Instead of turning to organometallic based photoredox catalysts, they speculated that red and orange organic dyes, which absorb green wavelengths of visible light, may also perform successfully as photocatalysts. Through initial studies, eosin Y emerged as the optimal substitute for more typical organometallic photocatalysts.<sup>33</sup> As a proof of concept with eosin Y, Zeidler was able to produce the same synergistic  $\alpha$ -alkylation of aldehydes with  $\alpha$ -bromocarbonyls as MacMillan's seminal photoredox organocatalysis. The proposed mechanism mirrors that of MacMillan with photoexcited eosin Y (\*EY) acting as the oxidant (requiring a sacrificial amount of enamine to initiate the photoredox cycle) and reduced eosin Y (EY<sup>•−</sup>) acting as the reductant (Scheme 21).

## 2.4 Other Synergistic Strategies Involving Enamine Catalysis

A powerful advantage of using a synergistic approach to enamine catalysis is the ability to generate reactive electrophiles in situ from non-electrophilic precursors. Klussmann and coworkers recognized this advantage and developed a direct oxidative Mannich-type coupling of cyclic tertiary amines **78** with methyl ketones **79** using a combination of vanadium and proline as catalysts (Scheme 22).<sup>34a</sup> In situ oxidation of tertiary amine **78** with VO(acac)<sub>2</sub> generates electrophilic iminium ion **81**. After proline activates methyl ketone **79**, transient enamine **82** adds to the cyclic iminium ion **81**. Hydrolysis of **83** liberates proline and delivers the Mannich-type product **80** in moderate to good yields. To close the vanadium catalytic cycle, the reduced form of the catalyst is reoxidized by *t*-BuOOH. Unfortunately, despite using a chiral organocatalyst, little to no enantioinduction was observed with proline. Further attempts with chiral vanadium complexes were also unsuccessful at an asymmetric reaction. These observations are attributed to facile racemization of  $\beta$ -amino ketones.

Recently, the same oxidative coupling reaction was addressed by Rueping and coworkers. Instead of using catalytic VO(acac)<sub>2</sub> to generate the intermediate iminium ion, photoredox catalysis with Ru(bpy)<sub>3</sub>(PF<sub>6</sub>)<sub>2</sub> was used in conjunction with proline instead (Scheme 22).<sup>34b</sup> The oxidation is proposed to proceed through the same radical mechanism, where the photoexcited \*Ru(bpy)<sub>3</sub>(PF<sub>6</sub>)<sub>2</sub> oxidizes tertiary amine **78** to form iminium ion **81**. Molecular oxygen oxidizes Ru(bpy)<sub>3</sub><sup>+</sup> to regenerate the photocatalyst. When compared to VO(acac)<sub>2</sub> oxidation, photoredox catalysis provides a noticeable increase in yield of the desired coupling product. Interestingly, use of 5W fluorescent light was found to be crucial to the high yields, as stronger light emission, whether from LED or UV light, resulted in diminished yields. This has been attributed to the interplay between the photoredox and organocatalytic cycles, since the strength of the light source can tune the rate of the photoredox cycle to match the



rate of enamine formation. As with Klussmann's protocol, Rueping's photoredox oxidative coupling also provided nearly racemic products (8% ee).

Recently, Pihko and coworkers reported a three-component domino reaction to generate  $\gamma$ -nitro aldehydes **86** using a combination of chiral secondary amine catalyst **84** and a multiple hydrogen bond donor (MHBD) catalyst (Scheme 23).<sup>35</sup> In this example, not only is the electrophile generated in situ through synergistic catalysis, it is subsequently consumed using the same combination of catalysts. Overall, the two step sequence involves the formation of nitroolefins from aldehydes and nitromethane, followed by the conjugate addition of the aldehyde to the nitroolefin via enamine catalysis. Attempting this domino process with a secondary amine catalyst alone results in aldol and aldol-type products, bypassing the nitromethane altogether. Furthermore, attempting just the second step of the domino sequence with pregenerated nitroolefins and an amine catalyst resulted in low yields of the  $\gamma$ -nitroaldehyde product **86** (< 20% yield), indicating both steps of this sequence benefit from synergistic catalysis.

In the first step, adding a MHBD catalyst activates nitromethane to form hydrogen-bonded anion **87** for a Knoevenagel-type condensation with iminium ion **88** (formed via condensation of the aldehyde and amine catalyst **84**). The in situ generation of nitroolefin **85** proceeds smoothly, even with challenging  $\beta$ -alkyl substitution. In the second step of the sequence, nitroolefin **85** is activated by the MHBD catalyst towards conjugate addition of chiral transient enamine **90** (derived from **84** and the second aldehyde). This synergistic domino process provides  $\gamma$ -nitroaldehydes **86** in good yields and excellent selectivities. The activation of reacting partners in both steps of this domino sequence allows for the desired reaction to proceed with high chemoselectivity over any aldol side products.

### 3. Reactions of $\alpha,\beta$ -unsaturated carbonyls

#### 3.1 Organocatalytic activation of unsaturated carbonyls

Although synergistic catalysis involving enamine and transition metal catalysis has been known since Córdova's allylic alkylation report in 1996,<sup>9</sup> synergistic catalysis involving iminium catalysis is much more recent. Just as synergistic catalysis expands the electrophile scope in enamine catalysis, this strategy should also expand the nucleophile scope of iminium catalyzed reactions to include those that were previously unsuccessful. Córdova and coworkers recognized this and developed a catalytic enantioselective silyl conjugate addition to  $\alpha,\beta$ -unsaturated aldehydes using  $\text{Me}_2\text{PhSi-B}(\text{pin})$  (**92**), an unlikely nucleophile in traditional iminium catalysis (Scheme 24).<sup>36</sup> Treating **92** with  $\text{CuCl}$  induces transmetalation to form nucleophilic  $\text{Cu(I)-silane}$  **94**. This complex intersects the iminium catalytic cycle and adds to the  $\beta$ -position of chiral transient iminium ion **95** (formed by condensation of the enal and amine catalyst **85**). The resultant copper-bound  $\beta$ -silyl iminium ion **96** provides the desired enantioenriched  $\beta$ -silyl aldehyde **93** in good yields and selectivities after protonation and hydrolysis of the amine catalyst. Although both aromatic and aliphatic enals react efficiently, selectivities are generally higher with aromatic enals.

Organocatalytic activation of enals is not limited to iminium catalysis. Condensation of an amine catalyst with an enal can also generate nucleophilic transient dienamines; this mode of activation has recently been combined synergistically with chiral Brønsted acid catalysis.<sup>37</sup> While developing a  $\gamma$ -benzylation of  $\alpha$ -branched enals, Melchiorre and coworkers found that trapping stabilized carbocations with chiral transient dienamines (derived from a cinchona alkaloid amine) provides only moderate enantioselectivities (up to 60% ee). Similarly, using a chiral phosphoric acid to induce carbocation formation, with achiral benzyl amine activating the enal, also leads to poor enantiocontrol (14% ee). When combined, however, the chiral cinchona alkaloid and chiral phosphoric acid together provide

excellent yield and enantioselectivity for the desired  $\gamma$ -benzylated enal **99** (up to 95% ee) (Scheme 25). It is believed that the cinchona alkaloid catalyst activates enal **97** through dienamine formation, creating vinylogous nucleophilicity at the  $\gamma$ -position. At the same time, the chiral phosphoric acid catalyst protonates dibenzyl alcohol **98**, inducing carbocation formation. The benzylic cation, with a chiral phosphate counterion, interacts with the dienamine through a network of non-covalent interactions, leading to a highly organized transition state (Scheme 25). The authors propose that the chiral phosphate counterion, associated with the benzylic cation, also participates in a hydrogen bond with the quinuclidine hydroxyl group at the 6'-position, presumably helping direct attack of the carbocation from the appropriate face of the dienamine. Evidence of the cooperation between the two catalysts can be seen with mismatched catalyst combinations, as this leads to dramatic loss in both reactivity and enantioselectivity ( $\leq 30\%$  yield,  $\leq 21\%$  ee). Interestingly, in all cases the phosphoric acid catalyst determines the major enantiomer of the product obtained.

The use of non-covalent ion-pairs in synergistic catalysis has also led to improvements in the organocatalytic enantioselective synthesis of tetrahydroxanthenones. In 2007, Córdova and coworkers reported the first catalytic enantioselective protocol for the synthesis of tetrahydroxanthenones **101** from salicylic aldehydes **100** and cyclohexenones via an iminium catalyzed oxa-Michael–Mannich domino reaction (Scheme 26A).<sup>38</sup> The transformation provides the desired tricyclic product in modest yields (42–56%), but good selectivities (85–91% ee). Realizing the power of synergistic catalysis, Xu and coworkers sought to improve this transformation through organocatalytic activation of both salicylic aldehyde **100** and cyclohexenone with catalysts that could bring the reacting partners together via an ion-pair assembly (Scheme 26B).<sup>39</sup> In Xu's protocol, the cyclohexenone is activated by chiral pyrrolidine derivative **103**, bearing a thiopyridine unit, to form iminium ion **104**. At the same time, salicylic aldehyde **100** is activated by *tert*-leucine, forming imine **105**. As a key design element, the two activated intermediates (**104** and **105**) form an ion-pair assembly through proton transfer from *tert*-leucine to the thiopyridine unit. This assembly brings together the two intermediates and ensures the domino oxa-Michael–Mannich reaction occurs with high efficiency and selectivity. Hydrolysis of catalyst **103** and subsequent elimination of *tert*-leucine regenerates both catalysts and delivers tetrahydroxanthenone **101** in excellent yields and enantioselectivities. Unsubstituted cyclohexenones provide significantly higher selectivities than that of the 4,4-disubstituted cyclohexenones (91–98% ee unsubstituted compared to 80% ee for 4,4-dimethylcyclohexenone).

### 3.2 Lewis acid activation of $\alpha,\beta$ -unsubstituted carbonyls

Chiral Lewis acid catalysis has been the cornerstone activation method for conjugate additions to  $\alpha,\beta$ -unsaturated carbonyl systems. In 2003, Jacobsen and coworkers reported a conjugate addition of hydrogen cyanide to unsaturated imides **108** using a (salen)AlCl complex.<sup>40</sup> Although excellent yields of highly enantioenriched cyanide adducts **109** were obtained, high catalyst loadings, long reaction times, and in some cases elevated temperatures were required. Through mechanistic studies, the authors found that the aluminum catalyst was activating both the imide and cyanide components. They hypothesized that the lower than desired reactivity was a result of inefficient activation of the cyanide component by the aluminum complex. To improve the conjugate cyanation protocol, Jacobsen and coworkers readdressed the same transformation, applying a synergistic catalysis strategy to effectively activate both reacting partners individually.<sup>41</sup> Chiral (pybox)lanthanide complexes, such as (pybox)ErCl<sub>3</sub>, are known to activate cyanide towards nucleophilic additions, but fail to effectively promote the conjugate cyanation alone (< 3% yield); this indicates the complex can activate the cyanide, but not imide **108**.

Similarly,  $\mu$ -oxo dimer (salen)Al<sub>2</sub>O is also ineffective as a single catalyst towards the conjugate cyanation (< 3% yield), however, this lack of reactivity is attributed to an unactivated cyanide component. Although alone, neither complex promotes the enantioselective conjugate cyanation, when used together to activate their respective component, the combination promotes a highly efficient and selective reaction (Scheme 27). By using synergistic catalysis, reaction times were reduced, catalyst loadings were lowered, and there was no longer a need to heat less reactive substrates.

## 4. Carbonyl and imine 1,2-Addition

### 4.1 Asymmetric alkynylation of imines via metal acetylides

Among the most straightforward methods for producing enantioenriched propargylic amines, important chiral building blocks, is the addition of a metal acetylide to an imine or iminium ion. In 2005, Chan and coworkers reported the first asymmetric alkynylation of  $\alpha$ -imino esters using chiral copper complexes.<sup>42a</sup> While high enantioselectivities can be obtained for aliphatic alkynes (up to 91% ee), aromatic alkynes resulted in much lower selectivities (up to 74% ee).<sup>42b</sup> Shortly after Chan's report, two synergistic catalysis strategies were introduced for the asymmetric addition of metal acetylides, both aromatic and aliphatic, to imines under chiral Brønsted acid and transition metal catalysis.

The successful merger of transition metal and Brønsted acid catalysis for the asymmetric alkynylation of imines relies on the concurrent propagation and interaction of the two independent catalytic cycles without protonation of the metal acetylide (**113**) (Scheme 28). Imine **110** is protonated by a chiral Brønsted acid to form chiral ion-pair **111**. Independently, terminal acetylene **112** interacts with the metal catalyst to form the activated metal acetylide nucleophile **113**. Combination of the two intermediates delivers the chiral propargylic amine **114** and returns both catalysts to their respective catalytic cycles.

In 2007, Rueping and coworkers successfully implemented this strategy for the alkynylation of  $\alpha$ -imino esters **115** using chiral binol-based phosphoric acid and AgOAc as catalysts (Scheme 29A).<sup>43</sup> Complementing Chan's method, the addition of electron-neutral and electron-rich aromatic acetylenes (**116**) to  $\alpha$ -imino esters **115** provides the propargylic amines **117** in good yields and enantioselectivities (up to 92% ee). The use of AgOAc as the acetylene activator may be key to the success of this synergistic catalytic system. Alkynyl-silver derivatives are known to be stable in protic media, requiring strong acids (e.g. HCl, TfOH) for hydrolysis.<sup>44a</sup> In addition, acetylides activated by AgOAc do not add to non-activated imines, preventing an achiral background reaction.<sup>44b</sup> Although the authors believe this transformation proceeds through the general mechanism outlined above (Scheme 28), they also acknowledge a possible counterion exchange between the silver acetate and chiral phosphoric acid that could generate chiral silver complex **118** (Scheme 29A). To investigate this, experiments were performed with chiral silver-binol complexes and achiral diphenyl hydrogen phosphates; however, these resulted in racemic propargylic amines. This suggests that the Brønsted acid cycle is responsible for the stereoinduction, regardless of the nature of the silver acetylide involved.

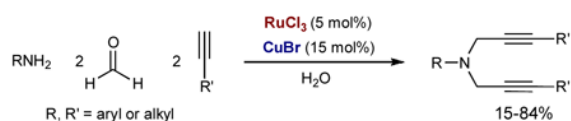
Recently, Arndtsen and coworkers were the second group to report a similar synergistic catalysis protocol for the addition of acetylides to imines (Scheme 29B).<sup>45</sup> Using *N*-Boc-proline as the chiral acid and ligated Cu(MeCN)<sub>2</sub>PF<sub>6</sub> to activate acetylene **119**, enantioenriched propargylic amines **121** are obtained in excellent yields and selectivities (up to 99% ee). Aryl-, vinyl- and alkyl-substituted acetylenes add to aryl- and *tert*-butylimines with little impact on yield or selectivity. While the authors also propose the general mechanism outlined above (Scheme 28), they recognize that an amino acid/copper secondary coordination might also be possible. Mechanistic studies, however, indicate that

the reaction rate has a first-order dependence on *N*-Boc-proline and a zero-order dependence on the copper catalyst. This disparity in reaction order suggests separate roles for the copper and acid catalysts. As the authors point out, an advantage to this protocol is the flexibility and modularity of the catalyst system. Even though the chiral information is held in the *N*-Boc-proline catalyst, the steric bulk located on the copper acetylide (via the ligands) has a significant influence on the enantioselectivity of the reaction. As there are many commercially available  $\alpha$ -amino acids and tertiary phosphines, this catalyst system is easily tuned for any given substrate.

#### 4.2 Racemic addition of metal acetylides to carbonyls and imines

In their efforts toward developing Grignard-like reactions in water, Li and coworkers reported a synergistic bimetallic system for the preparation of racemic propargylic alcohols.<sup>46</sup> Early in the investigation of metal acetylide addition to aldehydes, they observed that when a single transition metal catalyst was used, the acetylenes were consumed while the aldehydes remained unreacted. They speculated that water-tolerant Lewis acids may be needed to activate the carbonyl and this led to their successful  $\text{RuCl}_3/\text{In}(\text{OAc})_3$  bimetallic system (Scheme 30A).  $\text{RuCl}_3$ , reduced in situ to Ru(II), activates the acetylene via oxidative addition of the acetylene C–H bond. The resultant Ru(IV) acetylide **125** adds to the  $\text{In}(\text{OAc})_3$ -activated carbonyl **124** to deliver the desired propargylic alcohol **122**. Under this system, phenylacetylene adds to a broad range of non-enolizable aldehydes in moderate yields.

Li and coworkers quickly extended this synergistic protocol to the preparation of propargylic *N*-aryl amines **123** through a three-component coupling reaction of non-enolizable aldehydes, anilines, and phenylacetylene (via the in situ formation of imine) (Scheme 30B).<sup>47</sup> Although  $\text{In}(\text{OAc})_3$  was the optimal Lewis acid for carbonyl activation, it was ineffective for in situ generated imines. Further investigation revealed  $\text{CuBr}$  as the best imine activator. Using the synergistic combination of  $\text{RuCl}_3$  and  $\text{CuBr}$  in water, propargylic amines **123** are obtained in excellent yields. This powerful synergistic catalyst system has even been extended to a five-component coupling reaction for the formation of dipropargylic amines (Eq 3).<sup>48</sup>



(3)

#### 4.3 Asymmetric hydride transfer to imines

Asymmetric hydrogenation is a powerful technology for the synthesis of chiral compounds. The use of molecular hydrogen is particularly attractive due to its low cost and perfect atom economy. At this time, most asymmetric hydrogenations use precious late transition metal catalysts with specific chiral phosphines to impart stereocontrol.<sup>49</sup> Recently, Beller and coworkers saw an opportunity for synergistic catalysis to provide a different approach to asymmetric hydrogenation of imines using molecular hydrogen. In their strategy, Knölker's complex, a simple achiral iron hydrogenation catalyst, is used in combination with a chiral Brønsted acid to provide enantioenriched secondary amines **127** from corresponding imines **126** (Scheme 31).<sup>50</sup> Knölker's complex (**129**) is a molecularly defined iron complex that possess an iron hydride and an acidic hydrogen, both available for transfer to a polarized  $\pi$ -system.<sup>51</sup> In this synergetic design, imine **126** is protonated by (*S*)-TRIP to form chiral ion-

pair **128**. This intermediate accepts the hydride from Knölker's complex (**129**), producing enantioenriched secondary amine **127**. The acidic hydrogen of Knölker's complex is transferred to the (*S*)-TRIP anion, regenerating the Brønsted acid complex. The resultant 16-electron iron complex **130** coordinates a molecule of hydrogen and induces heterolytic cleavage to regenerate Knölker's complex and complete the iron catalytic cycle. While this transformation is successful for a broad range of both aryl aromatic and aliphatic *N*-aryl ketimines, aromatic ketimines provided noticeably higher selectivities. This is the first example of a highly enantioselective catalytic hydrogenation of imines that uses an achiral metal complex to activate molecular hydrogen.

Along with the asymmetric hydrogenation of imines, synergistic catalysis has also provided a similar strategy for the direct asymmetric reductive amination of ketones. Previously, Xiao and coworkers found that the half-sandwich complex Cp\*Ir(III)-diamine-(*R*)-TRIP (**134**) efficiently reduced *N*-aryl ketimines using hydrogen in high yields and selectivities.<sup>52</sup> When they tried to apply the same system to the reductive amination of aromatic ketones, very little amine product was observed. They reasoned that formation of the ketimine was rate-limiting and adding (*R*)-TRIP as an additional Brønsted acid catalyst may promote imine formation. Pleasingly, the synergistic catalyst combination of (*R*)-TRIP and Cp\*Ir(III)-diamine-(*R*)-TRIP (**134**) was effective in promoting the reductive amination of aromatic methyl ketones **131** and anilines with molecular hydrogen to yield stereogenic amines **132** in excellent yields and selectivities (Scheme 32).<sup>53</sup> It should be noted that the synergistic strategy is only required in the case of aromatic ketones; aliphatic ketones undergo reductive amination in the presence of the iridium catalyst alone.

The mechanism of this transformation begins with the Brønsted acid-catalyzed condensation of ketone **131** and aniline to form the protonated ketimine **133** with a chiral TRIP phosphate counterion. At the same time, iridium complex **134** coordinates a molecule of hydrogen and induces heterolytic cleavage to protonate the TRIP phosphate counterion (returning the free Brønsted acid catalyst) and generate iridium hydride **135**. Iridium hydride **135** transfers a hydride to chiral iminium phosphate **133**, providing enantioenriched secondary amine **132** and regenerating iridium complex **134**.

#### 4.4 Mannich-type addition to imines

In 2005, Hu and coworkers introduced a Rh<sub>2</sub>(OAc)<sub>4</sub>-catalyzed three-component reaction to couple diazoacetates with imines and alcohols.<sup>54</sup> The imine traps a rhodium oxonium ylide intermediate to build racemic β-amino-α-alkoxyesters. In order to suppress undesired side products, the scope was limited to highly electron-deficient imines and imines derived from 2-aminophenol (the phenol functionality activates the imine through an intramolecular hydrogen bond). Through the course of their study, the authors observed that the desired reaction is accelerated by Brønsted acids, presumably through activation of the imine. They reasoned that adding a Brønsted acid catalyst, in conjunction with rhodium, should expand the scope of this reaction to include less activated imines. Furthermore, incorporating a chiral Brønsted acid may lead to an asymmetric three-component reaction.

Implementing this synergistic catalysis strategy, Hu and coworkers found that Rh<sub>2</sub>(OAc)<sub>4</sub> with chiral phosphoric acid catalysts results in a highly efficient and selective coupling of diazoacetate **136** with a variety of imines **137** and benzyl alcohols to yield *syn*-β-amino-α-alkoxyesters **138** in high yields and selectivities (Scheme 33).<sup>55a</sup> Electronically diverse imines can now be used with no apparent impact on yield or selectivity. This protocol was also extended to water as a nucleophile, producing *syn*-β-amino-α-hydroxyesters **139** in good yields and excellent selectivities (Scheme 33).<sup>55b</sup>

This three-component transformation proceeds through the following mechanism (Scheme 34).  $\text{Rh}_2(\text{OAc})_4$  catalyzes the decomposition of diazoacetate **136** to form a rhodium carbenoid **140**. The alcohol nucleophile adds to carbenoid **140** and generates rhodium-bound oxonium ylide **141**. At the same time, imine **137** is protonated by the chiral phosphoric acid catalyst, forming chiral ion-pair **142**. Oxonium ylide **141** undergoes an enantioselective Mannich-type addition to **142**, forming the enantioenriched  $\beta$ -amino- $\alpha$ -alkoxyester. Without sufficient activation of the imine, oxonium ylide **141** may undergo an undesired 1,2-hydride shift to form  $\alpha$ -alkoxyester **143**, dramatically lowering the yield.

Hu and coworkers rationalized that along with activating the imine, the Brønsted acid catalyst might also induce its in situ formation from aldehyde **144** and amine **145**, creating a four-component coupling reaction.<sup>56</sup> This strategy would eliminate the need for prior imine preparation and isolation. The four component reaction proceeds smoothly under very similar conditions leading to high yields and selectivities (Scheme 35). Both electron-poor and electron-rich aromatic aldehydes perform well in the reaction (alkyl aldehydes suffer from low yield and selectivity); however, bulky 9-anthryl alcohol **146** is needed to increase both diastereoand enantioselectivity.

This robust synergistic system of a chiral phosphoric acid and  $\text{Rh}_2(\text{OAc})_4$  is also successful with carbamate nucleophile **147**, generating  $\alpha,\beta$ -diaminoester **148** in high yield and selectivity via the analogous ammonium ylide (Scheme 36).<sup>57</sup> Initially, the more basic diamine products appeared to poison the phosphoric acid catalyst through bidentate coordination. Adding *L*-tartaric acid alleviates this effect by neutralizing the basic diamine product and regenerating the chiral phosphoric acid. Although *L*-tartaric acid is also chiral, the Brønsted acid is the only source of enantiocontrol. Replacing *L*-tartaric acid with the racemic variant delivers the same high level of enantioselectivity, while absence of the chiral phosphoric acid catalyst results in racemic product.

An interesting element of stereocontrol is observed when the substitution of the binol-based phosphoric acid is altered. 3,5-Bis(trifluoromethyl)phenyl substituted binol provides the *syn* product, while changing to the larger triphenylsilyl substituted binol provides the *anti* product. The authors propose that with the 3,5-bis(trifluoromethyl)phenyl substitution, the phosphoric acid may form a bridge between the ammonium ylide and the imine, which leads to the *syn* product (Scheme 36, *syn*-TS). On the other hand, the much larger triphenylsilyl group cannot accommodate both the imine and the ylide and forms an open-chain transition state, leading to the *anti* product (Scheme 36, *anti*-TS).

The activation of imines in synergistic catalysis is not restricted to Brønsted acids. Chiral Lewis acids are traditionally designed to shield either the *Re*- or the *Si*-face of an electrophile, thereby restricting the nucleophile to attack the accessible face. For chiral tertiary anion nucleophiles there is the added challenge of differentiating between the easily interchangeable enantiomers of the pyramidal anion. This can often lead to high enantioselectivity, but little to no diastereoselectivity. However, synergistic activation of both the electrophile and the nucleophile by chiral catalysts can create a diastereomeric pair of activated chiral intermediates, which reduces the task of controlling selectivity to finding a matched set of catalysts.

Using this design strategy for the aza-Henry reaction with tertiary  $\alpha$ -nitroester **149**, Jørgensen and coworkers activated  $\alpha$ -iminoester **150** with chiral bisoxazoline-copper(II) complexes.<sup>58</sup> In order to create a diastereomeric pair of intermediates, the tertiary nitroester was activated by the chiral organic base quinine, creating chiral ammonium ion pair **152** (Scheme 37). Under these conditions, the anionic nucleophile added efficiently and selectively to the activated  $\alpha$ -iminoester providing the aza-Henry adduct **151** in 90% yield,

14:1 dr, and 98% ee. Through optimization and control reactions, Jørgensen and coworkers showed that both catalysts are, in fact, needed for efficiency and they must both be chiral for high enantioselectivity and diastereoselectivity. Absence of either catalyst leads to very little or no reaction (< 5% yield). Substituting the chiral BOX ligand with achiral 1,10-phenanthroline or 2,2'-bipyridine leads to the aza-Henry adduct with good diastereoselectivity (8:1 and 7:1 dr respectively), but no enantioselectivity. On the other hand, achiral Hünig's base, in conjunction with chiral Ph-BOX-Cu(OTf)<sub>2</sub>, leads to poor diastereoselectivity (2:1 dr) but good enantioselectivity (80 and 82% ee). This illustrates the synergistic relationship between the two chiral catalysts to control both the diastereoselectivity and the enantioselectivity.

#### 4.5 Lewis acid and Lewis base catalyzed enantioselective cyanation of carbonyls

In 1993, Corey and Wang reported one of the earliest examples of asymmetric synergistic catalysis.<sup>59</sup> In an effort towards a practical and efficient asymmetric cyanohydrin formation, they developed a dual catalytic system wherein a chiral Lewis acid activates an aldehyde while a chiral Lewis base creates a chiral cyanide nucleophile (Scheme 38). Initial reactions with cyclohexane carboxaldehyde and TMSCN show that 20 mol% of a chiral magnesium cyanobisoxazoline (Mg-BOX) complex delivers the cyanohydrin adduct in 85% yield, but with only moderate selectivity (65% ee). Selectivity dramatically increases (94% ee) when 12 mol% of a chiral Lewis basic bisoxazoline (BOX) is added. It became clear that both catalysts are required for this highly selective reaction as the BOX catalyst used alone results in racemic cyanohydrin adducts. Furthermore, there are clear matched and mismatched catalyst interactions; changing the enantiomer of just one catalyst results in considerably lower enantioselectivity (38% ee with the opposite enantiomer of the BOX catalyst). Mechanistically, the authors reason that adventitious traces of water hydrolyze TMSCN to form small amounts of HCN. The BOX catalyst activates HCN to create the chiral cyanide **154**. The chiral nucleophile forms a diastereomeric pair with the activated aldehyde **155** to react in a highly selective manner. The resulting cyanohydrin reacts with TMSCN to form cyanohydrin TMS ether **153** and generate HCN for another cycle. This transformation is highly selective for aliphatic, non-conjugated aldehydes (90–95% ee), but lower selectivities are observed for aryl- and  $\alpha,\beta$ -unsaturated aldehydes (52–87% ee).

A decade after Corey's report, Feng and coworkers also developed asymmetric Lewis acid/Lewis base catalyzed cyanation of ketones using TMSCN (Scheme 39).<sup>60</sup> In their first published report, a salen-Ti(IV) Lewis acid is combined with dimethylphenyl amine *N*-oxide (**156**) to provide the cyanohydrin adduct in moderate to good yields and selectivity (up to 83% yield, up to 84% ee).<sup>60a,b</sup> Subsequent improvements are observed in both yield and selectivity when the Lewis acid is changed to a salen-Al(III) complex (the Lewis base remains the same); excellent yields and selectivities are now seen for both aliphatic and aromatic ketones (up to 99% yield, up to 94% ee).<sup>60c</sup>

In this system, the Lewis acid activates the ketone via carbonyl coordination to the metal (Scheme 40A). The amine *N*-oxide is believed to activate TMSCN through coordination of the *N*-oxide oxygen to silicon (Scheme 40B) As the intermediates approach each other, the silicon of TMSCN also coordinates the ketone carbonyl, forming an organized transition state (Scheme 40C). The *N*-oxide complex transfers the cyanide to the ketone with concurrent TMS trapping to form the cyanohydrin TMS ether.

## 5 Lewis Base-Catalyzed Cycloadditions and Cyclizations

### 5.1 Hetero [2 + 2] cycloadditions

Inspired by the importance of  $\beta$ -lactams in pharmaceutical science and biochemistry,<sup>61</sup> Lectka and coworkers reported several studies towards the catalytic, asymmetric synthesis

of these important synthons.<sup>62</sup> In their protocol, chiral amine catalysts (generally cinchona alkaloid derivatives) activate acyl chlorides to form ketene-derived zwitterionic enolates that subsequently add to electrophilic imines, a process that is mechanistically distinct from the Staudinger reaction. Although enantioselectivities were excellent (generally >95% ee), the yields were consistently low, ranging from 40–65%. The authors believed the low yields are a result of the zwitterionic enolate being consumed through side reactions before addition to the imine can occur. To address this, they envisaged adding a catalytic Lewis acid to activate the imine and increase the rate of the desired reaction and suppress any side products. They found that adding hard Lewis acidic metals with low azophilicity (e.g. Sc<sup>3+</sup>, Al<sup>3+</sup>, Zn<sup>2+</sup>, In<sup>3+</sup>) leads to a significant increase in yield while maintaining high levels of selectivity. After optimization, the combination of In(OTf)<sub>3</sub> and benzoylquinine emerged as the optimal Lewis acid/Lewis base pair for their synergistic strategy towards the synthesis of β-lactams from acyl chlorides and α-iminoesters (Scheme 41).<sup>63</sup>

Mechanistic studies<sup>64</sup> suggest that the transformation begins with addition of the benzoylquinine to acyl chloride **157**, creating ketene-derived zwitterionic enolate **160**. At the same time, In(OTf)<sub>3</sub> activates α-iminoester **158**, through bidentate coordination, increasing its electrophilicity. Zwitterionic enolate **160** adds to metal-bound imine **161**, furnishing the new carbon-carbon bond. Subsequent transacylation of **162** regenerates both catalysts and releases β-lactam **159** in excellent yield (> 90% yield) and selectivities (>9:1 dr, >95% ee).

Following Lectka's report, similar synergistic systems were developed for the preparation of β-lactones<sup>65</sup> and β-sultones<sup>66</sup> (Scheme 42). Calter and coworkers reported the synthesis of β-lactones **163** from acyl chlorides and benzaldehydes using quinidine trimethylsilyl ether and a Lewis acidic metal triflate (Scheme 42A). The reaction proceeds through a similar mechanism as the β-lactam synthesis, wherein ketene-derived zwitterionic enolates add to Lewis acid-activated aldehydes. For alkyl substituted acyl chlorides, Sc(OTf)<sub>3</sub> provides the best yield and selectivity, while Er(OTf)<sub>3</sub> is optimal with α-oxy acyl chlorides. It should be noted that due to the coordination ability of oxygen, the α-oxy acyl chlorides provide predominately the *cis* product (**163-syn**) while the alkyl substituted acyl chlorides provide predominately *trans* (**163-trans**).

Recently, Peters and Koch also applied this synergistic Lewis acid/Lewis base strategy to the preparation of β-sultones from sulfonyl chlorides and trichloroacetaldehyde (Scheme 42B).<sup>66</sup> Sulfonyl chloride **164** is deprotonated to generate sulfene **167**, which reacts with the quinuclidine catalyst, (DHQ)<sub>2</sub>PYR, to form the zwitterionic nucleophile **168**. Analogous to the previously described mechanism, zwitterion **168** adds to the Lewis acid-activated trichloroacetaldehyde **165** to provide β-sultone **166**.

## 5.2 N-Heterocyclic carbene-catalyzed cyclizations

Just as cinchona alkaloid catalysts are able to create nucleophiles from acyl chlorides, nucleophilic Lewis base catalysts can also render α,β-unsaturated aldehydes or ketones nucleophilic rather than electrophilic. N-Heterocyclic carbenes (NHC), for example, can combine transiently with an α,β-unsaturated aldehyde (or ketone) to generate homoenolate equivalents, which are nucleophilic at the β-position. Scheidt and coworkers used this strategy in a synergistic route to stereogenic γ-lactams **171** (Scheme 43).<sup>67</sup> Treating an α,β-unsaturated aldehyde and an N-acyl hydrazone with a chiral NHC catalyst alone provides the γ-lactam in only moderate yields. Further examination revealed incomplete consumption of the hydrazone, indicating electrophilicity may be the problem. To increase the electrophilicity of the hydrazone, the authors pursued a synergistic strategy and screened a variety of Lewis acidic metal salts. Previously, NHCs have not been used synergistically with Lewis acids, presumably because these species are excellent ligands for late transition metals.<sup>68</sup> Combining the NHC with Mg(*Ot*-Bu)<sub>2</sub>, however, increased both the yield and the



stereoselectivity of the [3 + 2] annulation, leading to a highly efficient reaction. In this catalytic system, chiral azolium precatalyst **175** is deprotonated by 1,5,7-triazabicyclo[4.4.0]dec-5-ene (TBD) to form the active NHC catalyst **176**. NHC **176** adds to  $\alpha,\beta$ -unsaturated aldehyde **170**, forming homoenolate equivalent **173** that is nucleophilic at the  $\beta$ -position. At the same time,  $\text{Mg}(\text{O}t\text{-Bu})_2$  activates hydrazone **170** through bidentate coordination. Transient homoenolate **173** adds to activated hydrazone **172** and subsequent cyclization of **174** furnishes  $\gamma$ -lactam **171** in good yields and stereoselectivities.

## 6 Synergistic Cross-Coupling Reactions

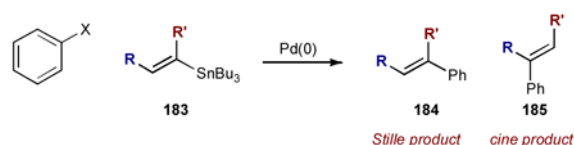
### 6.1 Synergistic catalysis in traditional Pd-catalyzed cross coupling reactions

For several decades, cross-coupling has been considered a cornerstone technology to form carbon-carbon bonds in organic chemistry. It should not be surprising that the earliest examples of synergistic catalysis are found within this realm. The most well known example of synergism in cross coupling is the Sonogashira reaction. This transformation, which couples terminal acetylenes with aryl or vinyl halides, was discovered by Sonogashira, Tohda, and Hagihara in 1975 and is arguably one of the first examples of synergistic catalysis in organic synthesis.<sup>69</sup> Just prior to Sonogashira's report, Cassar along with Dieck and Heck published simultaneous accounts of the same transformation using palladium alone, however, these single catalyst methods generally required high temperatures.<sup>70</sup> Sonogashira and coworkers realized the power of a synergistic strategy and added catalytic copper(I) iodide to initiate a copper-mediated transmetalation of the acetylide to the palladium. The result of this synergistic system is a much milder and robust method for the alkynylation of arenes and alkenes. This transformation is believed to proceed through the two synergistic catalytic cycles described in Scheme 44. The palladium is assumed to participate in a traditional C-C cross coupling mechanism wherein the active Pd(0) complex oxidatively inserts into the Ar-X bond of **177**, generating Pd(II) intermediate **180**. While this is occurring, acetylene **178** is activated by the Cu(I) catalyst to presumably generate transient copper acetylide **181** (possibly through coordination of the Cu(I) and subsequent deprotonation by the amine base). The two catalytic cycles intersect as the intermediates transmetalate to form alkynylpalladium(II) complex **182**, which upon reductive elimination, delivers alkynylated product **179**.

Since Sonogashira's first report in 1975, there have been a vast number of catalyst systems developed for many different substrate types. The scope has moved well beyond the original reported scope of aryl iodides, pyridyl bromides, and vinyl bromides. It now includes, but is not limited to, aryl chlorides and diazonium salts, numerous aromatic and non-aromatic heterocycles, alkynyl halides, vinyl tosylates, and even primary and secondary alkyl bromides (Fig 4).<sup>71</sup> In addition to expanding the substrate scope, considerable work has been devoted towards the development of mild single catalyst systems; however, most Sonogashira reactions still use the synergistic combination of palladium and copper.

Although Stille coupling is generally considered to be a reaction involving one metal catalyst and one stoichiometric metallic reagent, this transformation has also benefitted from synergistic catalysis. Traditional Stille coupling involves the union of aryl or vinyl halides (or triflates) and organostannanes under palladium catalysis. For certain substrates, Stille couplings can prove to be troublesome with low yields and undesired side products. In particular, sterically hindered 1-substituted vinylstannanes **183** had remained a challenging substrate class, often leading to low yields of desired product **184** and/or as a mixture with *cine* type coupling product **185** (Eq 4).<sup>72</sup> To overcome these challenges, copper(I) salts can be added to help promote Stille reactions that will not proceed effectively via palladium catalysis alone.<sup>73</sup> This palladium/copper system was first formally studied by Liebeskind and coworkers; interestingly they found that the role of the copper(I) salt is solvent

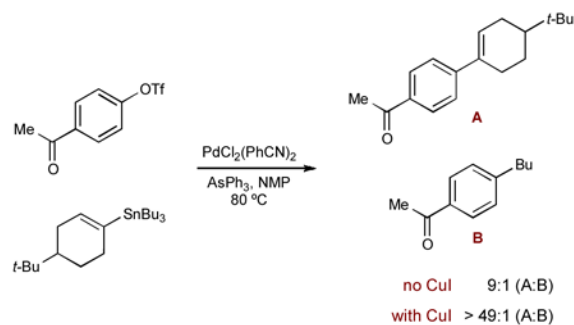
dependent.<sup>73b</sup> In ethereal solvents (such as THF or dioxane), the copper(I) is proposed to scavenge free ligand that otherwise decreases the rate-determining transmetalation step. This role of copper is not within the realm of synergistic catalysis. In polar solvents such as DMF or NMP, however, the copper is believed to transmetalate with the organostannane **186** to produce the more reactive organocopper intermediate **188**; this species enters the palladium catalytic cycle for a second transmetalation with arylpalladium(II) intermediate **187** (Scheme 45). As transmetalation is responsible for the group transfer selectivity of unsymmetrical stannanes, an intermediate transmetalation to copper could be expected to affect the transfer ratio. In their studies of copper catalysis in Stille coupling,



(4)

Liebesskind and coworkers observed a large selectivity increase by the addition of copper(I), lending support to the transmetalation mechanism (Eq 5).<sup>73b</sup>

Both Corey and Baldwin are among the many that have exploited this synergistic relationship to significantly enhance challenging Stille reactions.<sup>74</sup> Corey and coworkers developed a Pd(PPh<sub>3</sub>)<sub>4</sub>/CuCl/LiCl system in DMSO for coupling 1-substituted vinylstannanes **190** with aryl triflate or nonaflates **189** (Scheme 46A), a reaction that generally results in low yields and mixtures of position-isomeric coupling products.<sup>74a</sup> By adding CuCl and LiCl, the resulting styrenyl products **191** are obtained in excellent yields under mild conditions. The authors propose the Sn/Cu transmetalation to generate the more reactive vinylcopper species. It is also believed that LiCl suppresses homocoupling of the vinylstannanes, which otherwise leads to diminished yields.



(5)

Baldwin and coworkers also developed a similar system to enhance difficult Stille couplings, whether the difficulty stems from sterics or electronics. They found that a Pd(PPh<sub>3</sub>)<sub>4</sub>/CuI/CsF system could effectively promote the coupling between aryl iodides or triflates and a wide variety of aryl- and vinylstannanes (including 1-substituted vinylstannanes) (Scheme 46B).<sup>74b</sup> A similar system of PdCl<sub>2</sub>/Pt-Bu<sub>3</sub>/CuI/CsF was also developed for aryl bromides and electron-deficient aryl chlorides. The desired coupling products were obtained in excellent yields under very mild conditions and generally short reaction times. Through optimizing the coupling of 4-iodotoluene (**192**) and 4-(tri-*n*-

butylstannyl)nitrobenzene (**193**), the large positive effect of CuI became clear. Using palladium as a single catalyst, the reaction only provides 2% of coupling product **194**. Adding CuI increases the yield of **194** to 46%, while combining CuI and CsF results in nearly quantitative conversion (98% yield). It should also be noted that both Pd(PPh<sub>3</sub>)<sub>4</sub> and CsF alone fail to promote the reaction efficiently, as does CuI/CsF without palladium. CsF is believed to remove the Bu<sub>3</sub>SnCl byproduct through formation of the insoluble Bu<sub>3</sub>SnF. When used with the copper catalyst, this should help drive the formation of the more reactive organocopper species.

Palladium-catalyzed cyanation of aryl halides offers a practical alternative to the Rosenmund-von Braun reaction, which cyanates aryl halides via stoichiometric CuCN and high reaction temperatures (150–250 °C).<sup>75</sup> Although the palladium-catalyzed variant offers much milder conditions than its predecessor, it experiences the inherent problem that cyanide interferes with the oxidative addition of the aryl halide to palladium(0); this requires minimizing the exposure of palladium(0) to free cyanide. One successful approach is to use stoichiometric metal cyanide complexes of a more covalent nature, such as Zn(CN)<sub>2</sub> and CuCN; unfortunately, this leads to significant amounts of metallic waste. Andersen and coworkers at Eli Lilly and Company found that catalytic amounts of CuI (or ZnI<sub>2</sub>) work synergistically with palladium(0) to promote the same transformation using KCN or NaCN (Scheme 47A).<sup>76</sup> Catalytic copper(I) salts act as a cyanide shuttle between the sparingly soluble alkali-metal cyanide **195** and the arylpalladium(II) intermediate **196**. This shuttle mechanism functions through sequential transmetalations involving the copper catalyst. First, the copper(I) interacts with alkali-metal cyanide **195** to form a substoichiometric amount of copper cyanide **197**. This intermediate transmetalates with arylpalladium(II) **196** (produced via aryl halide oxidative addition to palladium(0)). The resulting cyano(aryl)palladium(II) intermediate **198** reductively eliminates to deliver the benzonitrile product with excellent yields.

Following this report, Yang and Williams at Merck Research Laboratories disclosed a similar synergistic palladium-catalyzed cyanation of aryl halides and triflates, this time using catalytic Bu<sub>3</sub>SnCl as the cyanide shuttle.<sup>77</sup> Prior attempts at using stoichiometric Me<sub>3</sub>SnCN as the cyanide source were ineffective, as rapid reaction between Me<sub>3</sub>SnCN and Pd(0) quickly terminated the catalytic cycle.<sup>78</sup> Through further exploration, the authors found that with very low catalytic loadings, Bu<sub>3</sub>SnCl acts as a highly effective cyanide shuttle between KCN and arylpalladium(II), through a similar mechanism as described above (Scheme 47B). Based on NMR studies, the authors believe that the active cyano species is tin ate complex **199**, formed through the addition of KCN to Bu<sub>3</sub>SnCl without the loss of chloride (Eq 6). This may be the key to the success of this reaction, as ate complex **199** may favor transmetalation with arylpalladium(II), while suppressing deactivation of palladium(0). With this protocol, a wide variety of benzonitriles are produced with just 0.5 mol% Pd<sub>2</sub>(dba)<sub>3</sub> and 0.14 mol% Bu<sub>3</sub>SnCl.



(6)

## 6.2 Synergistic catalysis in non-traditional cross-coupling reactions

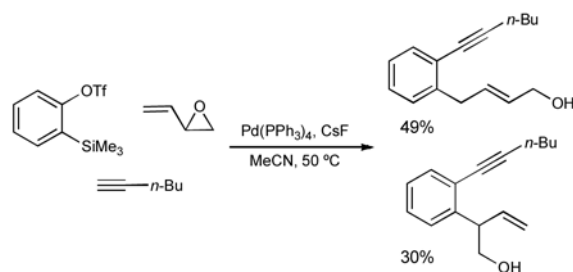
Synergistic catalysis has enabled many cross-coupling reactions that do not fall under the traditional named reactions. For example, palladium-catalyzed coupling reactions involving

transient copper acetylides extend beyond the traditional Sonogashira reaction. Recently, Kang and coworkers at Johnson & Johnson Pharmaceutical Research and Development reported a direct dehydrative coupling of tautomerizable heterocycles with alkynes using synergistic palladium and copper catalysts (Scheme 48).<sup>79</sup> This coupling proceeds via chemoselective activation of C–H and C–OH bonds to achieve carbon-carbon bond formation. This transformation is termed a dehydrative cross-coupling since the substrates together formally lose an equivalent of water to form a carbon-carbon bond. By directly activating C–H and C–OH bonds via synergistic catalysis, the need to prepare carbon-halogen or carbon-metal substrates is eliminated, along with the harmful waste they generate.

This efficient transformation proceeds via a Sonogashira-type coupling mechanism. Before coupling takes place, the C–OH bond of the phenol tautomer of heterocycle **200** is activated by phosphonium **202** to generate pseudo-aryl halide **203**. Phosphonium-activated heterocycle **203** enters the palladium catalytic cycle and oxidatively adds to palladium(0). Resulting palladium(II) phosphonium **204** transmetalates with copper acetylide **205** (generated in the copper catalytic cycle) to produce aryl(alkynyl)palladium(II) intermediate **206**. This species reductively eliminates to deliver alkynylated heterocycle **201**.

While copper acetylides are common intermediates in cross-coupling reactions, Cheng and coworkers show that other organocopper species are also useful in non-traditional cross-couplings. Using benzyne, allylic epoxides, and terminal alkynes, they developed a palladium- and copper-catalyzed three-component coupling reaction to form 1,2-disubstituted arenes **207** (Scheme 49).<sup>80</sup> Using only palladium to catalyze this coupling, the product is isolated as a mixture of regioisomers (Eq 7). During efforts to improve selectivity, the authors found that adding catalytic CuI, in conjunction with the palladium, allows coupling product **207** to be obtained as a single regioisomer.

This coupling is proposed to take place via the synergistic mechanism outlined in Scheme 49. Catalytic CuI activates the acetylene to form copper acetylide **208**. This acetylide undergoes an alkynylcupration with in situ-generated benzyne **209** to generate key arylcopper species **210**. Simultaneously, the allylic epoxide oxidatively adds to palladium(0), forming  $\pi$ -allyl intermediate **211**. At this point, the copper and palladium cycles intersect as arylcopper **210** adds to **211** at the least hindered position, regenerating the copper(I) catalyst and forming palladium-bound 1,2-disubstituted arene **212**. Dissociation of the palladium catalyst delivers desired product **207**.

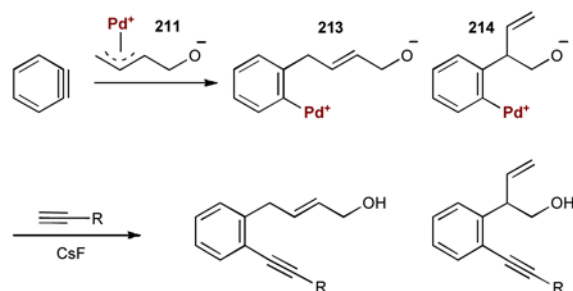


(7)

The enhancement of regioselectivity by CuI is most likely the result of a change in mechanism. When catalyzed by palladium alone, the authors propose an alternate mechanism wherein palladium  $\pi$ -allyl intermediate **211** adds across benzyne to produce a mixture of linear and branched arylpalladium species (**213** and **214**), which subsequently

react with the acetylene (Eq 8).<sup>81</sup> Attack of an unsubstituted benzyne is much less sterically hindered than the 1,2-disubstituted arylcopper intermediate proposed for the dual catalyzed system, which leads to poor regioselectivity.

Copper is not the only metal to be used synergistically with palladium-catalyzed cross-coupling. As an alternative to



(8)

carbonylative coupling, Chang and coworkers developed a palladium- and ruthenium-catalyzed coupling of aryl halides with 2-pyridylmethyl formate (**215**) to form corresponding benzoates **216** (Scheme 50).<sup>82</sup> In previous studies, the authors discovered that  $\text{Ru}_3(\text{CO})_{12}$  catalyzed the decarbonylation of formate **215**, generating the corresponding carbinol and CO, a process driven by coordination of the pyridine nitrogen to ruthenium.<sup>83</sup> The authors hypothesized that the same ruthenium intermediate (**221**), bearing the chelated carbinol and CO, could also be used in a palladium-catalyzed coupling mechanism to generate aryl esters without the need for a CO atmosphere.

The interaction of chelated ruthenium intermediate **221** with palladium-catalyzed coupling proceeds through the intersecting cycles outlined in Scheme 50. The aryl halide oxidatively adds to palladium(0) and the resulting arylpalladium(II) intermediate **220** transmetalates with ruthenium carbinol **221** as CO inserts into the Pd-carbinol bond. The resulting palladium(II) complex **222** reductively eliminates to deliver ester benzoate **216**. The authors were pleased to find that the synergistic combination of  $\text{Ru}_3(\text{CO})_{12}$  and  $\text{PdCl}_2$  successfully coupled 2-pyridylmethyl formate (**215**) with a variety of aryl iodides, as well as vinyl iodides and imidoyl triflates, providing the ester products in excellent yields (**217–219**).

Shortly after their report with 2-pyridylmethyl formate, Chang and workers expanded this concept to similar couplings with *N*-(2-pyridyl)formamide (**223**) and 8-quinolinecarboxaldehyde (**224**) (Scheme 51).<sup>84</sup> Using the same catalytic system, the corresponding benzamides **225** and aryl ketones **226** were also obtained in excellent yields. At this time, it is unclear whether these couplings proceed through ruthenium-catalyzed decarbonylation prior to reacting with the arylpalladium(II) intermediate, or if the key ruthenium intermediate is the five-membered chelate (via insertion into the C-H bond of the formyl group, see **227** and **228**) formed prior to decarboxylation.

## 7 Conclusions and Future Outlook

Although examples of synergistic catalysis have been known for more than 35 years, when thought of as an area of catalysis the concept is still in its infancy. We believe that synergistic catalysis will continue to grow and be recognized as a powerful catalysis strategy. As the examples in this perspective illustrate, the synergistic interaction of two catalytic

cycles brings about several benefits, specifically (i) introducing new, novel reactivity not attainable with a single catalyst; (ii) improving existing reactions, often by suppressing side reactions; (iii) creating or improving stereocontrol through highly organized transition states. Although this concept may be perceived to have inherent problems, such as catalyst compatibility or kinetics involving small concentration of key intermediates, we hope this perspective has illustrated these challenges are easily overcome with the right catalyst combination. For example, Lewis acids and Lewis bases are compatible in synergistic systems when together they form labile complexes, which avoids catalyst quenching.

Currently, the vast majority of synergistic catalysis strategies use systems where at least one catalytic intermediate is formed reversibly and/or is relatively stable. While these strategies are powerful, we believe this is just the beginning and more is possible with respect to this concept. Synergistic catalysis also has the potential to couple many types of irreversibly-formed, fleeting intermediates, as exemplified with Trost and Luan's palladium- and vanadium-catalyzed synthesis of  $\alpha$ -allylated- $\alpha,\beta$ -unsaturated ketones (Section 2.1, Scheme 8).<sup>12</sup> Both reactive intermediates are formed irreversibly, but still find each other and react to form the desired product before either engage in side reactions. As the concept of synergistic catalysis expands, the number of new and novel transformations this strategy provides will continue to grow. This will lead to new bond disconnections and recognized synthons in organic synthesis, expanding our synthetic toolbox. Traditional catalysis changed the way we approach the synthesis of molecules in a laboratory and the concept of synergistic catalysis will continue to increase the power of catalysis.

## Acknowledgments

Financial support was provided by NIHGM (R01 GM078201-05) and kind gifts from Merck, Amgen, Abbott Research Laboratories and Bristol-Myers Squibb.

## Notes and references

1. For reviews on bifunctional catalysis, see: (a) Shibasaki M, Kanai M, Matsunaga S, Kumagai N. *Acc Chem Res.* 2009; 42:1117. [PubMed: 19435320] (b) Breslow R. *J Molec Catal.* 1994; 91:161. (c) Shibasaki M, Yoshikawa N. *Chem Rev.* 2002; 102:2187. [PubMed: 12059266] (d) Wang Y, Deng L, Ojima I. *Catalytic Asymmetric Synthesis* (3). John Wiley & Sons New Jersey 2010:59. (e) Shibasaki M, Kanai M, Mikami K, Lautens M. *New Frontiers in Asymmetric Catalysis*. John Wiley & Sons New Jersey 2007:383.
2. For examples of double activation catalysis, see: (a) Xu H, Zuend SJ, Woll MG, Tao Y, Jacobsen EN. *Science.* 2010; 327:986. [PubMed: 20167783] (b) Rubina M, Conley M, Gevorgyan V. *J Am Chem Soc.* 2006; 128:5818. [PubMed: 16637651] (c) Mukherjee S, List B. *J Am Chem Soc.* 2007; 129:11336. [PubMed: 17715928] (d) Shi Y, Peterson SM, Haberaecker WW III, Blum SA. *J Am Chem Soc.* 2008; 130:2168. [PubMed: 18229930] (e) Park YJ, Park JW, Jun CH. *Acc Chem Res.* 2008; 41:222. [PubMed: 18247521]
3. For examples of cascade catalysis, see: (a) Belot S, Vogt KA, Besnard C, Krause N, Alexakis A. *Angew Chem Int Ed.* 2009; 48:8923. (b) Han ZY, Xiao H, Chen XH, Gong LZ. *J Am Chem Soc.* 2009; 131:9182. [PubMed: 19518048] (c) Sorimachi K, Terada M. *J Am Chem Soc.* 2008; 130:14452. [PubMed: 18850704] (d) Cai Q, Zhao ZA, You SL. *Angew Chem Int Ed.* 2009; 48:7428. (e) Simmons B, Walji AM, MacMillan DWC. *J Am Chem Soc.* 2009; 48:4349. (f) Lathrop SP, Rovis T. *J Am Chem Soc.* 2009; 131:13628. [PubMed: 19731910]
4. Strater N, Lipscomb WN, Klabunde T, Krebs B. *Angew Chem Int Ed.* 1996; 35:2024.
5. (a) Brown KA, Kraut J. *Faraday Discuss.* 1992; 93:217. [PubMed: 1290933] (b) Polshakov VI. *Russ Chem Bull, Int Ed.* 2001; 50:1733.
6. (a) Pearson RG. *J Am Chem Soc.* 1963; 85:3533. (b) Woodward S. *Tetrahedron.* 2002; 58:1017.

7. (a) Tsuji J, Takahashi H, Morikawa M. *Tetrahedron Lett.* 1965; 6:4387.(b) Trost BM, Fullerton TJ. *J Am Chem Soc.* 1973; 95:292. For a review on transition metal-catalyzed asymmetric allylic alkylations, see: (c) Trost BM, Van Vranken DL. *Chem Rev.* 1996; 96:395. [PubMed: 11848758]
8. Sawamura M, Sudoh M, Ito Y. *J Am Chem Soc.* 1996; 118:3309.
9. Ibrahim I, Córdova A. *Angew Chem Int Ed.* 2006; 45:1952.
10. Zhao X, Liu D, Xie F, Liu Y, Zhang W. *Org Biomol Chem.* 2011; 9:1871. [PubMed: 21283877]
11. (a) Nakoji M, Kanayama T, Okino T, Takemoto Y. *Org Lett.* 2001; 3:3329. [PubMed: 11594826] (b) Nakoji M, Kanayama T, Okino T, Takemoto Y. *J Org Chem.* 2002; 67:7418. [PubMed: 12375973] Another report of a phase-transfer- and palladium-catalyzed allylic alkylation of glycine iminoesters was reported just prior to the work of Takemoto and coworkers, however, significantly lower selectivities were observed, see: (c) Chen G, Deng Y, Gong L, Mi A, Cui X, Jiang Y, Choi MCK, Chan ASC. *Tetrahedron: Asymmetry.* 2001; 12:1567.
12. (a) Trost BM, Luan X. *J Am Chem Soc.* 2011; 133:1706. [PubMed: 21244050] (b) Trost BM, Luan X, Miller Y. *J Am Chem Soc.* 2011; 133:12824. [PubMed: 21714524]
13. Trost BM, Oi S. *J Am Chem Soc.* 2001; 123:1230. [PubMed: 11456678]
14. Mukherjee S, Yang JW, Hoffmann S, List B. *Chem Rev.* 2007; 107:5471. [PubMed: 18072803]
15. Ding Q, Wu J. *Org Lett.* 2007; 9:4959. [PubMed: 17960938]
16. Allen AE, MacMillan DWC. *J Am Chem Soc.* 2010; 132:4986. [PubMed: 20297822]
17. (a) Eisenberger P, Gischig S, Togni A. *Chem-Eur J.* 2006; 12:2579. [PubMed: 16402401] (b) KIELTSCH I, Eisenberger P, Togni A. *Angew Chem Int Ed.* 2007; 46:754.(c) Eisenberger P, KIELTSCH I, Armanino N, Togni A. *Chem Commun.* 2008:1575.(d) KIELTSCH I, Eisenberger P, Stanek K, Togni A. *Chemia.* 2008; 62:260.(e) Koller R, Stanek K, Stolz D, Aardoom R, Niedermann K, Togni A. *Angew Chem Int Ed.* 2009; 48:4332.
18. (a) Ikeda M, Miyake Y, Nishibayashi Y. *Angew Chem Int Ed.* 2010; 49:7289.(b) Yoshida A, Ikeda M, Hattori G, Miyake Y, Nishibayashi Y. *Org Lett.* 2011; 13:592. [PubMed: 21222439]
19. (a) Motoyama K, Ikeda M, Miyake Y, Nishibayashi Y. *Eur J Org Chem.* 2011:2239. Shortly after Nishibayashi's report, Cozzi and coworkers published a very similar account with slightly higher diastereomeric ratios. They also previously demonstrated this amine/ $\text{InBr}_3$  strategy is successful for the  $\alpha$ -allylic alkylation of aldehydes using allyl alcohols, see: (b) Sinisi R, Vita MV, Gualandi A, Emer E, Cozzi PG. *Chem Eur J.* 17:7404.(c) Capdevila MG, Befatti F, Zoli L, Stenta M, Cozzi PG. *Chem Eur J.* 2010; 16:11237. [PubMed: 20721994]
20. Sibi MP, Hasegawa M. *J Am Chem Soc.* 2007; 129:4124. [PubMed: 17362013]
21. (a) Van Humbeck JF, Simonovich SP, Knowles RR, MacMillan DWC. *J Am Chem Soc.* 2010; 132:10012. [PubMed: 20608675] (b) Simonovich SP, Van Humbeck JF, MacMillan DWC. *Chem Sci.* 201110.1039/C1SC00556A
22. Allen AE, MacMillan DWC. *J Am Chem Soc.* 2011; 133:4260. [PubMed: 21388207]
23. Lockhart TP. *J Am Chem Soc.* 1983; 105:1940.(b) The MacMillan group has performed mechanistic studies that provide evidence to support this mechanism. Results of this study are forthcoming.
24. (a) Conrad JC, Kong J, Laforteza BN, MacMillan DWC. *J Am Chem Soc.* 2009; 131:11640. [PubMed: 19639997] (b) Alemán J, Cabrera S, Maerten E, Overgaard J, Jørgensen KA. *Angew Chem Int Ed.* 2007; 46:5520.
25. For a review on photoredox catalysis, see: Narayanam JMR, Stephenson CRJ. *Chem Soc Rev.* 2011; 40:102. [PubMed: 20532341]
26. For selected carbonyl  $\alpha$ -alkylation examples, see: (a) Ooi T, Maruoka K. *Angew Chem Int Ed.* 2007; 46:4222.(b) Imai M, Hagihara A, Kawasaki H, Manabe K, Koga K. *J Am Chem Soc.* 1994; 116:8829.(c) Doyle AG, Jacobsen EN. *J Am Chem Soc.* 2005; 127:62. [PubMed: 15631449] (d) Dai X, Strotman NA, Fu GC. *J Am Chem Soc.* 2008; 130:3302. [PubMed: 18302392]
27. Intramolecular organocatalytic asymmetric  $\alpha$ -alkylation of aldehydes using alkyl iodides has been accomplished for specific substrate scopes, see: (a) Vignola N, List B. *J Am Chem Soc.* 2004; 126:450. [PubMed: 14719926] (b) Enders D, Wang C, Bats JW. *Angew Chem Int Ed.* 2008; 47:7539.
28. Nicewicz DA, MacMillan DWC. *Science.* 2008; 322:77. [PubMed: 18772399]

29. For references on the reductive cleavage of alkyl halides using photoredox catalysis, see: Fukuzumi S, Mochizuki S, Tanaka T. *J Phys Chem.* 1990; 94:722.
30. Nagib DA, Scott ME, MacMillan DWC. *J Am Chem Soc.* 2009; 131:10875. [PubMed: 19722670]
31. Shih H-W, Vander Wal MN, Grange RL, MacMillan DWC. *J Am Chem Soc.* 2010; 132:13600. [PubMed: 20831195]
32. (a) Shaikh RR, Mazzanti A, Petrini M, Bartoli G, Melchiorre P. *Angew Chem Int Ed.* 2008; 47:8707.(b) Cozzi PG, Benfatti F, Zoli L. *Angew Chem Int Ed.* 2009; 48:1313.(c) Brown AR, Kuo WH, Jacobsen EN. *J Am Chem Soc.* 2010; 132:9286. [PubMed: 20568761]
33. Neumann M, Fuldner S, König B, Zeitler K. *Angew Chem Int Ed.* 2011; 50:951.
34. (a) Sud A, Sureshkumar D, Klussmann M. *Chem Commun.* 2009:3169.(b) Rueping M, Vila C, Koenigs RM, Poschary K, Fabry DC. *Chem Commun.* 2011; 47:2360.
35. Rahaman H, Madarász Á, Pápai I, Pihko PM. *Angew Chem Int Ed.* 2011; 50:6123.
36. Ibrahem I, Santoro S, Himo F, Córdova A. *Adv Synth Catal.* 2011; 353:245.
37. Bergonzini G, Vera S, Melchiorre P. *Angew Chem Int Ed.* 2010; 49:9685.
38. Rios R, Sundén H, Ibrahem I, Córdova A. *Tetrahedron Lett.* 2007; 48:2181.
39. Xia A-B, Xu D-Q, Luo S-P, Jiang J-R, Tang J, Wang Y-F, Xu Z-Y. *Chem Eur J.* 2010; 16:801. [PubMed: 19946910]
40. Sammis GM, Jacobsen EN. *J Am Chem Soc.* 2003; 125:4442. [PubMed: 12683813]
41. Sammis GM, Danjo H, Jacobsen EN. *J Am Chem Soc.* 2004; 126:9928. [PubMed: 15303860]
42. (a) Ji JX, Wu J, Chan ASC. *Proc Natl Acad Sci U S A.* 2005; 102:11196. [PubMed: 16061808] (b) Shao ZH, Wang J, Ding K, Chan ASC. *Adv Synth Catal.* 2007; 349:2375.
43. Rueping M, Antonchick AP, Brinkmann C. *Angew Chem Int Ed.* 2007; 47:6903.
44. (a) Halbes-Letinois U, Weibel JM, Pale P. *Chem Soc Rev.* 2007; 36:759. [PubMed: 17471400] (b) Ji JX, Au-Yeung TTL, Wu J, Yip CW, Chan ASC. *Adv Synth Catal.* 2004; 346:42.
45. Lu Y, Johnstone TC, Arndtsen BA. *J Am Chem Soc.* 2009; 131:11284. [PubMed: 19630398]
46. Wei C, Li C-J. *Green Chemistry.* 2002; 4:39.
47. Li C-J, Wei C. *Chem Commun.* 2002:268.
48. Bonfield ER, Li C-J. *Org Biomol Chem.* 2007; 5:435. [PubMed: 17252122]
49. For reviews of asymmetric hydrogenations, see: (a) Xie JH, Zhu SF, Zhou QL. *Chem Rev.* 2011; 111:1713. [PubMed: 21166392] (b) Tang W, Zhang X. *Chem Rev.* 2003; 103:3029. [PubMed: 12914491]
50. Zhou S, Fleischer S, Junge K, Beller M. *Angew Chem Int Ed.* 2011; 50:5120.
51. For the isolation of Knölker's complex, see: Knölker H-J, Baum E, Goesmann H, Klauss R. *Angew Chem Int Ed.* 1999; 38:2064. For its development as a hydrogenation catalyst, see: Casey CP, Guan H. *J Am Chem Soc.* 2007; 129:5816. [PubMed: 17439131]
52. Li C, Wang C, Villa-Marcos B, Xiao J. *J Am Chem Soc.* 2008; 130:14450. [PubMed: 18839940]
53. Li C, Villa-Marcos B, Xiao J. *J Am Chem Soc.* 2009; 131:6967. [PubMed: 19402701]
54. (a) Lu CD, Liu H, Chen ZY, Hu WH, Mi AQ. *Org Lett.* 2005; 7:83. [PubMed: 15624983] (b) Huang H, Guo X, Hu W. *Angew Chem Int Ed.* 2007; 46:1337. For the three-component reaction of diazoacetates, imines, and anilines, see: (c) Wang Y, Zhu Y, Chen Z, Mi A, Hu W, Doyle MP. *Org Lett.* 2003; 5:3923. [PubMed: 14535744]
55. (a) Hu W, Xu X, Zhou J, Liu WJ, Huang H, Hu J, Yang L, Gong LZ. *J Am Chem Soc.* 2008; 130:7782. [PubMed: 18512907] (b) Qian Y, Jing C, Shi T, Ji J, Tang M, Zhou J, Zhai C, Hu W. *ChemCatChem.* 2011; 3:653.
56. Xu X, Zhou J, Yang L, Hu W. *Chem Commun.* 2008:6564.
57. Jiang J, Xu H-D, Xi J-B, Ren B-Y, Lv F-P, Guo X, Jiang L-Q, Zhang Z-Y, Hu W-H. *J Am Chem Soc.* 2011; 133:8428. [PubMed: 21553930]
58. Knudsen KR, Jørgensen KA. *Org Biomol Chem.* 2005; 3:1362. [PubMed: 15827627]
59. Corey EJ, Wang Z. *Tetrahedron Lett.* 1993; 34:4001.
60. (a) Chen FX, Feng X, Qin B, Zhang G, Jiang Y. *Org Lett.* 2003; 5:949. [PubMed: 12633113] (b) Chen FX, Qin B, Feng X, Zhang G, Jiang Y. *Tetrahedron.* 2004; 60:10449.(c) Chen FX, Zhou H, Liu X, Qin B, Feng X, Zhang G, Jiang Y. *Chem Eur J.* 2004; 10:4790. [PubMed: 15372678]



61. Alcaide B, Almendros P, Aragoncillo C. *Chem Rev.* 2007; 107:4437. [PubMed: 17649981]
62. (a) Taggi AE, Wack H, Hafez AM, France S, Lectka T. *Org Lett.* 2002; 4:627. [PubMed: 11843608] (b) Dudding T, Hafez AM, Taggi AE, Wagerle TR, Lectka T. *Org Lett.* 2002; 4:387. [PubMed: 11820886] (c) Hafez AM, Taggi AE, Dudding T, Lectka T. *J Am Chem Soc.* 2001; 123:10853. [PubMed: 11686686] (d) Hafez AM, Taggi AE, Wack H, Drury WJ III, Lectka T. *Org. Lett.* 2000; 2:3963. [PubMed: 11112618] (e) Taggi AE, Hafez AM, Wack H, Young B, Drury WJ III, Lectka T. *J Am Chem Soc.* 2000; 122:7831.
63. France S, Wack H, Hafez AM, Taggi AE, Watsil DR, Lectka T. *Org Lett.* 2002; 4:1603. [PubMed: 11975639]
64. France S, Shah MH, Weatherwax A, Wack H, Roth JP, Lectka T. *J Am Chem Soc.* 2005; 127:1206. [PubMed: 15669860]
65. Calter MA, Tretyak OA, Flaschenriem C. *Org Lett.* 2005; 7:1809. [PubMed: 15844912]
66. Koch FM, Peters R. *Angew Chem Int Ed.* 2007; 46:2685.
67. Raup DEA, Cardinal-David B, Holte D, Scheidt KA. *Nature Chem.* 2010; 2:766. [PubMed: 20729898]
68. (a) Burgess K, Perry MC. *Tetrahedron: Asymmetry.* 2003; 14:951.(b) Lin JCY, Huang RTW, Lee CS, Bhattacharyya A, Hwang WS, Lin IJ. *Chem Rev.* 2009; 109:3561. [PubMed: 19361198] (c) Glorius, FE. *N-Heterocyclic Carbenes in Transition Metal Catalysis.* Springer-Verlag; Berlin Heidelberg: 2010.
69. Sonogashira K, Tohda Y, Hagihara N. *Tetrahedron Lett.* 1975; 16:4467.
70. (a) Cassar L. *J Organomet Chem.* 1975; 93:253.(b) Dieck H, Heck F. *J Organomet Chem.* 1975; 93:259.
71. For reviews on Sonogashira coupling, see: (a) Sonogashira K. *J Organomet Chem.* 2002; 653:46. (b) Chinchilla R, Nájera C. *Chem Rev.* 2007; 107:874. [PubMed: 17305399] (c) Doucet H, Hierso JC. *Angew Chem Int Ed.* 2007; 46:834.(d) Heravi MM, Sadjadi S. *Tetrahedron.* 2009; 65:7761.(e) Chinchilla R, Nájera C. *Chem Soc Rev.* 201110.1039/c1cs15071e
72. For a review on Stille coupling, see: Farina V, Krishnamurthy V, Scott WJ. *Org React.* 1997; 50:1.
73. (a) Liebeskind LS, Fengl RW. *J Org Chem.* 1990; 55:5359.(b) Farina V, Kapadia S, Krishnan B, Wang C, Liebeskind LS. *J Org Chem.* 1994; 59:5905. Marino and Long had previously documented using PdCl<sub>2</sub>(PPh<sub>3</sub>)<sub>2</sub> and CuI to couple a vinylstannane and a vinyl tosylate in a footnote, but never elaborated on this finding, see: (c) Marino JP, Long JK. *J Am Chem Soc.* 1988; 110:7916.
74. (a) Han X, Stoltz BM, Corey EJ. *J Am Chem Soc.* 1999; 121:7600.(b) Mee SPH, Lee V, Baldwin JE. *Angew Chem Int Ed.* 2004; 43:1132.
75. For a recent review on palladium-catalyzed cyanation of aryl halides, see: Anbarasan P, Schareina T, Beller M. *Chem Soc Rev.* 201110.1039/c1cs15004a
76. Anderson BA, Bell EC, Ginah FO, Harn NK, Pagh LM, Wepsiec JP. *J Org Chem.* 1998; 63:8224.
77. Yang C, Williams JM. *Org Lett.* 2004; 6:2837. [PubMed: 15330627]
78. (a) Kingsbury WD, Boehm JC, Jakas DR, Holden KG, Hecht SM, Gallagher G, Caranga MJ, McCabe FL, Faucette LF, Johnson RK, Hertzberg RP. *J Med Chem.* 1991; 34:98. [PubMed: 1846923] (b) Nagamura S, Kobayashi E, Gomi K, Saito H. *Bioorg, Med Chem.* 1996; 4:1379. [PubMed: 8879561]
79. Kang FA, Lanter JC, Cai C, Sui Z, Murray WV. *Chem Commun.* 2010; 46:1347.
80. Jeganmohan M, Bhuvaneswari S, Cheng C-H. *Angew Chem Int Ed.* 2009; 48:391.
81. This mechanism was proposed for a very similar palladium-catalyzed three-component coupling reaction of benzyne, allyl chlorides, alkynylstannanes see: Jeganmohan M, Cheng C-H. *Org Lett.* 6:2821. [PubMed: 15281778]
82. Ko S, Lee C, Choi M-G, Na Y, Chang S. *J Org Chem.* 2003; 68:1607. [PubMed: 12585917]
83. Ko S, Na Y, Chang S. *J Am Chem Soc.* 2002; 124:750. [PubMed: 11817940]
84. (a) Ko S, Han H, Chang S. *Org Lett.* 2003; 5:2687. [PubMed: 12868890] (b) Ko S, Kang B, Chang S. *Angew Chem Int Ed.* 2005; 44:455.

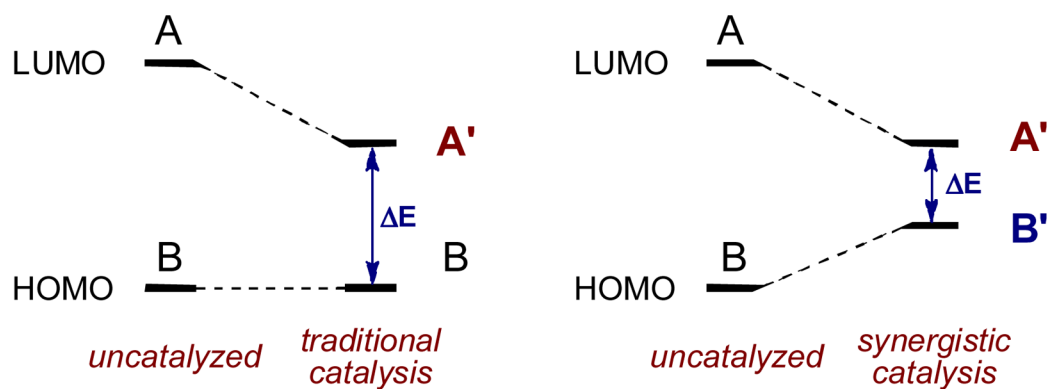
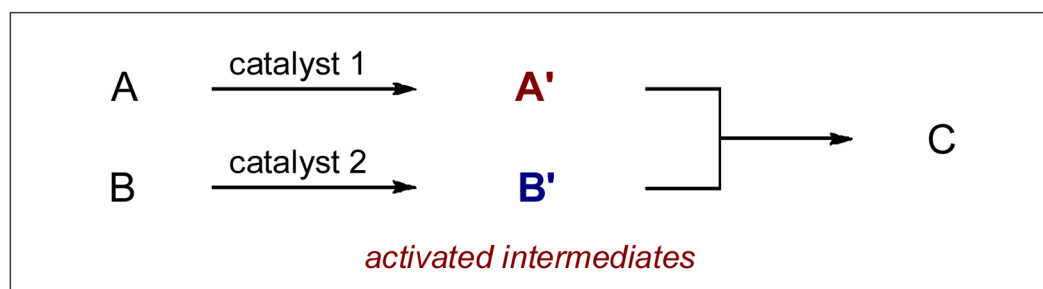
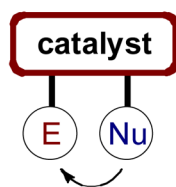
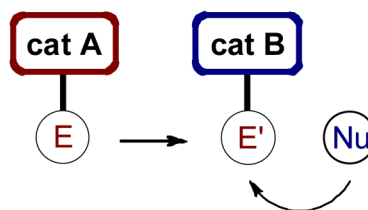


**Fig. 1.**  
The concept of synergistic catalysis.

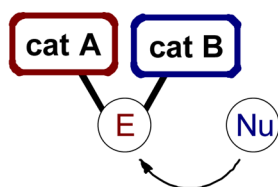
(A) Bifunctional Catalysis



(C) Cascade Catalysis



(B) Double Activation Catalysis



(D) Synergistic Catalysis

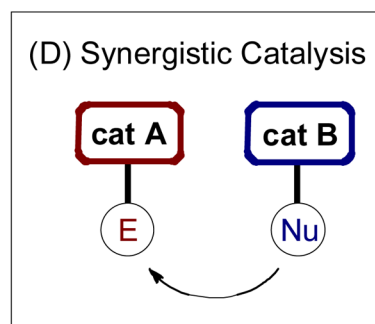


**Fig. 2.**  
Classification of catalytic systems involving two catalysts.

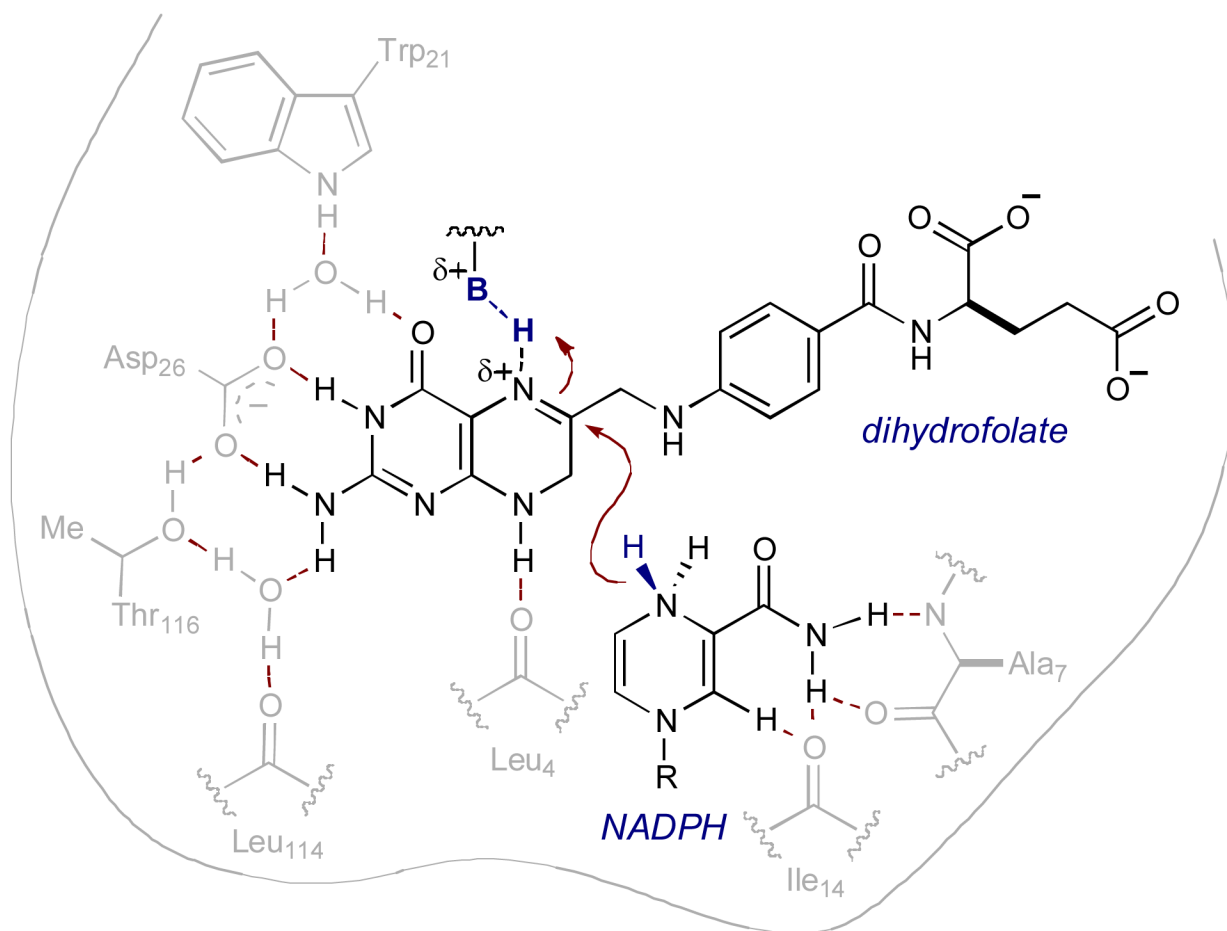


**Fig. 3.**  
Synergistic catalysis in dihydrofolate reductase.

### Total Number of Publications in Asymmetric Synergistic Catalysis (Jan 1993 - May 2011)

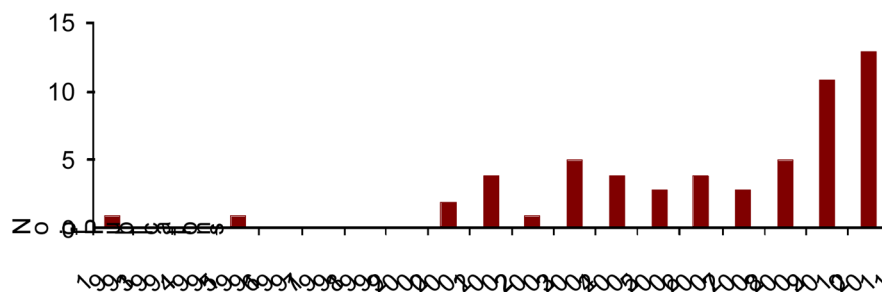


**Fig. 4.** The total number of publications describing asymmetric synergistic catalysis from January 1993 to May 2011.

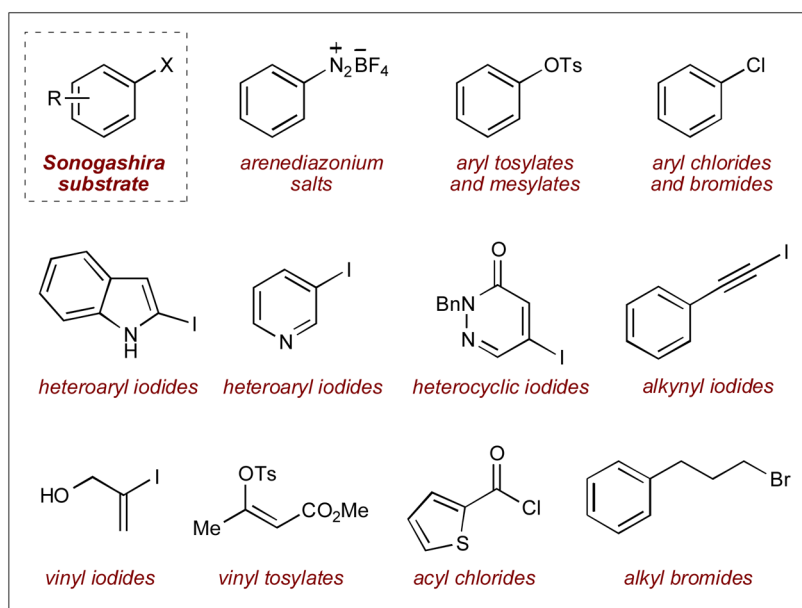
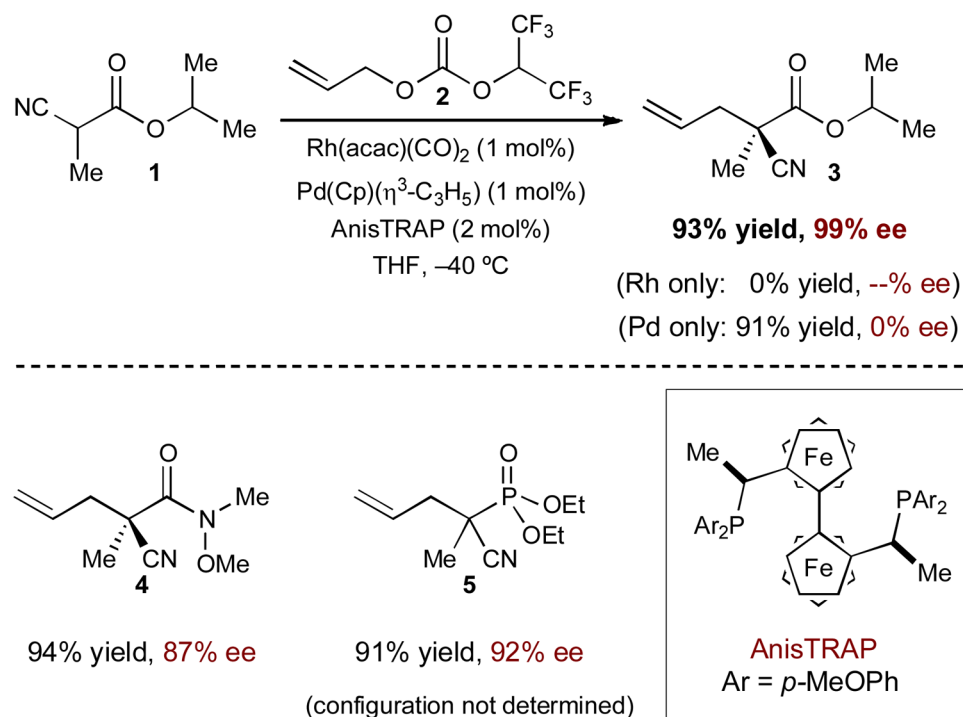
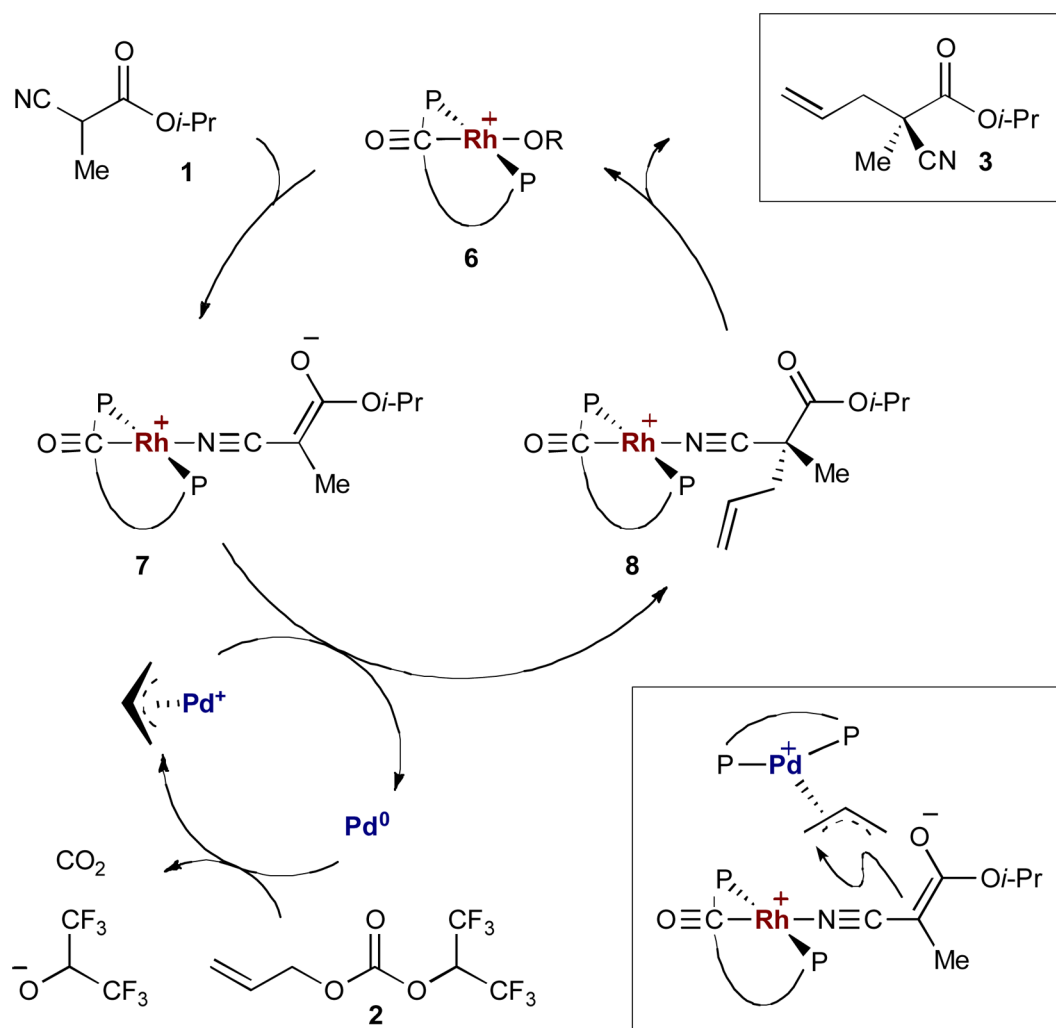


**Fig. 5.** Examples of Sonogashira substrates that undergo alkylation using synergistic palladium- and copper-catalysis.<sup>71</sup>

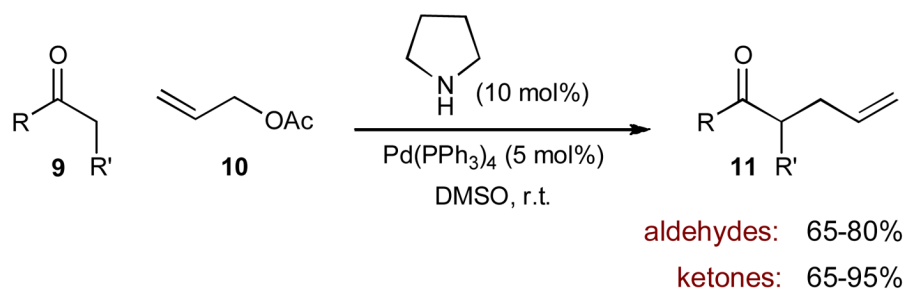


**Scheme 1.**  
 Rhodium- and palladium-catalyzed enantioselective allylic alkylation of  $\alpha$ -cyano carbonyls.

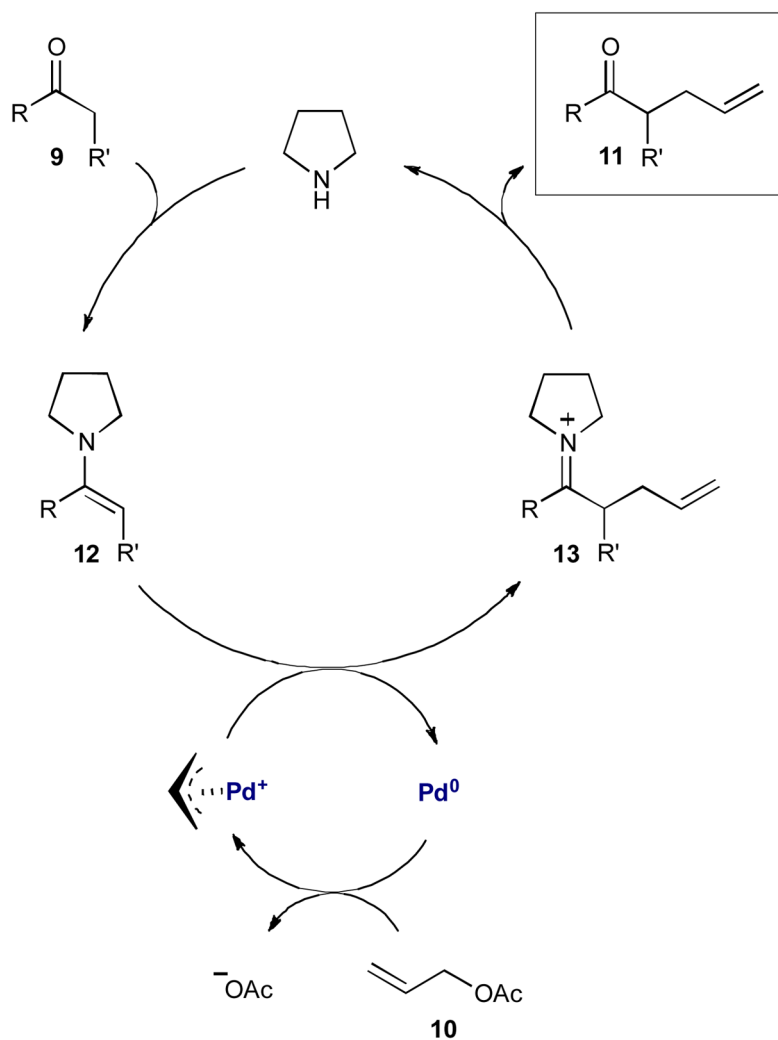


**Scheme 2.**  
Mechanism of the rhodium- and palladium-catalyzed allylic alkylation of  $\alpha$ -cyano carbonyls.

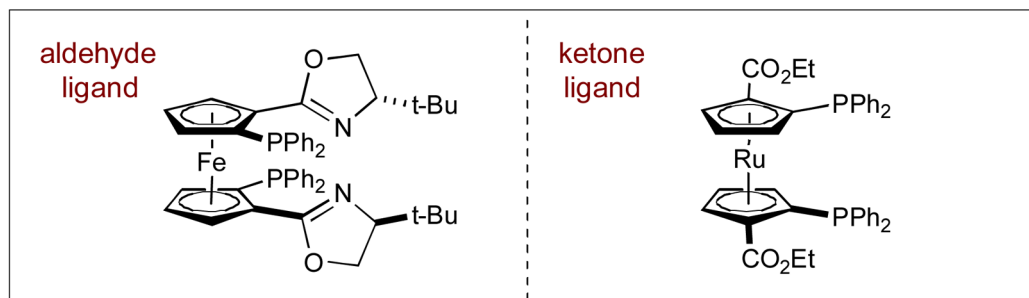
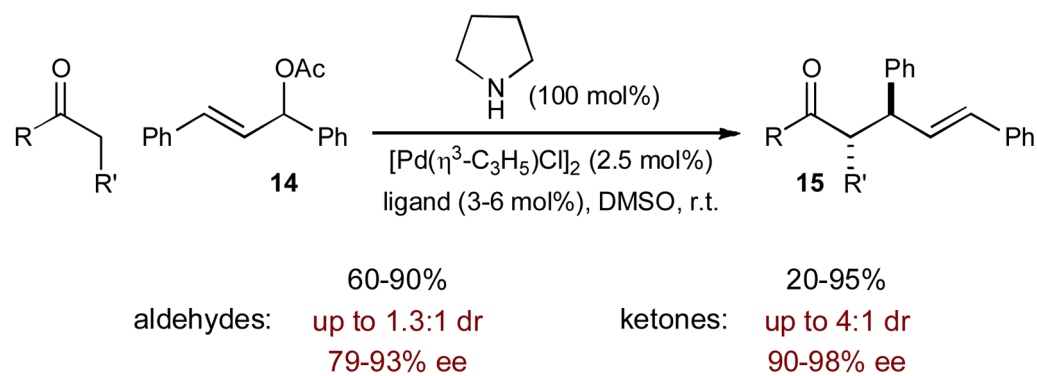


**Scheme 3.**

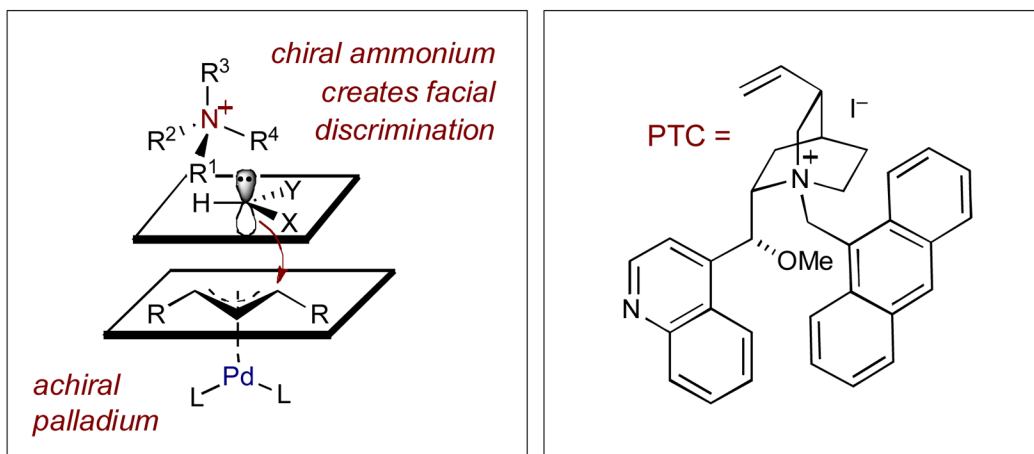
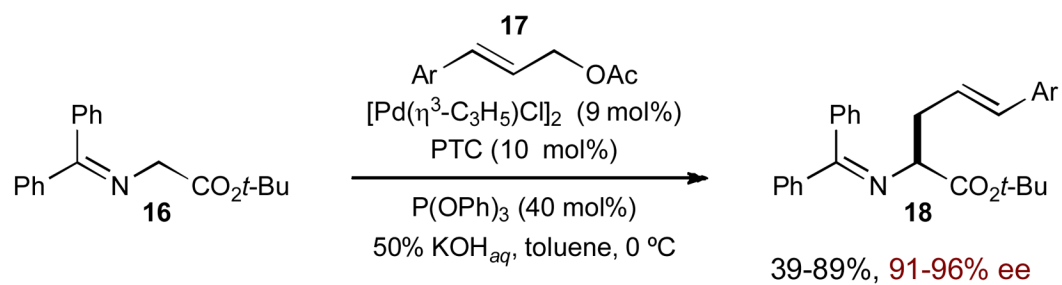
Córdova's direct  $\alpha$ -allylation of unactivated aldehydes and ketones via enamine and palladium  $\pi$ -allyl intermediates.



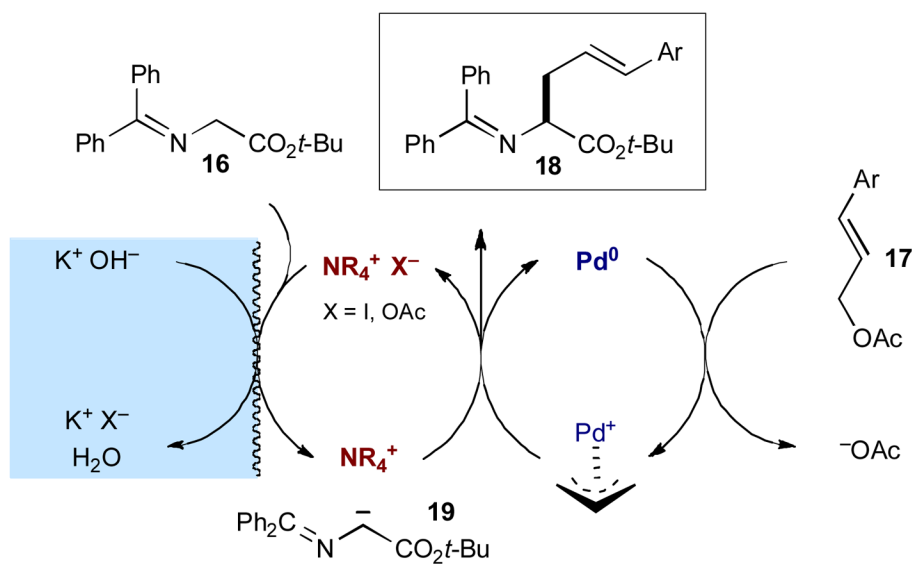
**Scheme 4.** Mechanism of the enantioselective  $\alpha$ -allylation of aldehydes and ketones via enamine and palladium  $\pi$ -allyl intermediates.

**Scheme 5.**

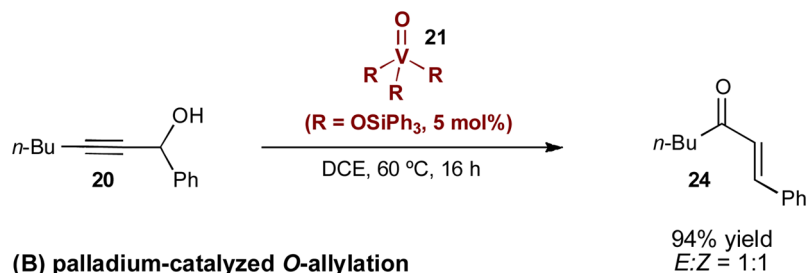
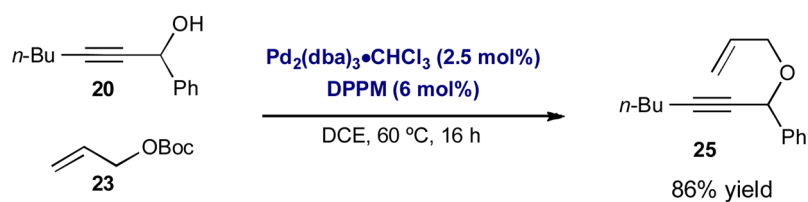
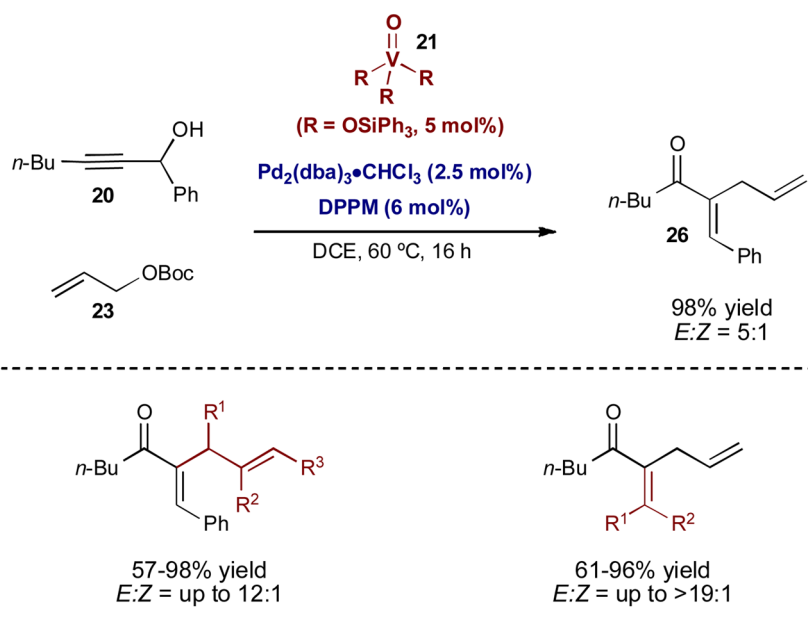
An enantioselective  $\alpha$ -allylation of aldehydes and ketones via enamine and palladium  $\pi$ -allyl intermediates.

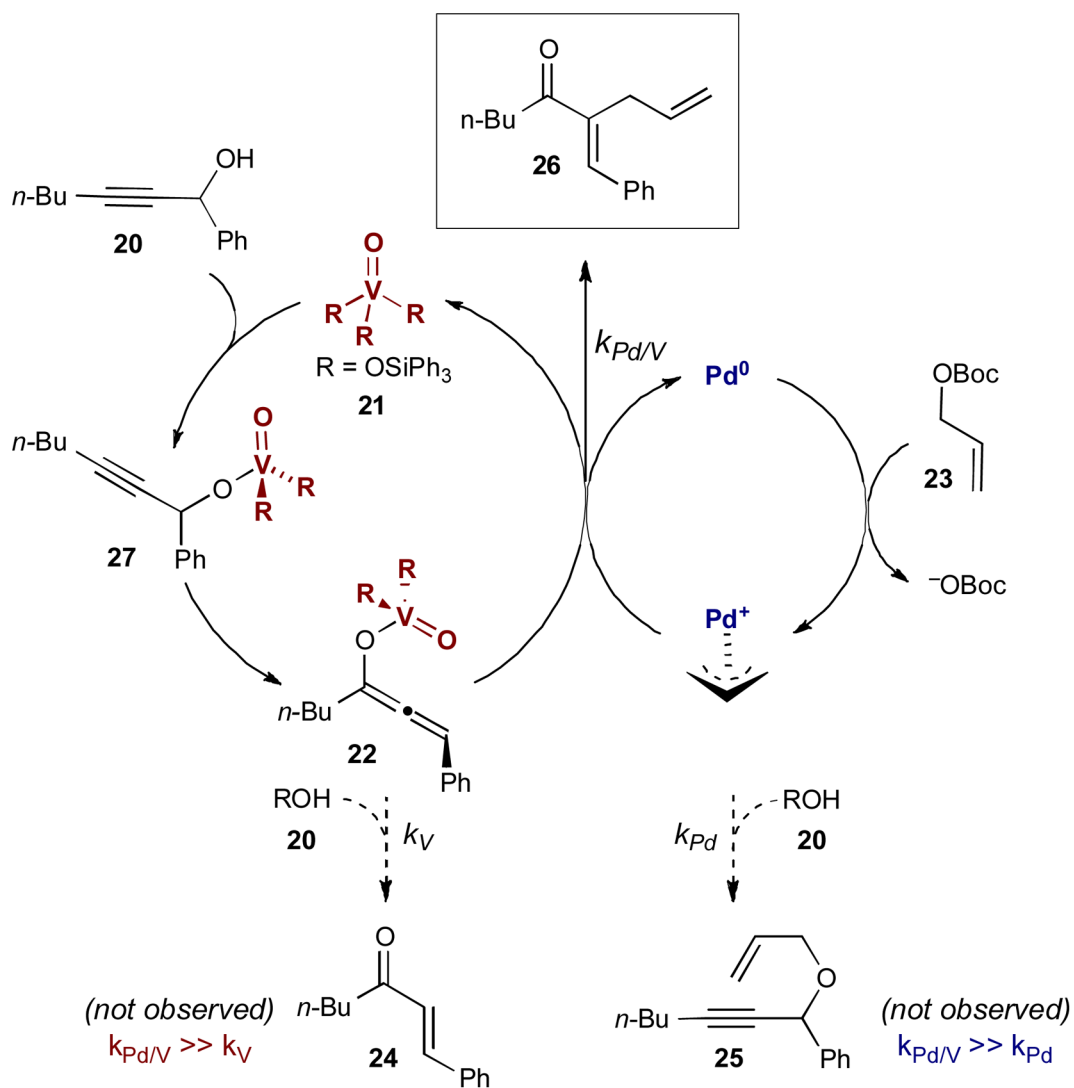


**Scheme 6.**  
Takemoto's  $\alpha$ -allylic alkylation of glycine imino esters.

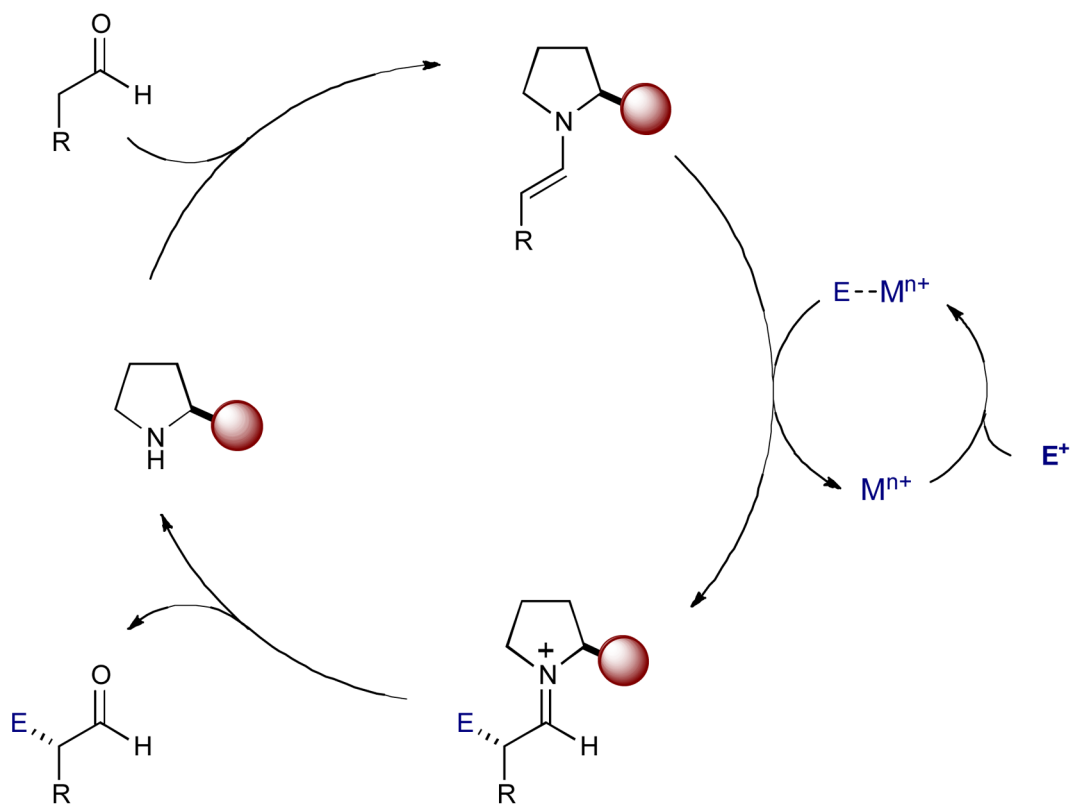


**Scheme 7.**  
 $\alpha$ -Allylic alkylation of glycine imino esters via phase transfer and palladium catalysis.

**(A) vanadium-catalyzed 1,3-transposition of propargyl alcohols****(B) palladium-catalyzed O-allylation****(C) palladium- and vanadium-catalyzed generation of  $\alpha$ -allyl enones****Scheme 8.**Trost's palladium- and vanadium-catalyzed synthesis of  $\alpha$ -allyl- $\alpha,\beta$ -unsaturated ketones.

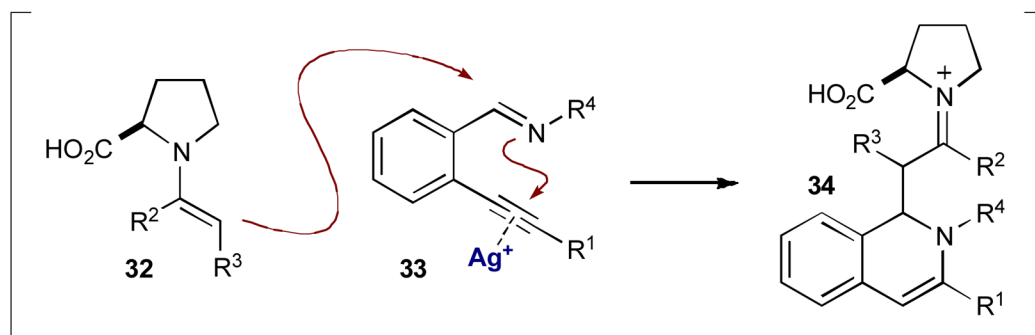
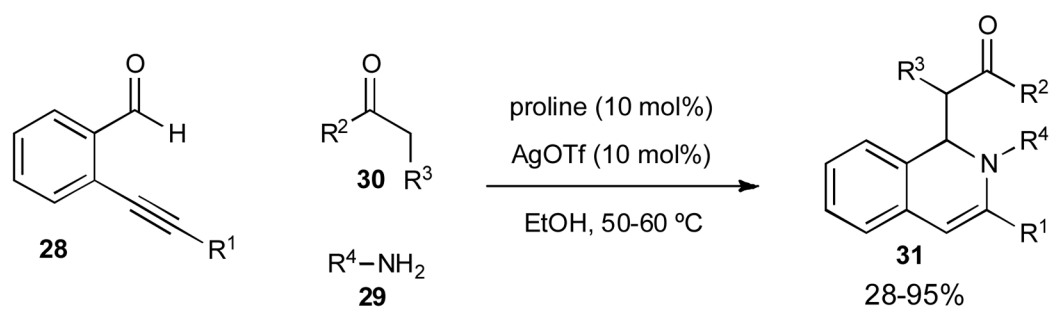


**Scheme 9.**  
Mechanism of the palladium- and vanadium-catalyzed  $\alpha$ -allyl enone formation.

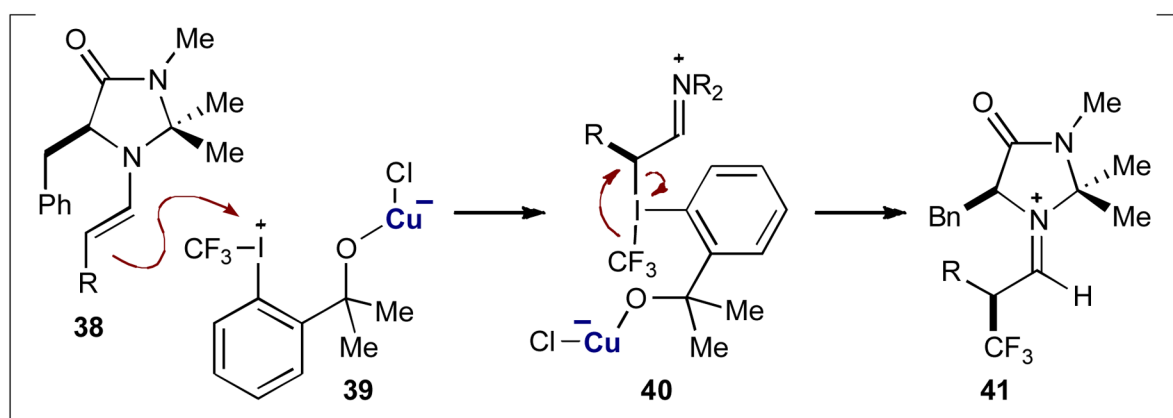
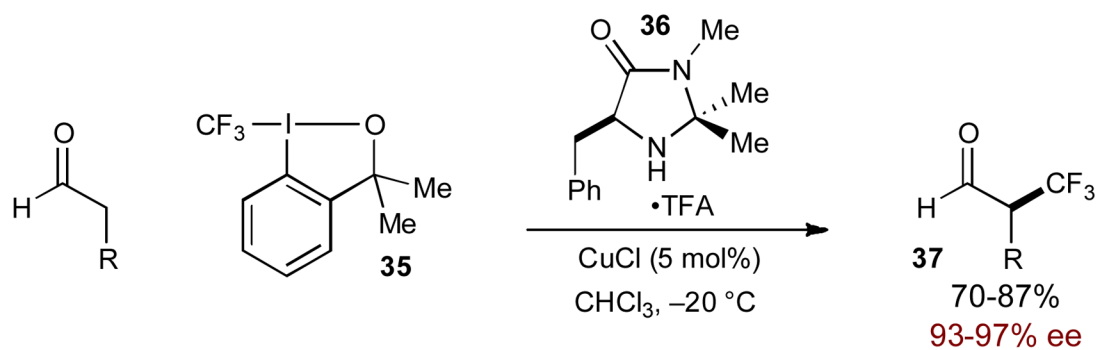


**Scheme 10.** General mechanism of enamine catalysis with metal-bound electrophiles to generate  $\alpha$ -substituted carbonyls.

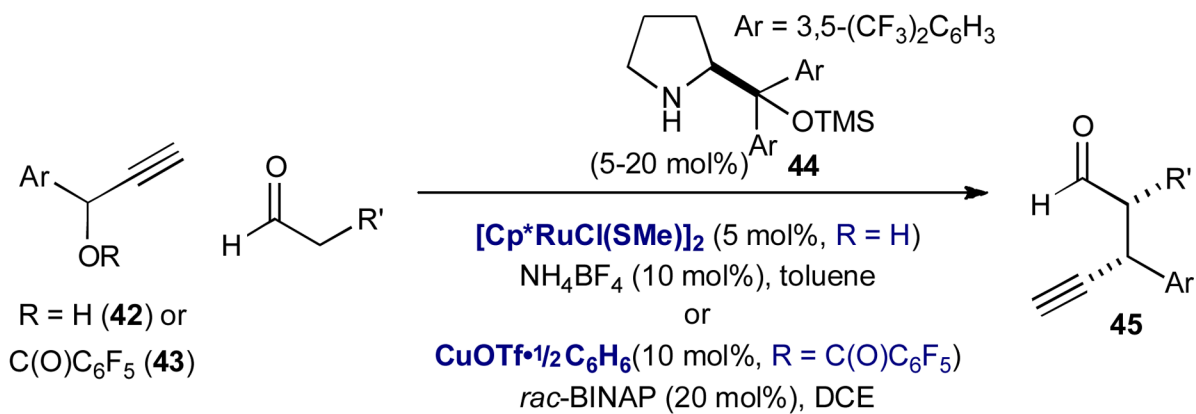




**Scheme 11.**  
Wu's synthesis of 1,2-dihydroisoquinoline derivatives.



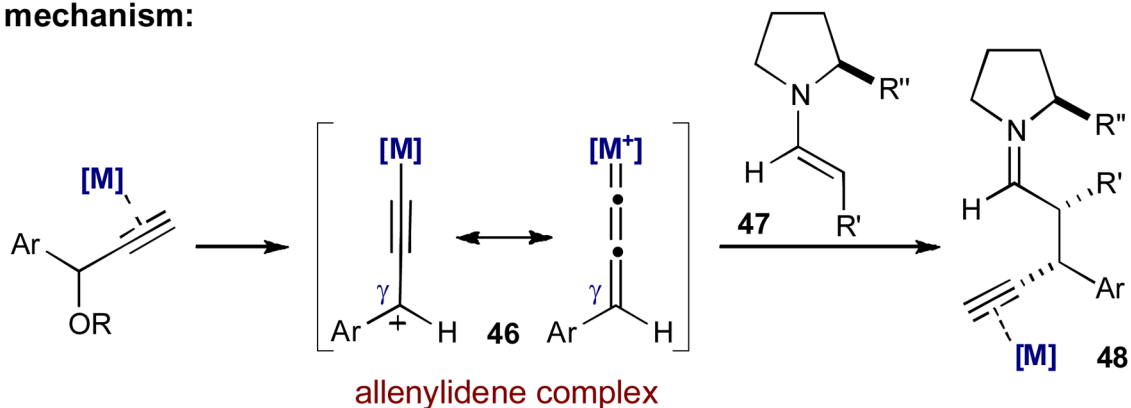
**Scheme 12.**  
MacMillan's organocatalytic  $\alpha$ -trifluoromethylation of aldehydes using Togni's reagent and CuCl.



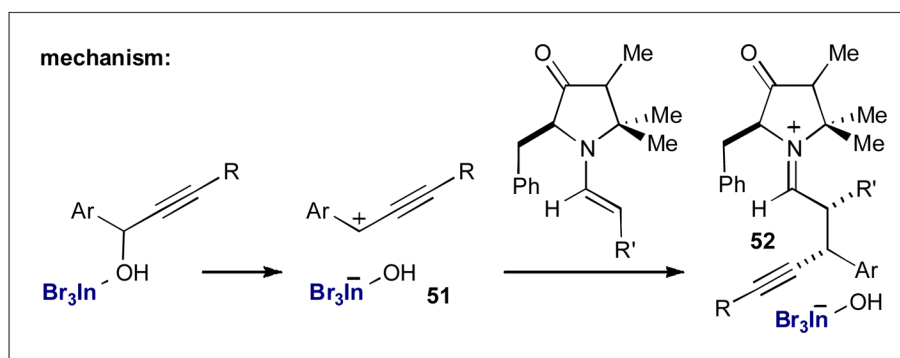
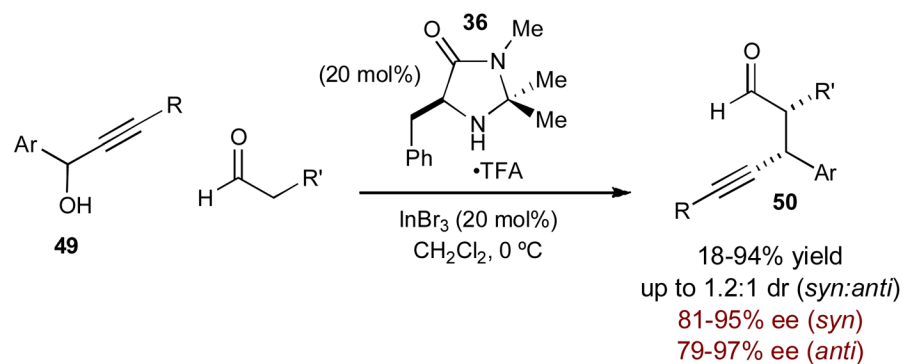
Ru: 80-93% yield  
up to 3.3:1 dr (*syn:anti*)  
92-99% ee (*syn*), 52-95% ee (*anti*)

Cu: 52-64% yield  
up to 3.8:1 dr (*syn:anti*)  
84-99% ee (*syn*), 94-97% ee (*anti*)

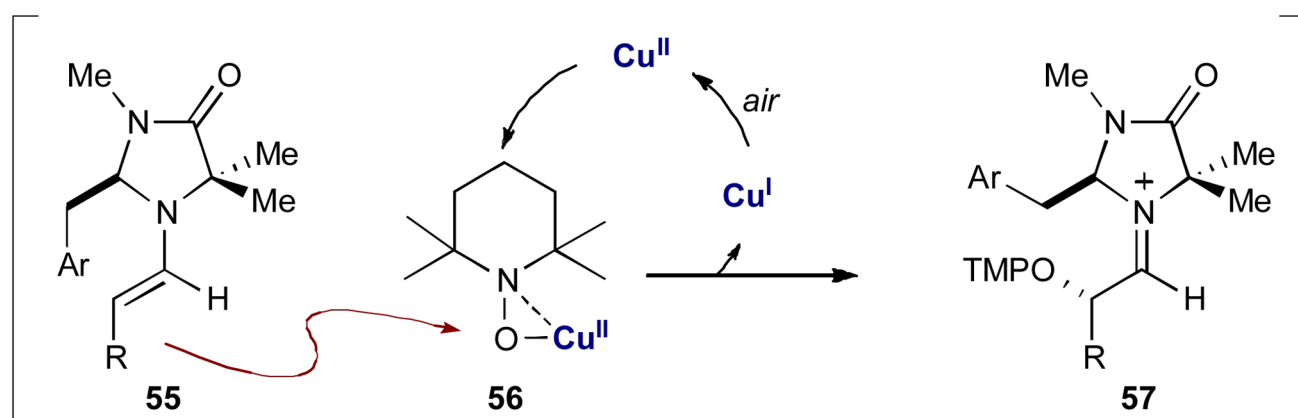
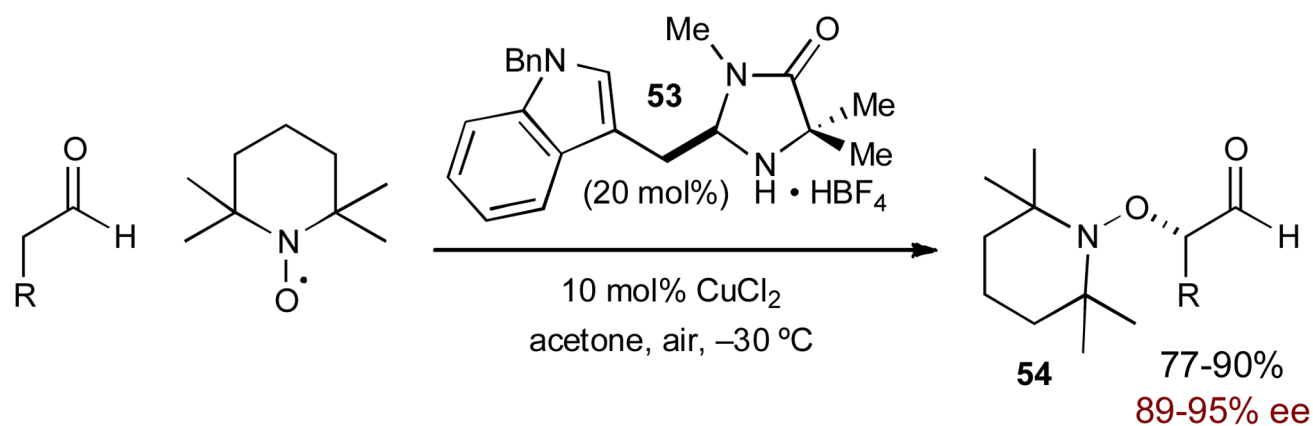
**mechanism:**



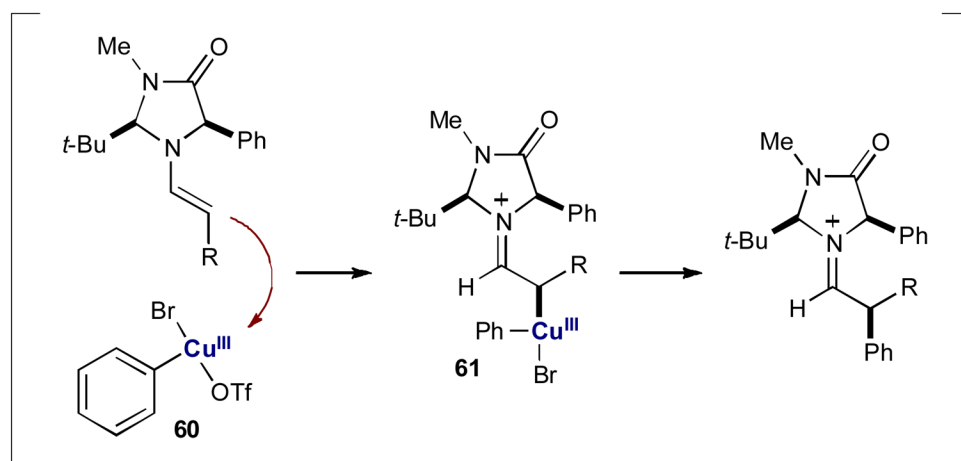
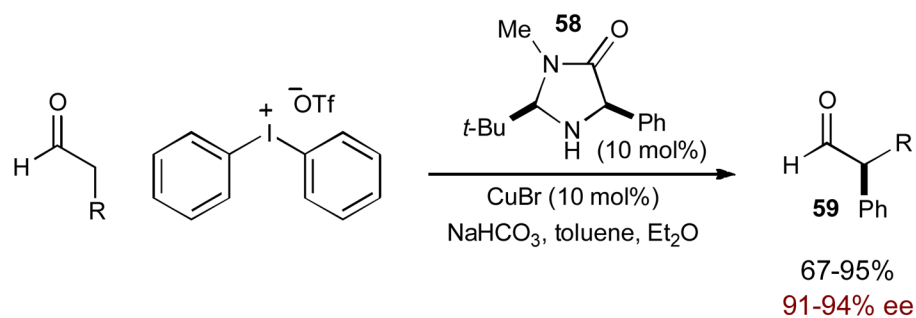
**Scheme 13.**  
Nishibayashi's enantioselective  $\alpha$ -propargylation of aldehydes via enamine and transition metal catalysis.

**Scheme 14.**

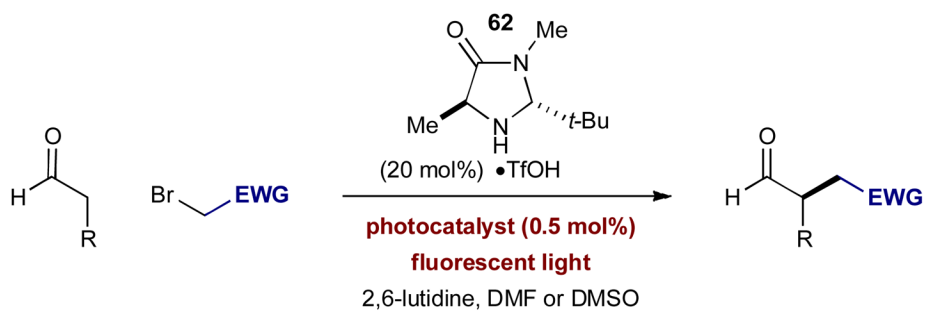
Nishibayashi's enantioselective  $\alpha$ -propargylation of aldehydes using internal alkynes via enamine and indium catalysis.



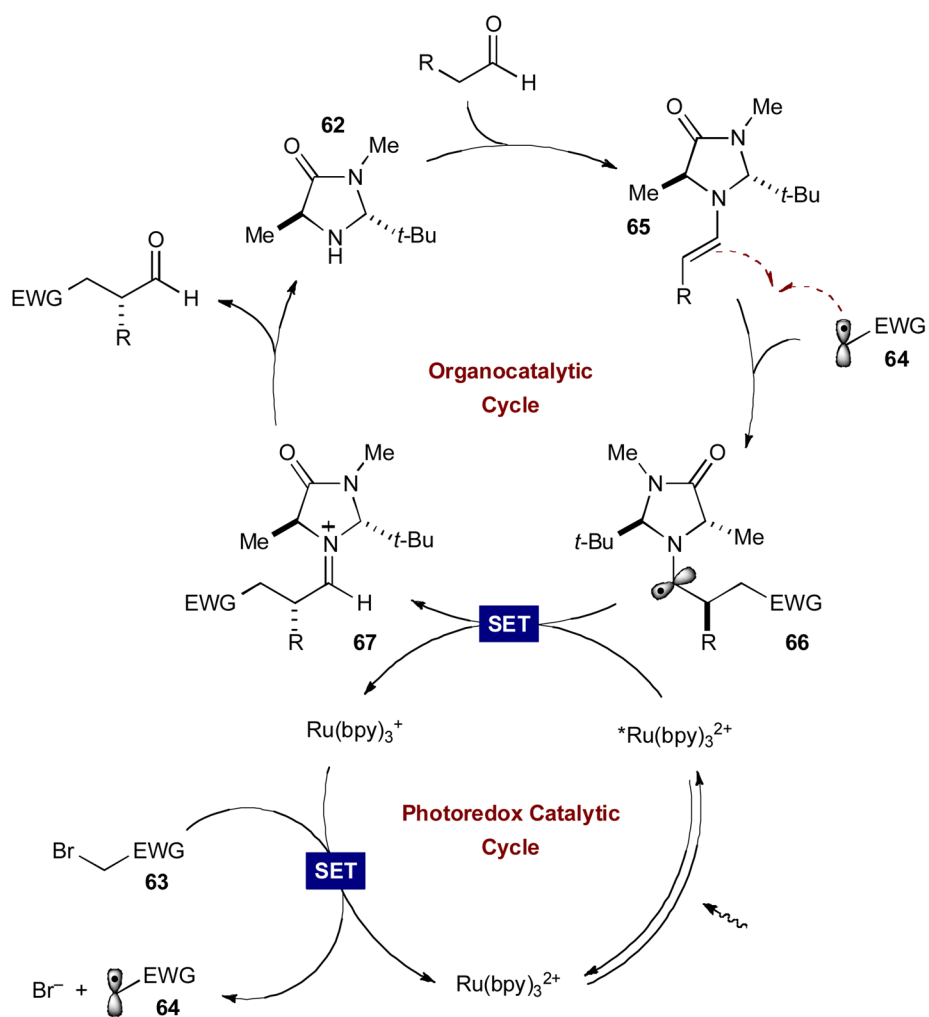
**Scheme 15.** MacMillan's copper-catalyzed enantioselective  $\alpha$ -oxyamination of aldehydes.



**Scheme 16.** Organocatalytic  $\alpha$ -arylation of aldehydes via the merger of enamine and copper catalysis.

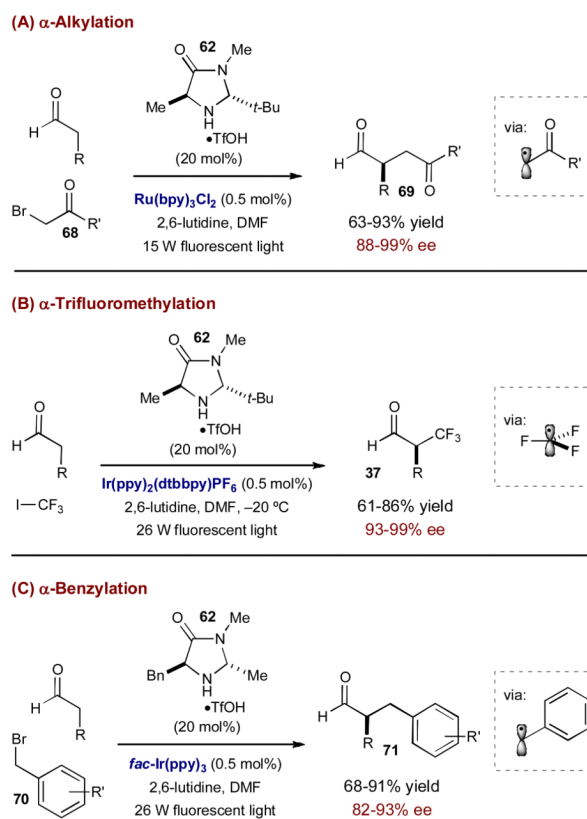
**Scheme 17.**

The reductive cleavage of electron-poor alkyl bromides for use in photoredox organocatalysis.

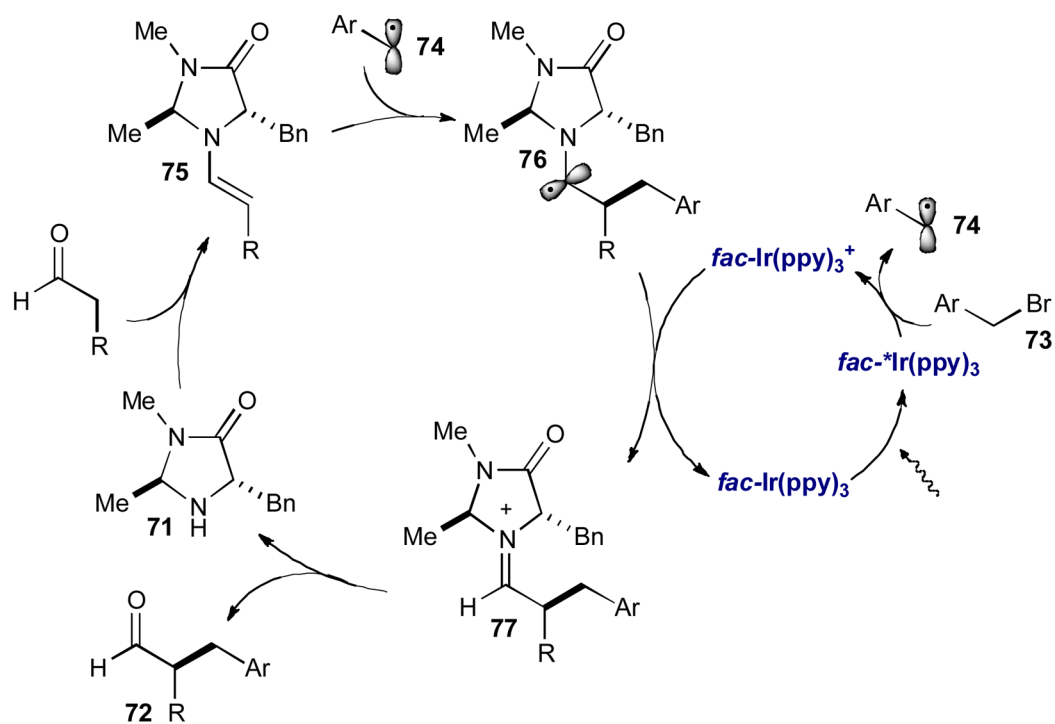


**Scheme 18.**  
General mechanism for the photoredox enantioselective  $\alpha$ -alkylation of aldehydes.

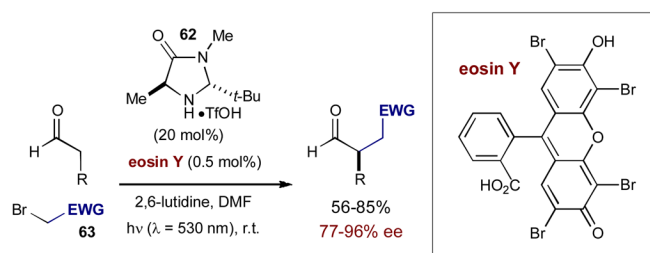




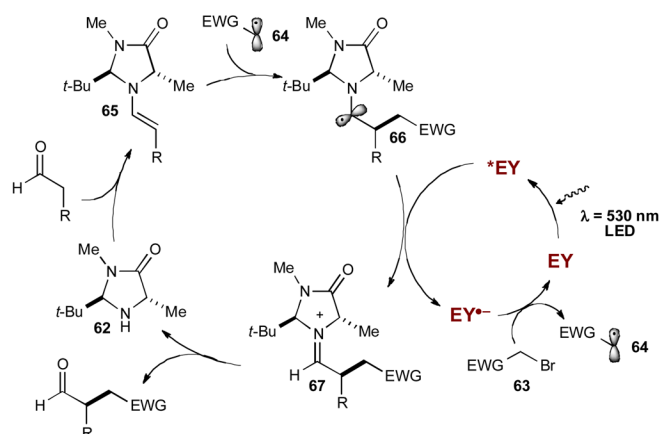
**Scheme 19.**  
Examples of photoredox organocatalysis reported by MacMillan and coworkers.



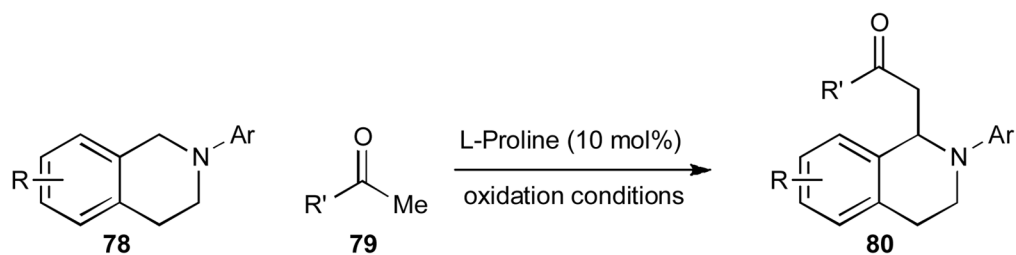
**Scheme 20.**  
Mechanism of the photoredox organocatalytic  $\alpha$ -benzylation of aldehydes.



**mechanism**



**Scheme 21.**  
Zeitler's photoredox protocol using organic photocatalysts.



**oxidation conditions:**

**Klussmann**

**VO(acac)<sub>2</sub> (5 mol%)**

*t*-BuOOH, MeOH

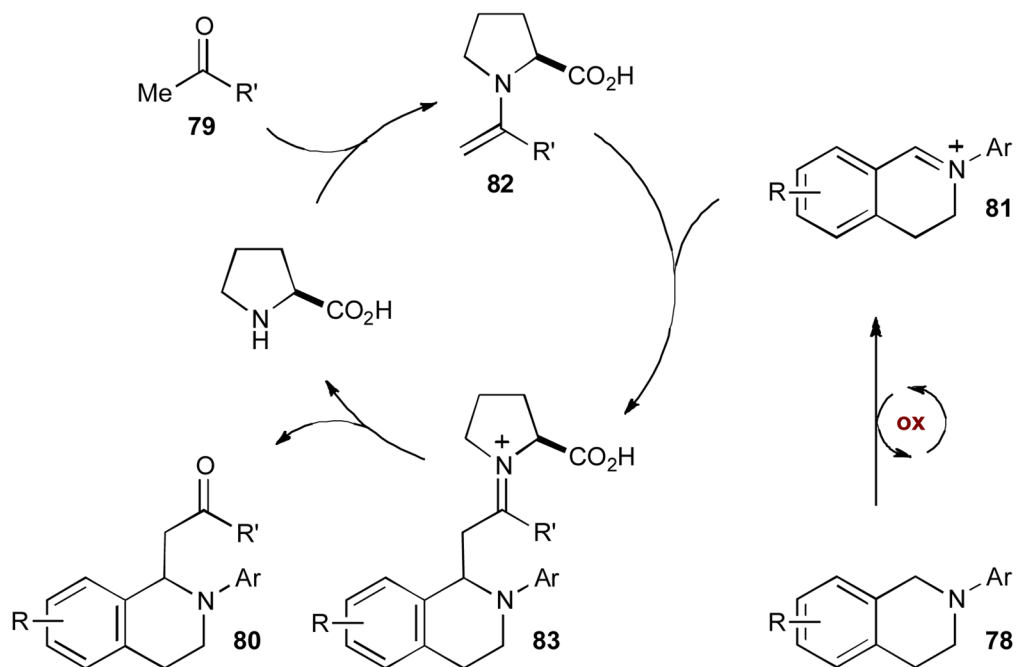
32-69% yield

**Rueping**

**Ru(bpy)<sub>3</sub>(PF<sub>6</sub>)<sub>2</sub> (1 mol%)**

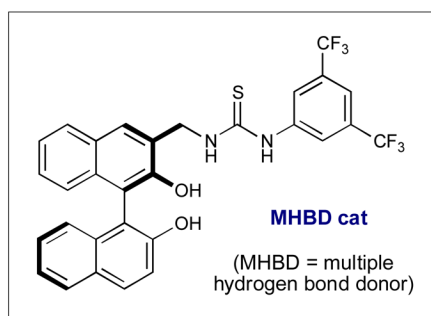
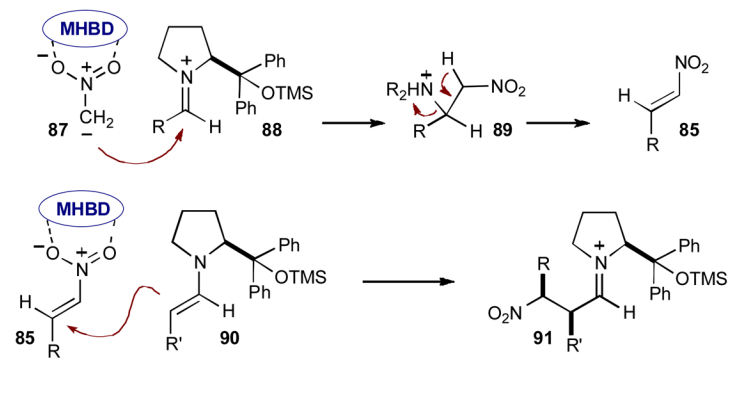
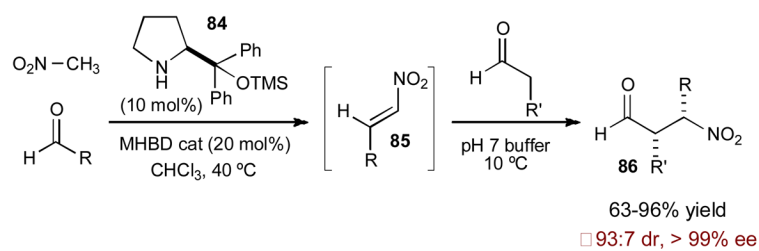
5W fluorescent light, MeCN, O<sub>2</sub>

47-95% yield

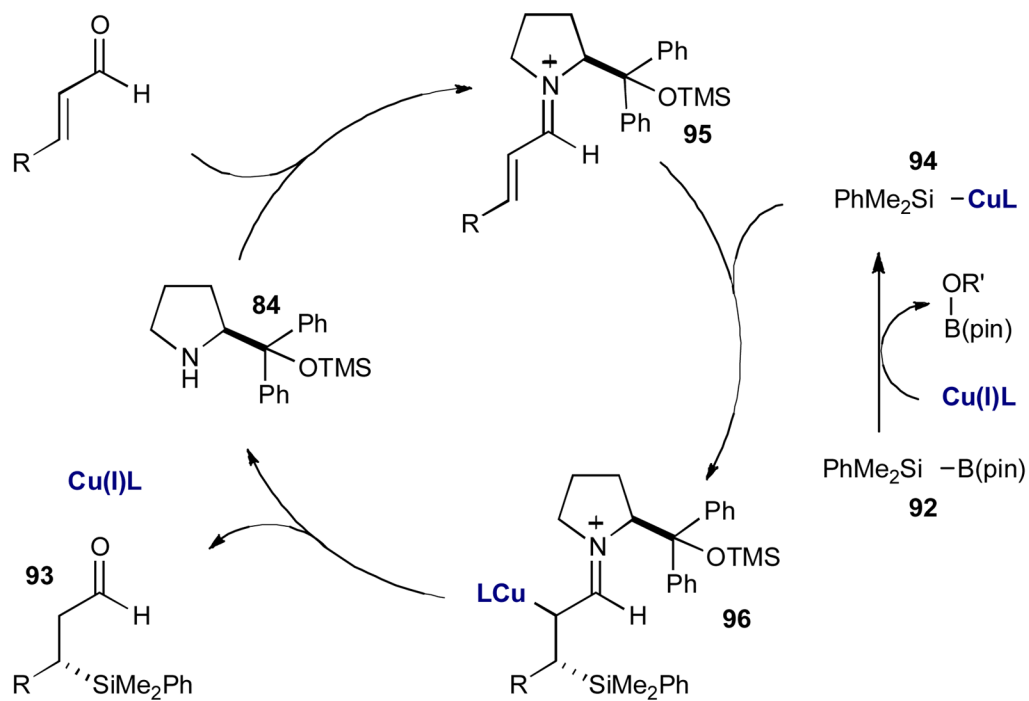
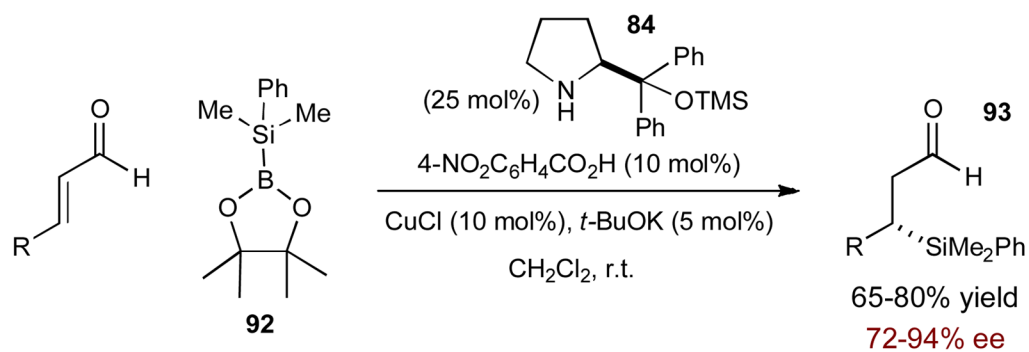


**Scheme 22.**

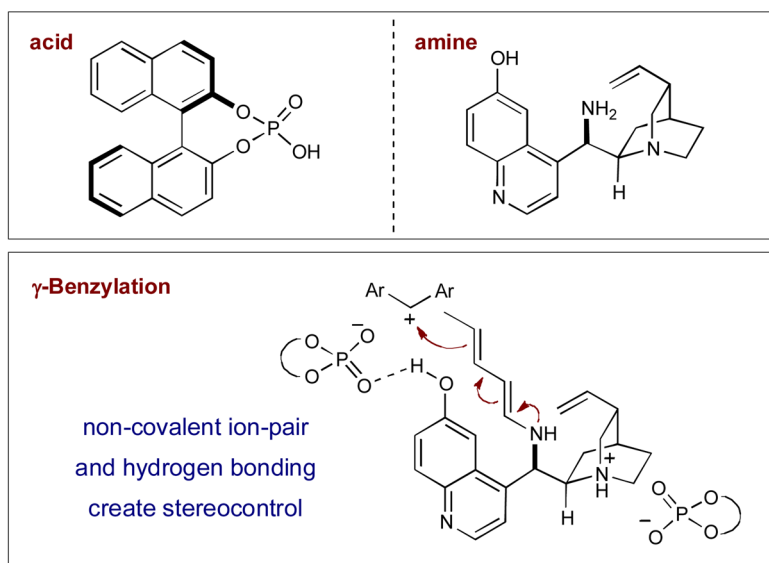
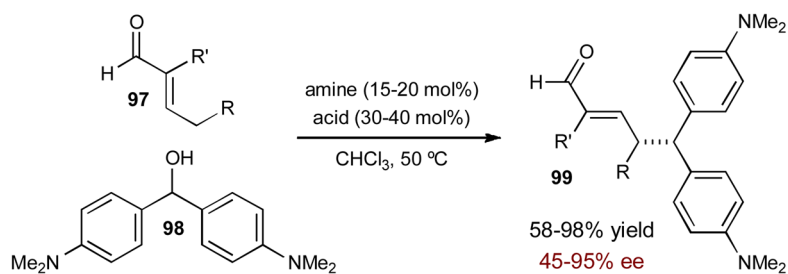
Oxidative coupling reactions of cyclic tertiary amines and methyl ketones reported by Klussmann and Rueping.

**Scheme 23.**

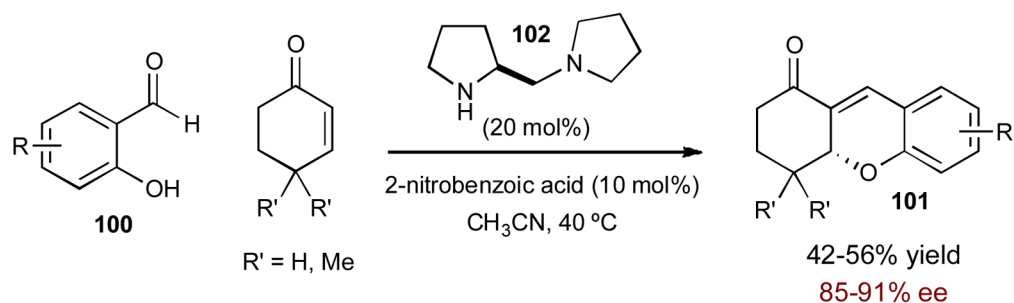
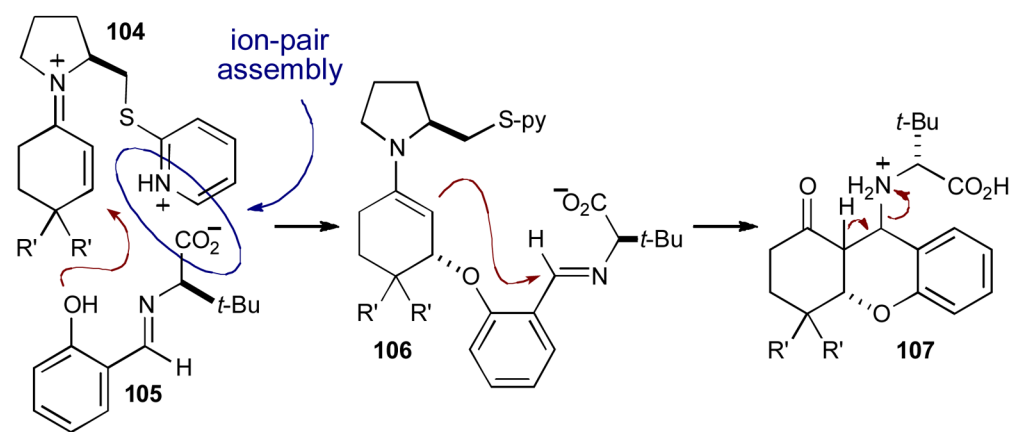
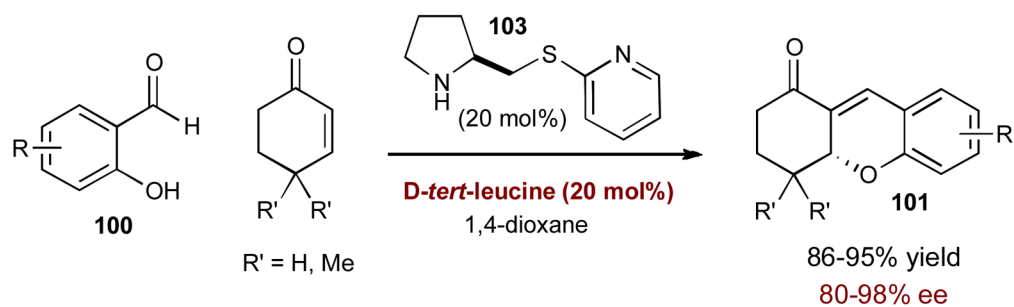
An enantioselective three-component domino reaction via synergistic hydrogen-bond and enamine catalysis.

**Scheme 24.**

Córdova's catalytic enantioselective silyl conjugate addition to  $\alpha,\beta$ -unsaturated aldehydes via copper and iminium catalysis.

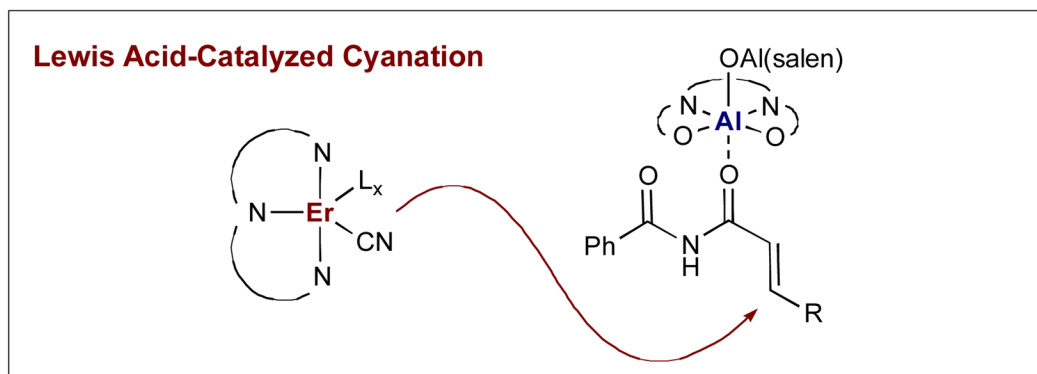
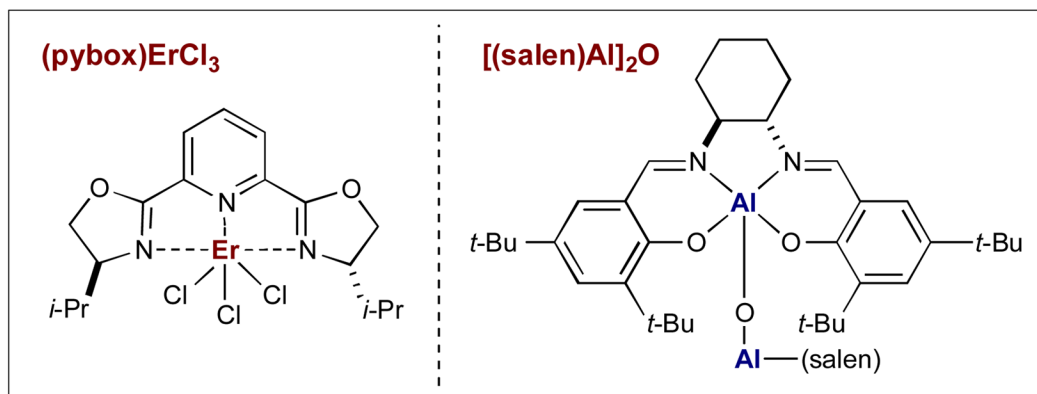
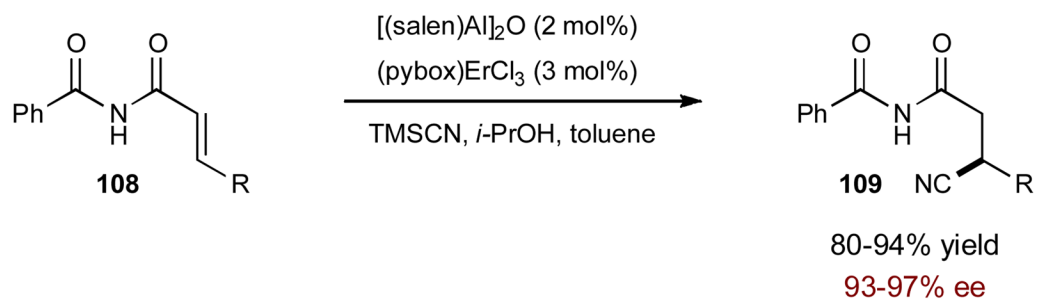


**Scheme 25.** Direct  $\gamma$ -benzylic alkylation of  $\alpha$ -branched enals via the merger of chiral dienamine and Brønsted acid catalysis.

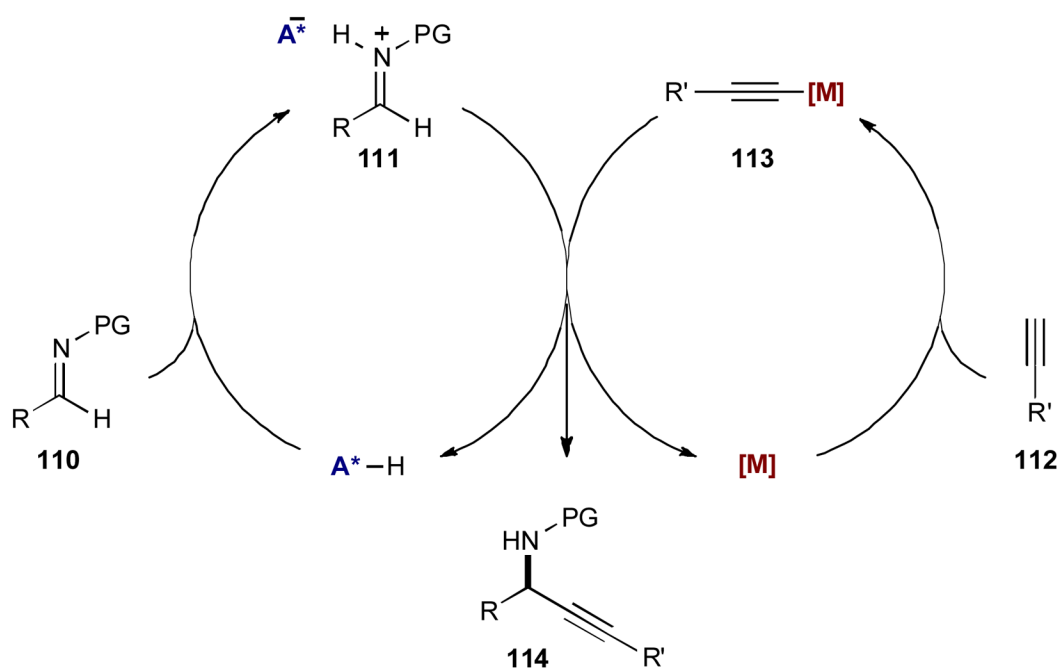
**(A) Córdova (2007) – Conventional Catalysis****(B) Xu (2010) – Synergistic Catalysis**

**Scheme 26.** Formation of tetrahydroxanthenones via organocatalytic enantioselective oxa-Michael-Mannich reaction.

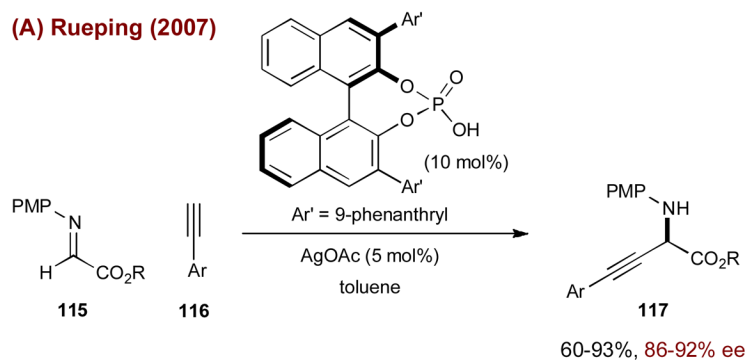




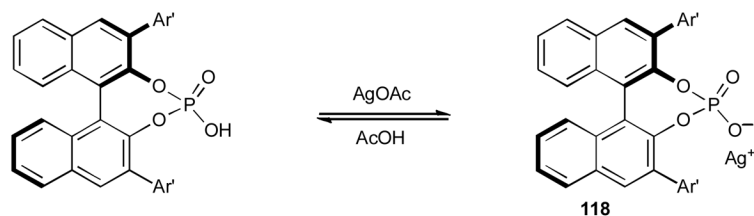
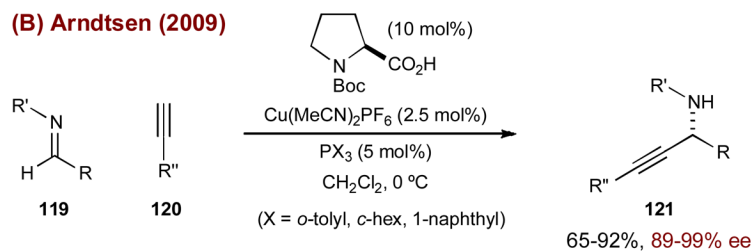
**Scheme 27.**  
Jacobsen's conjugate cyanation of unsaturated imides.



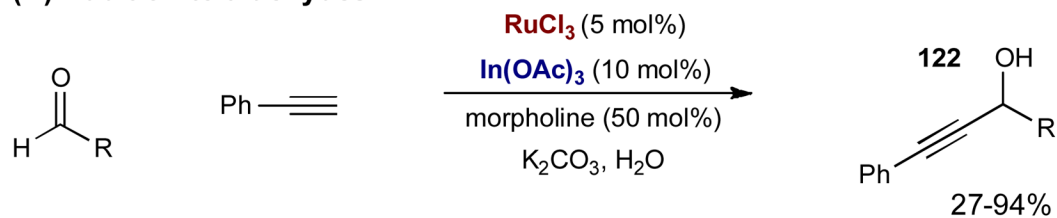
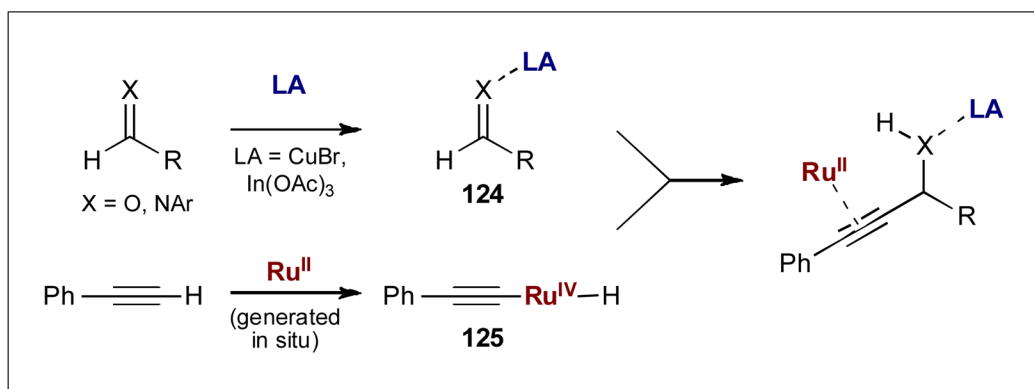
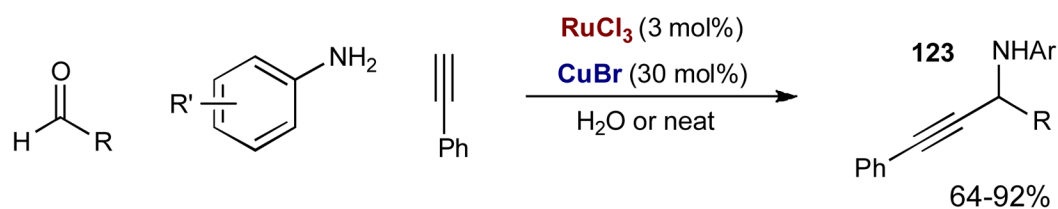
**Scheme 28.**  
General mechanism for the addition of metal acetylides to Brønsted acid activated imines.

**(A) Rueping (2007)**

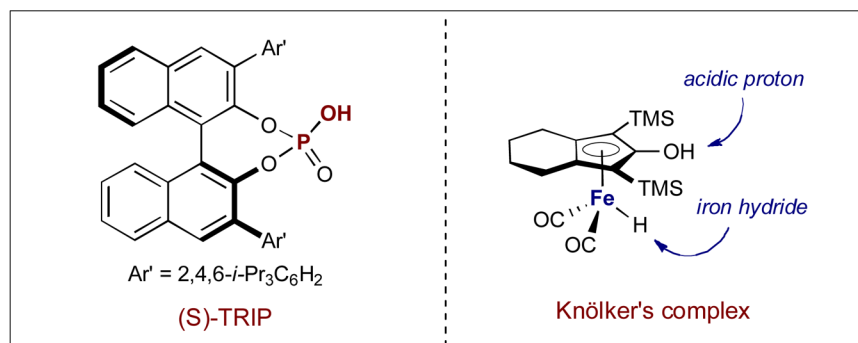
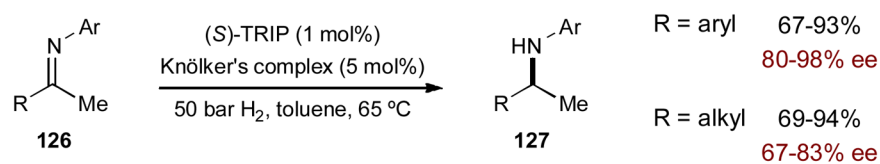
possible counterion exchange:

**(B) Arndtsen (2009)****Scheme 29.**

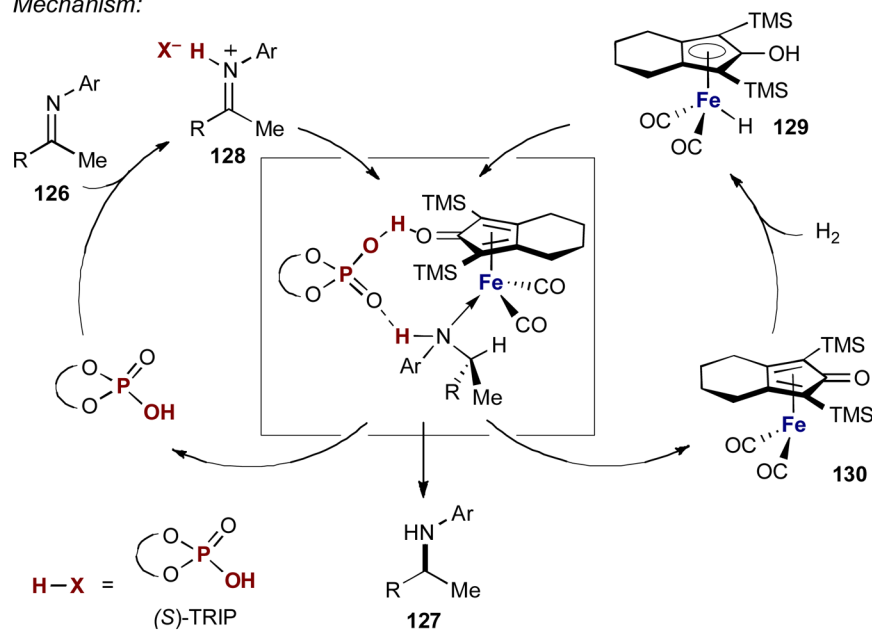
Asymmetric synthesis of propargylic amines via the merger of transition metal catalysis with Brønsted acid catalysis.

**(A) Addition to aldehydes****(B) Addition to in situ imines****Scheme 30.**

Li's ruthenium- and copper-catalyzed synthesis of propargyl alcohols and amines.

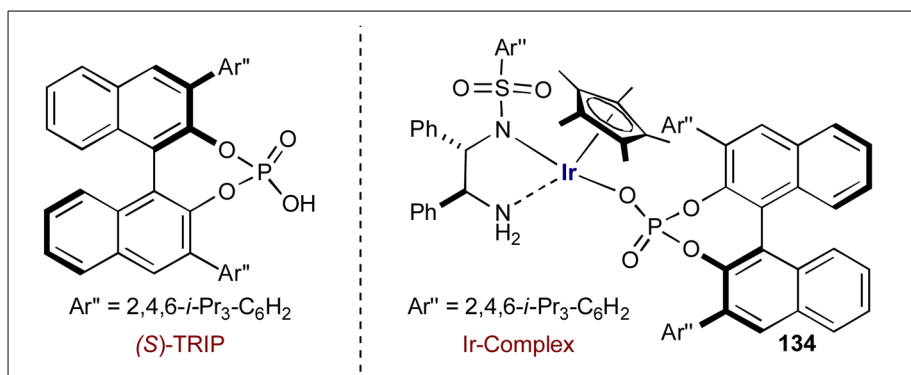
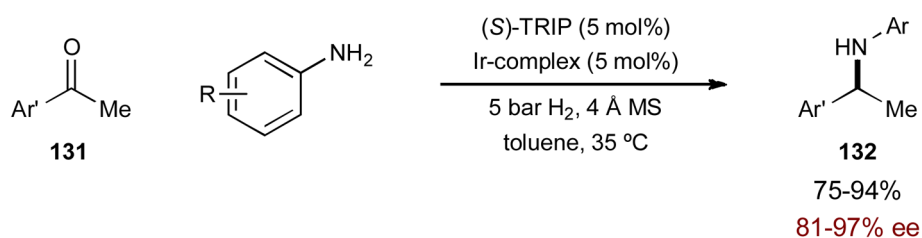


Mechanism:

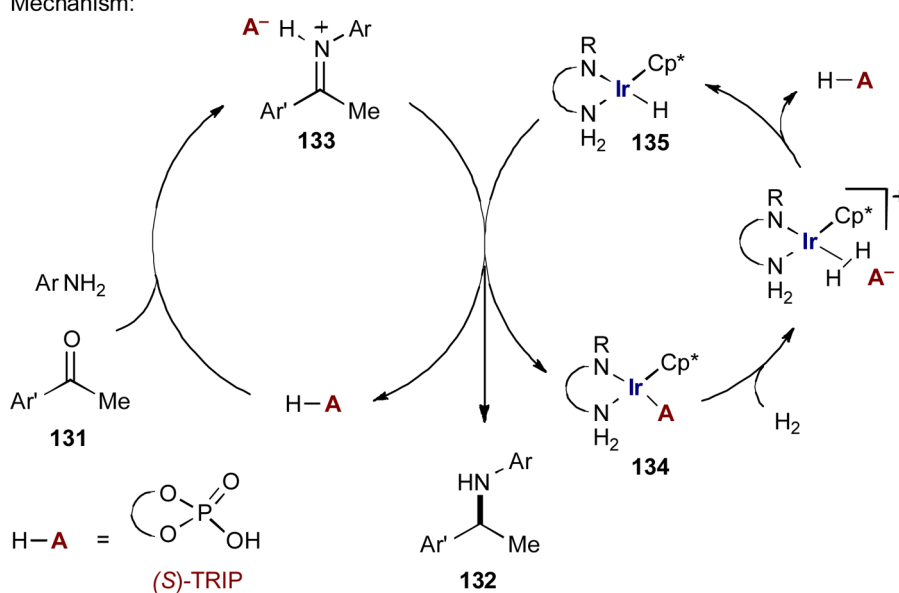


**Scheme 31.**

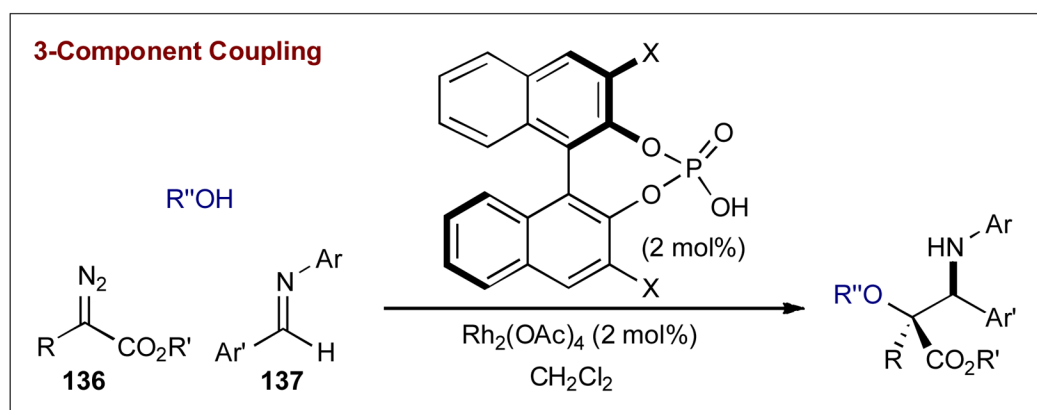
Beller's catalytic asymmetric hydrogenation of imines using a simple achiral iron catalyst and a chiral Brønsted acid catalyst.



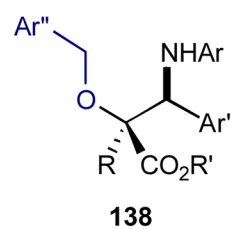
Mechanism:

**Scheme 32.**

The reductive amination of methyl ketones catalyzed by a chiral iridium complex and a chiral Brønsted acid.



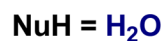
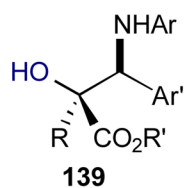
## oxygen nucleophiles



$\text{Ar}''$ , X = 9-phenanthryl

43-98%

□99:1 dr, 83-99% ee



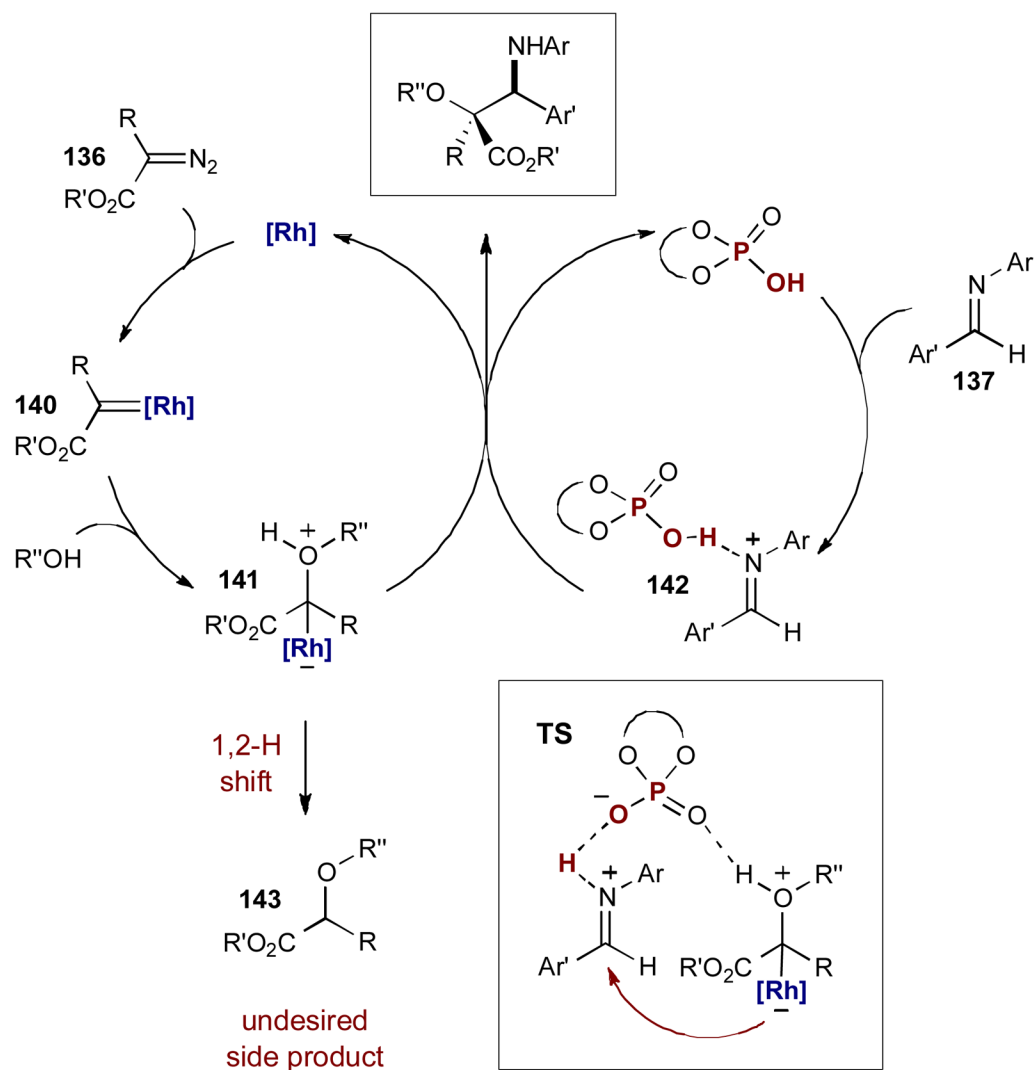
X =  $\text{SiPh}_3$

62-86%

□4:1 dr, 93-97% ee

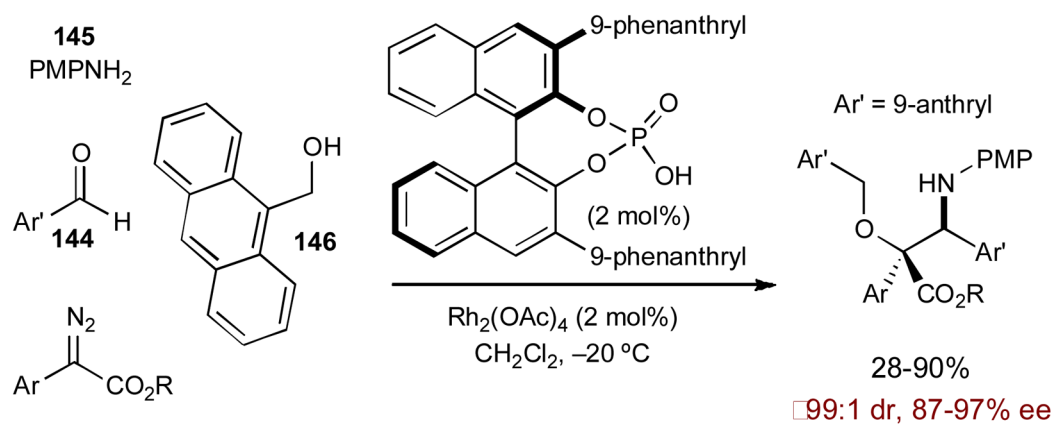
## Scheme 33.

The three-component coupling of diazoacetates, alcohols, and imines catalyzed by chiral Brønsted acids and  $\text{Rh}_2(\text{OAc})_4$ .

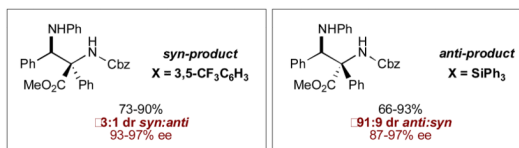
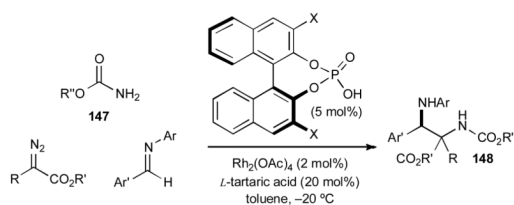
**Scheme 34.**

Mechanism of the three-component coupling of diazoacetates, alcohols, and imines via rhodium- and Brønsted acid catalysis.

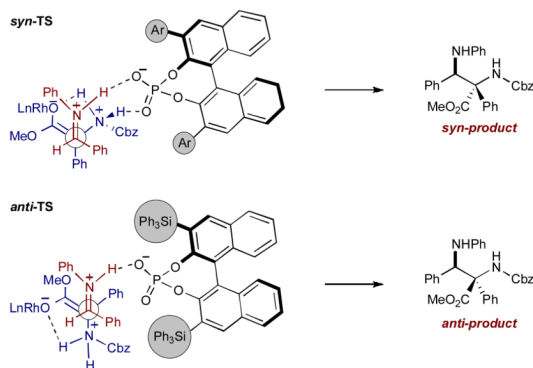


**Scheme 35.**

The four-component coupling of diazoacetates with alcohol, aldehydes, and amines to generate  $\beta$ -amino- $\alpha$ -hydroxyesters.

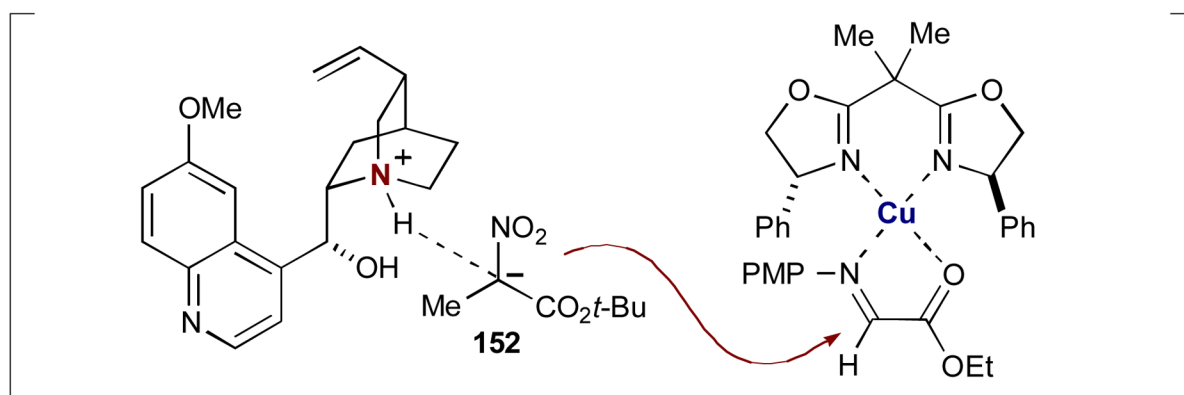
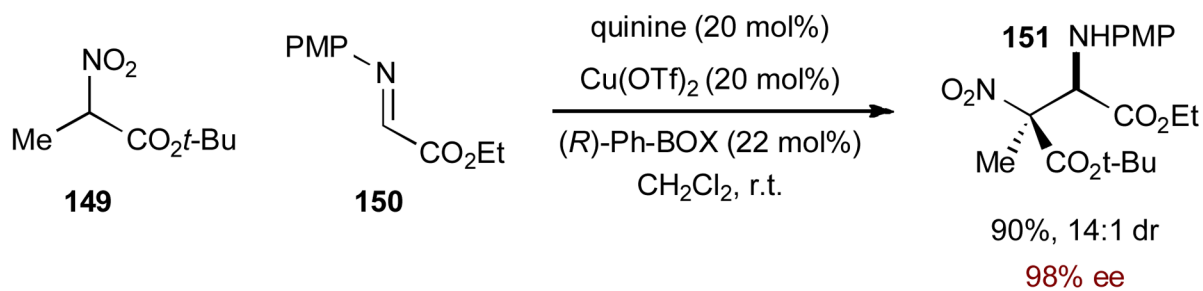


proposed transition states for diastereoselectivity switch

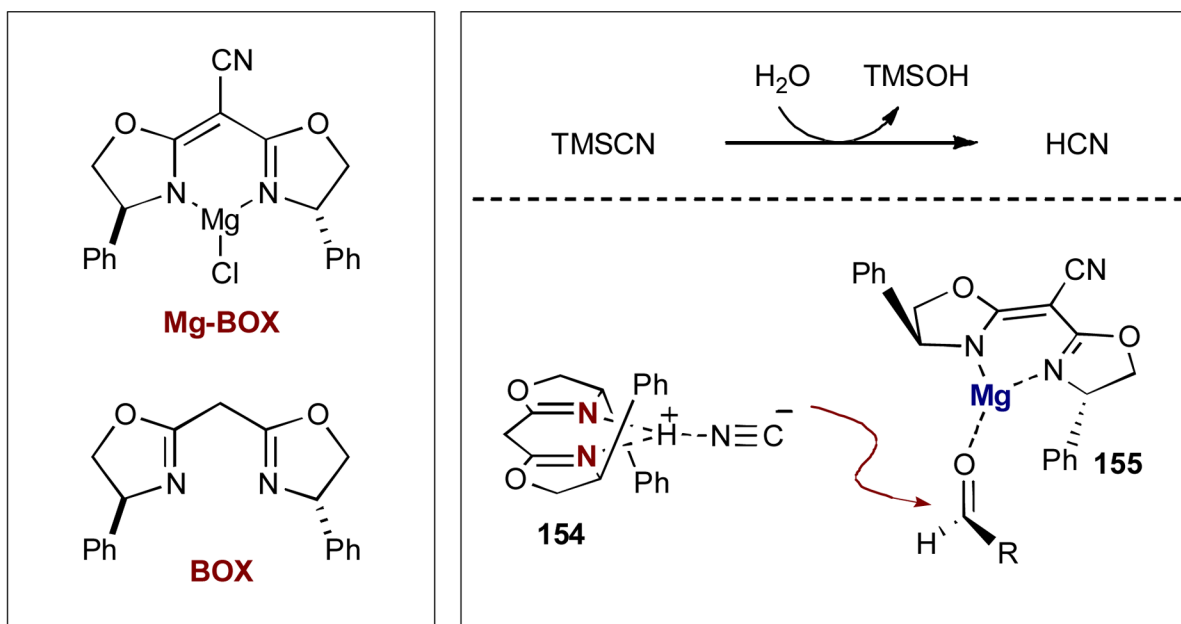
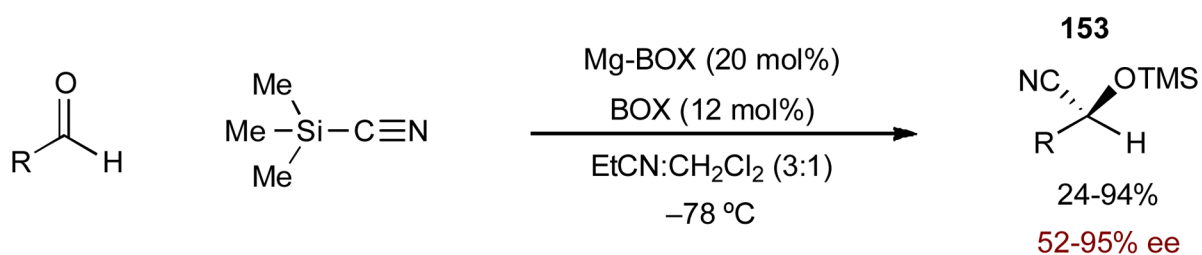


### Scheme 36.

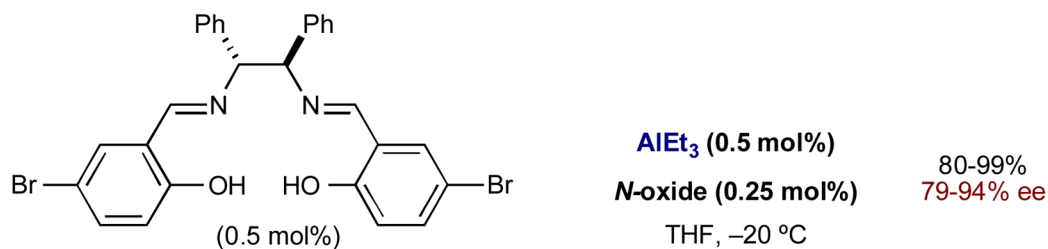
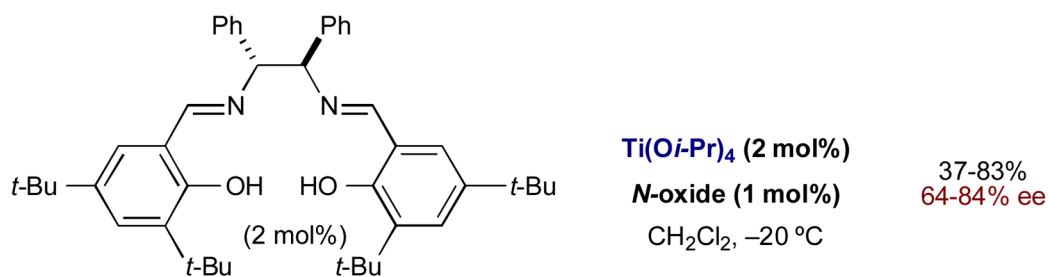
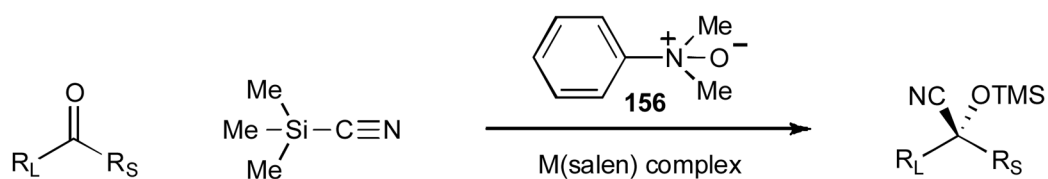
The three-component coupling of diazoacetates, carbamates, and imines using a chiral Brønsted acid and  $\text{Rh}_2(\text{OAc})_4$ .



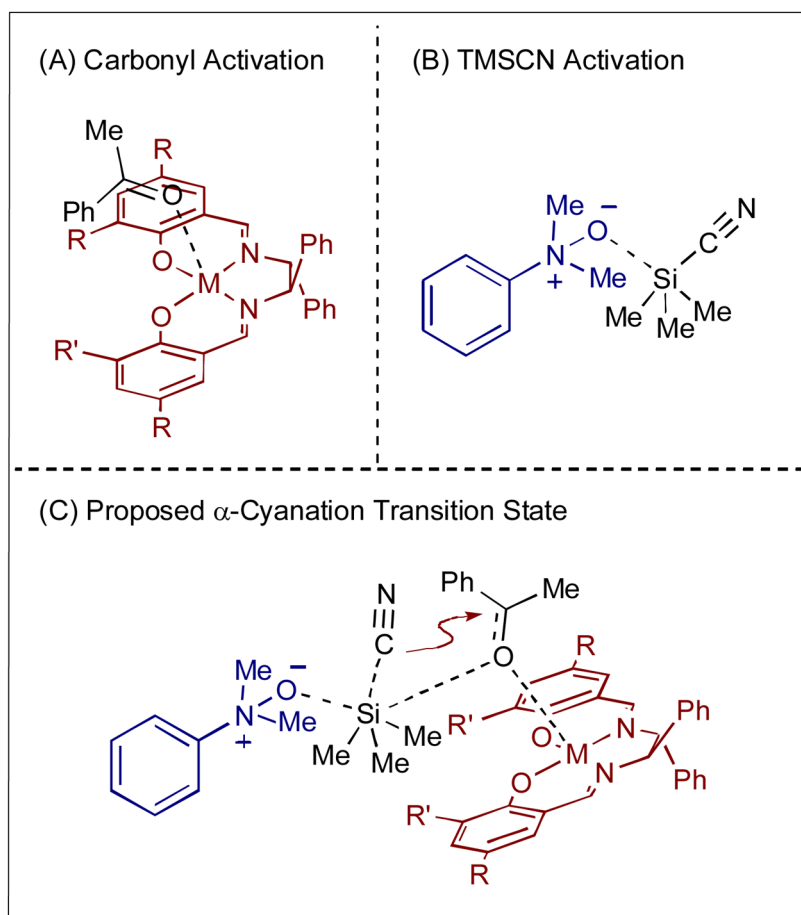
**Scheme 37.**  
Enantioselective aza-Henry reaction via chiral organic and Lewis acid catalysis.

**Scheme 38.**

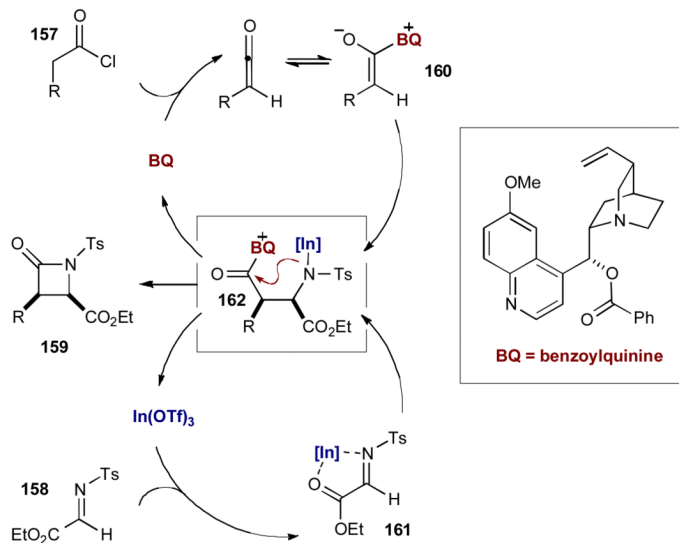
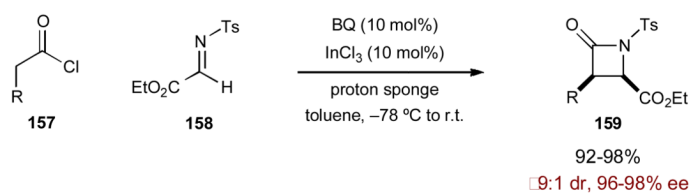
Corey's enantioselective cyanation of aldehydes using TMSCN with Lewis acid and Lewis base catalysts.

**Scheme 39.**

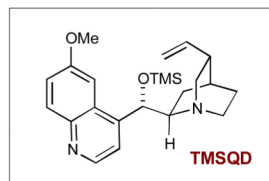
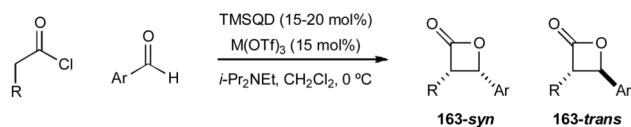
The enantioselective cyanation of ketones catalyzed by metal-salen complexes and dimethylphenylamine  $N$ -oxide.

**Scheme 40.**

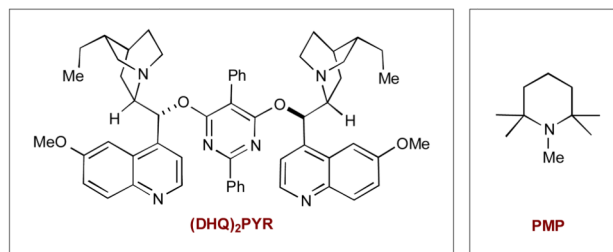
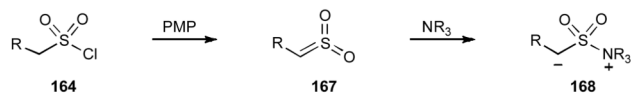
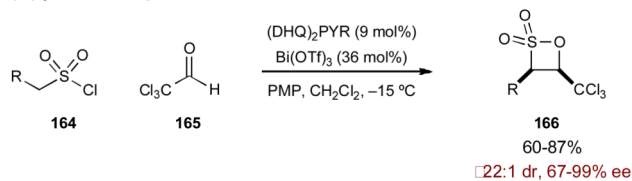
Proposed transition states for the Lewis acid and Lewis base catalyzed cyanation of ketones.



**Scheme 41.**  
The asymmetric synthesis of  $\beta$ -lactams catalyzed by benzoylquinine and  $\text{In(OTf)}_3$ .

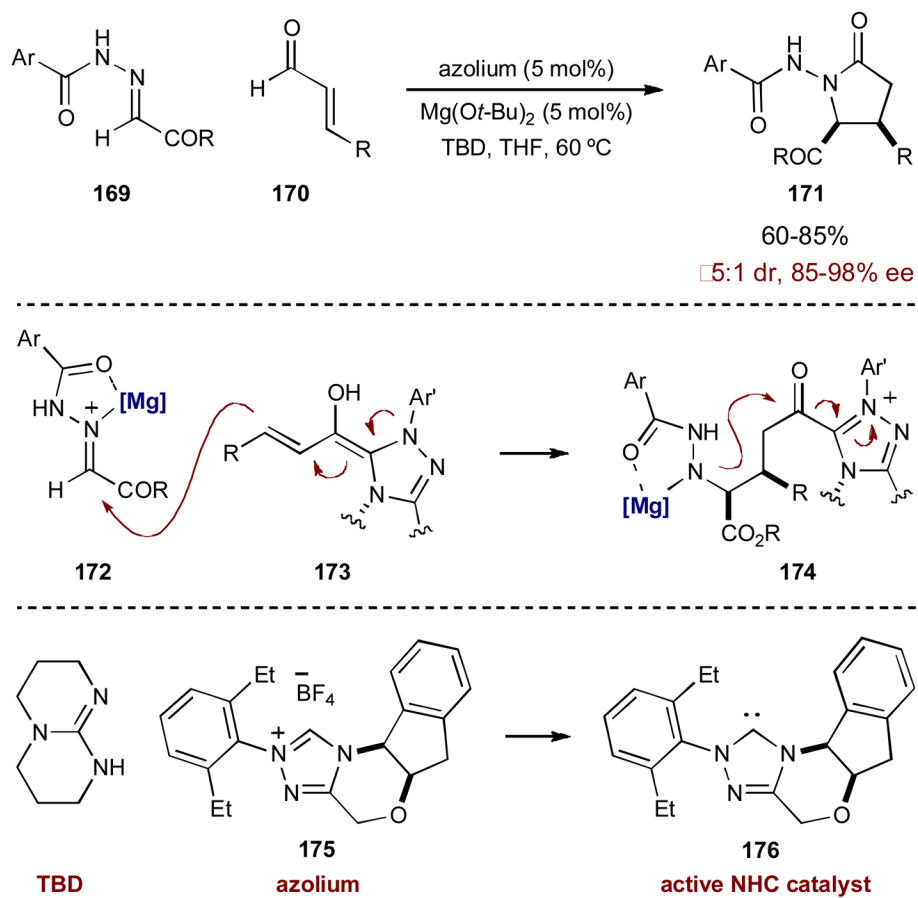
**(A)  $\beta$ -lactone synthesis**

**R = alkoxy**      55-88%  
**M = Er**       $\square$ 87:13 dr *cis:trans*  
                          >99% ee  
  
**R = alkyl**      75-82%  
**M = Sc**       $\square$ 91:9 dr *trans:cis*  
                          92-99% ee

**(B)  $\beta$ -sultone synthesis****Scheme 42.**

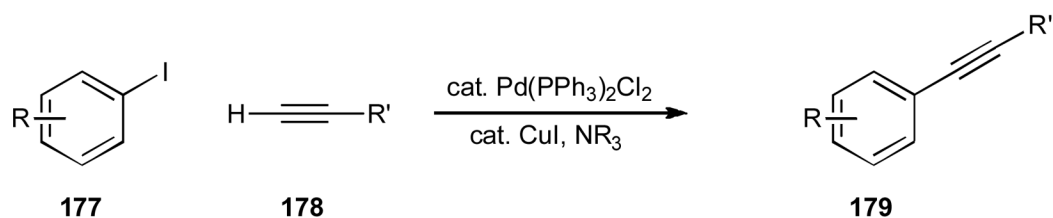
The asymmetric synthesis of (A)  $\beta$ -lactones and (B)  $\beta$ -sultones using cinchona alkaloid and metal Lewis acid catalysts.



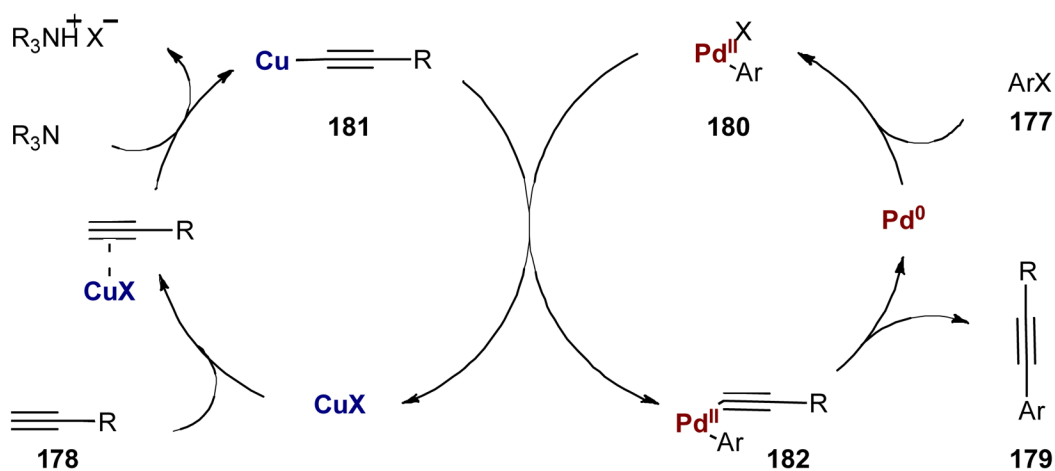


**Scheme 43.** Scheidt's  $\gamma$ -lactam formation via a [3 + 2] annulation catalyzed by an *N*-heterocyclic carbene and a Lewis acid.

## Sonogashira cross-coupling

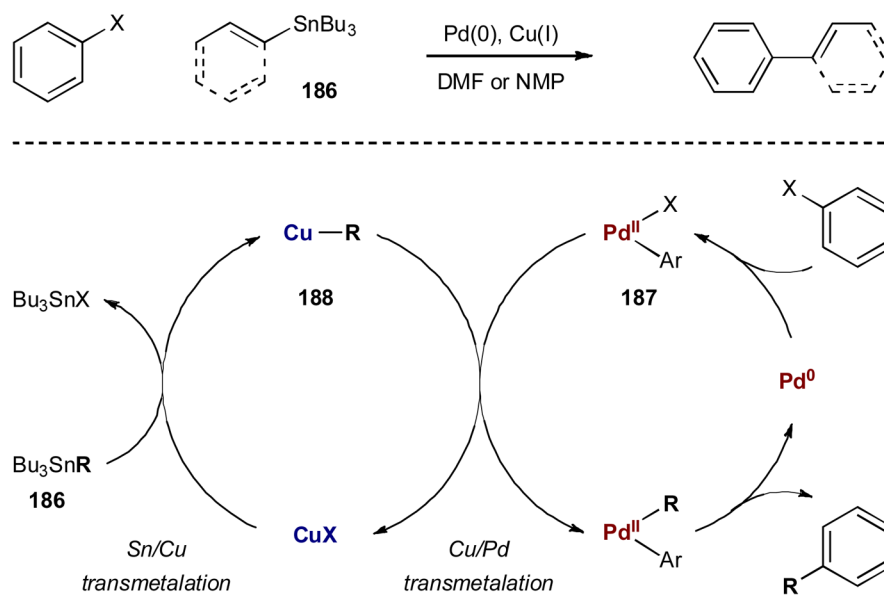


### mechanism

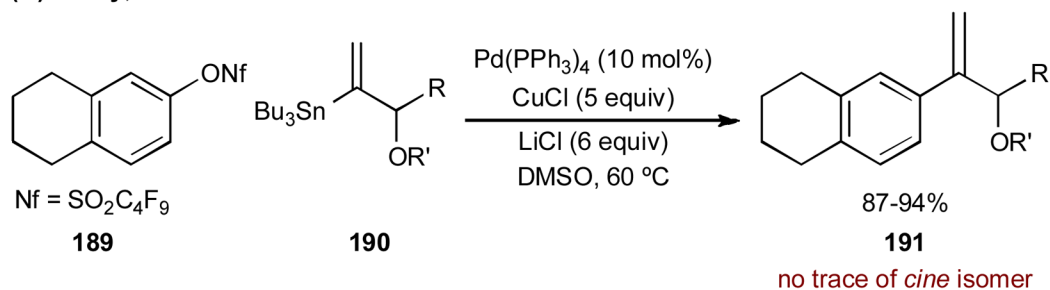
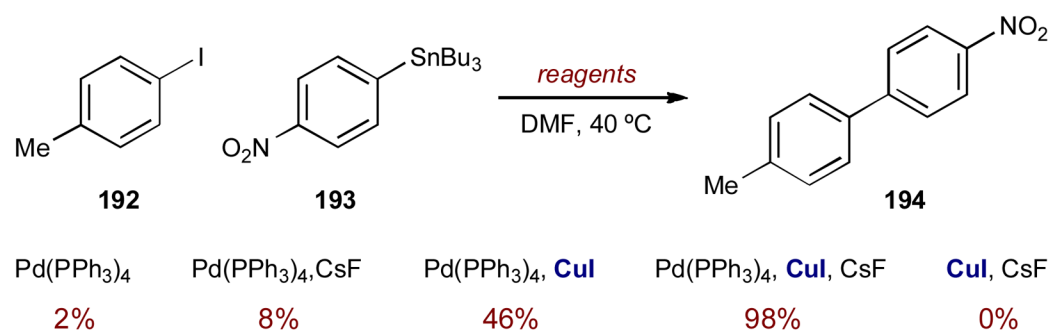
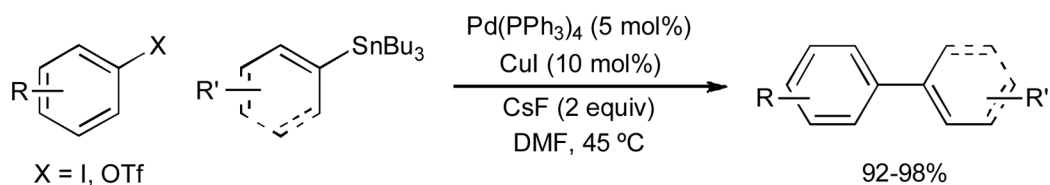


#### Scheme 44.

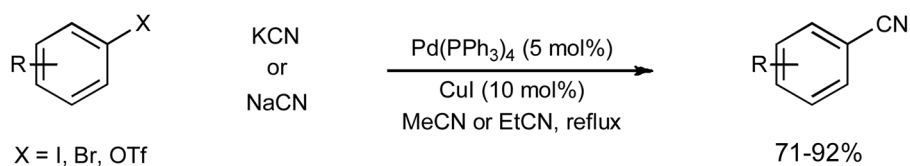
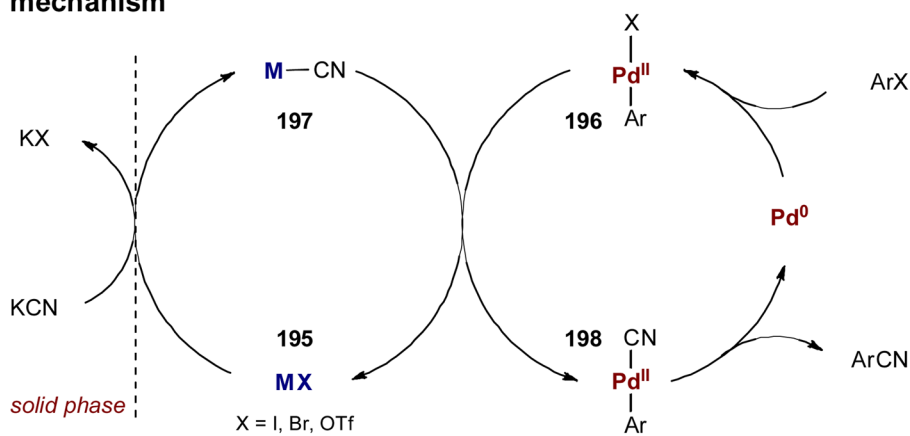
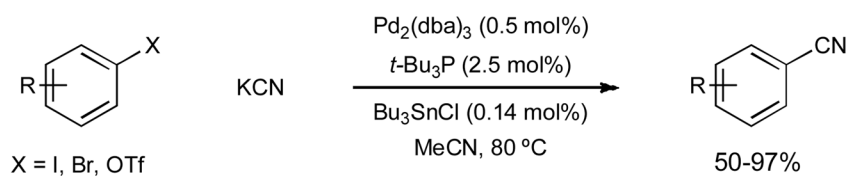
The Sonogashira coupling reaction first disclosed in 1975 by Sonogashira, Tohda, and Hagihara.



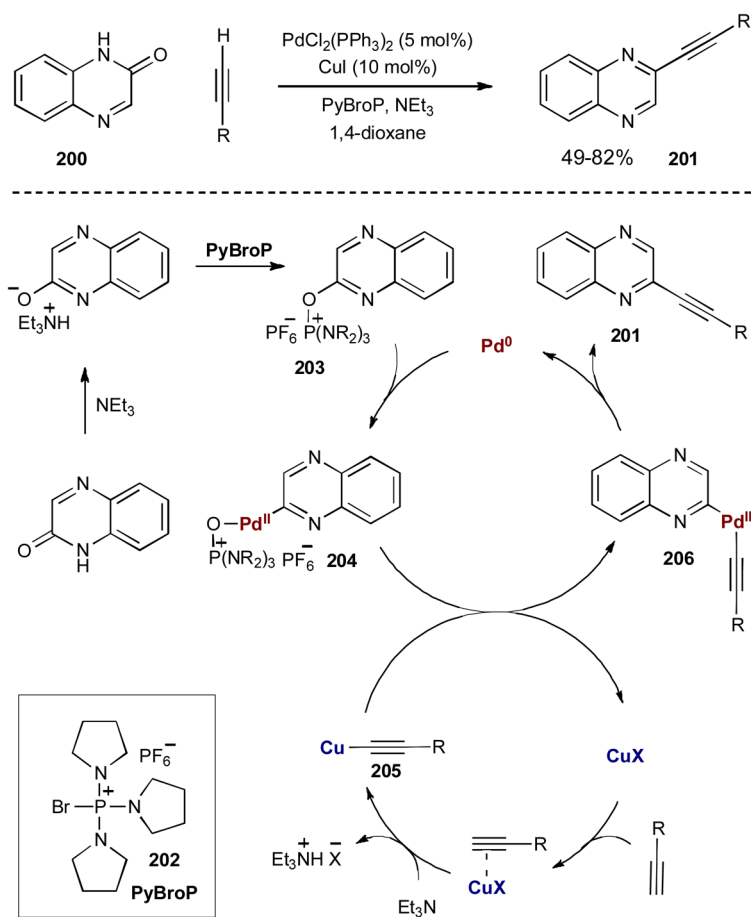
**Scheme 45.**  
Palladium- and copper-catalyzed Stille coupling reaction.

**(A) Corey, 1999:****(B) Baldwin, 2004:****Scheme 46.**

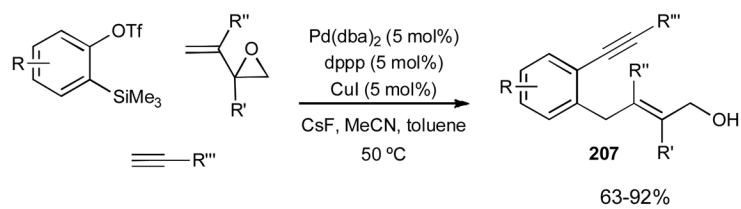
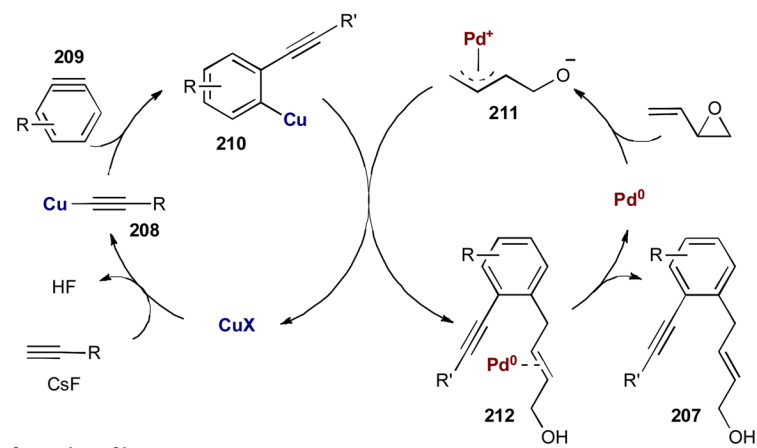
Palladium- and copper-catalyzed Stille coupling reactions.

**(A) palladium- and copper-catalyzed cyanation****mechanism****(B) palladium- and tin-catalyzed cyanation**

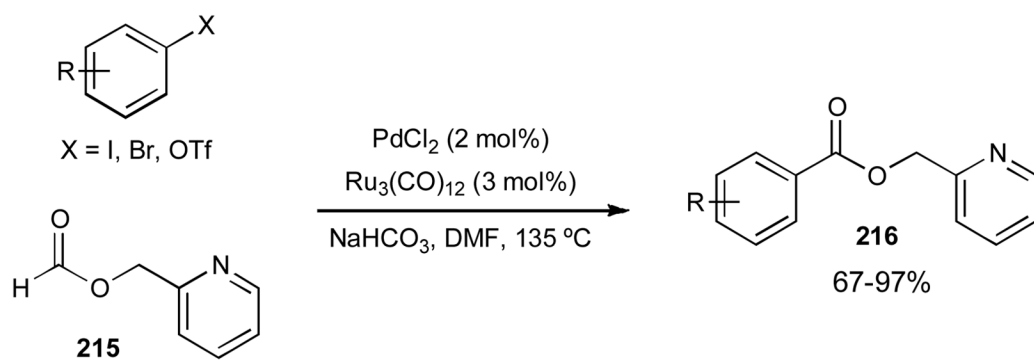
**Scheme 47.**  
Synergistic palladium-catalyzed cyanation of aryl halides.



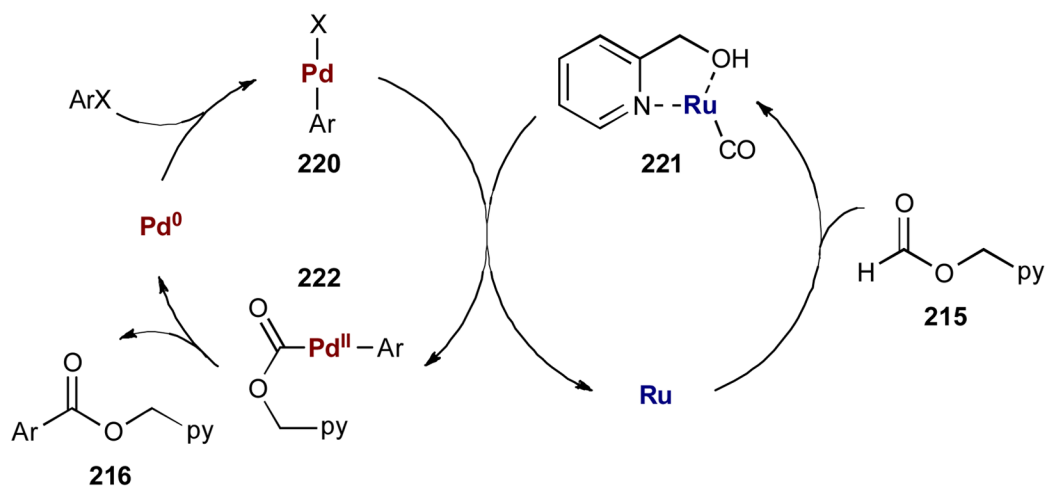
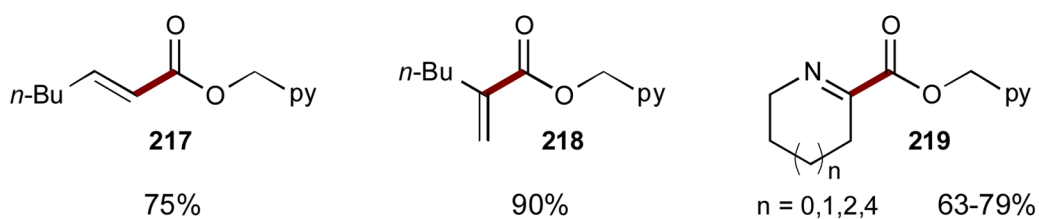
**Scheme 48.** Direct dehydrative cross-coupling of tautomerizable heterocycles and alkynes via palladium and copper catalysis.

**mechanism****formation of benzyne:**

**Scheme 49.** Three-component coupling of benzyne, allylic epoxides, and terminal acetylenes.



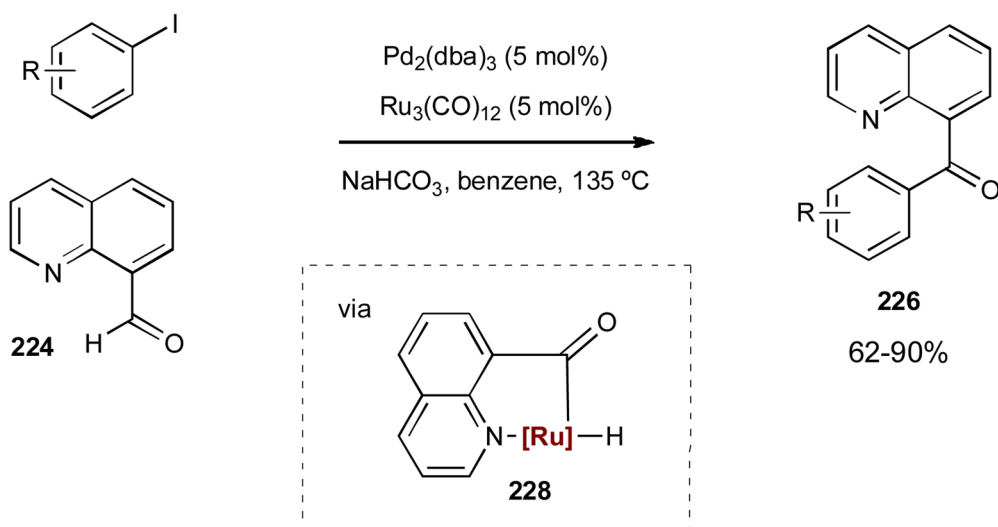
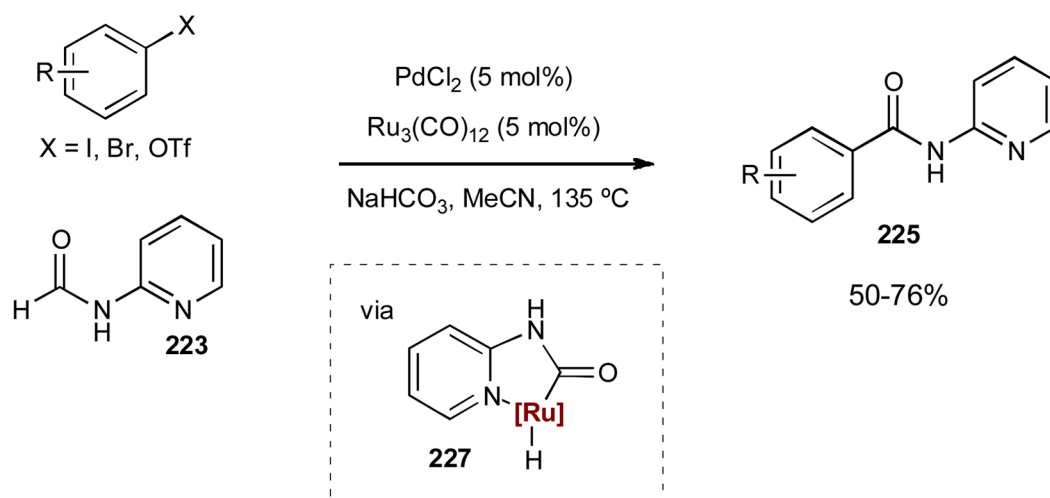
vinyl and imidoyl substrates



**Scheme 50.**

Palladium- and ruthenium-catalyzed coupling of 2-pyridylmethyl formate with aryl and vinyl halides.





**Scheme 51.**  
Palladium- and ruthenium-catalyzed coupling of aryl formates with aryl halides.